NAVAL POSTGRADUATE SCHOOL
Monterey, California

THESIS

ELECTRONIC COUNTERMEASURES (ECM) AND ACOUSTIC COUNTERMEASURES SUPPORTED PROTECTION FOR MERCHANT SHIPS AGAINST SSM/ASM MISSILES AND MINES

by

Bo L. Wallander

December 1989

Thesis Advisor: Robert L. Partelow
Co-Advisor: Alan B. Coppens

UNCLASSIFIED

SECURITY CLASSIFICATION OF THIS PAGE

REPORT DOCUMENTATION PAGE

Form Approved OMB No 0704-0188

1a REPORT SECURITY CLASSIFICATION: Unclassified	1b RESTRICTIVE MARKINGS
2a SECURITY CLASSIFICATION AUTHORITY	3 DISTRIBUTION / AVAILABILITY OF REPORT: approved for public relased; distribution is unlimited
2b. DECLASSIFICATION / DOWNGRADING SCHEDULE	
4. PERFORMING ORGANIZATION REPORT NUMBER(S)	5 MONITORING ORGANIZATION REPORT NUMBER(S)
6a NAME OF PERFORMING ORGANIZATION: Naval Postgraduate School; 6b OFFICE SYMBOL (If applicable)	7a. NAME OF MONITORING ORGANIZATION: Naval Postgraduate School
6c. ADDRESS (City, State, and ZIP Code): Monterey, CA 93943-5000	7b ADDRESS (City, State, and ZIP Code): Monterey, CA 93943-5000
8a. NAME OF FUNDING / SPONSORING ORGANIZATION; 8b. OFFICE SYMBOL (If applicable)	9 PROCUREMENT INSTRUMENT IDENTIFICATION NUMBER
8c. ADDRESS (City, State, and ZIP Code)	10 SOURCE OF FUNDING NUMBERS: PROGRAM ELEMENT NO; PROJECT NO; TASK NO; WORK UNIT ACCESSION NO

11 TITLE (Include Security Classification): Electronic Countermeasures (ECM) and Acoustic Countermeasures (ACM) Supported Protection for Merchant Ships Against SSM/ASM Missiles and Mines

12 PERSONAL AUTHOR(S): Wallander, Bo L.

13a TYPE OF REPORT	13b TIME COVERED	14 DATE OF REPORT (Year, Month, Day)	15 PAGE COUNT
Master's Thesis	FROM _____ TO _____	December 1989	196

16 SUPPLEMENTARY NOTATION: The views expressed in this thesis are those of the author and do not reflect the official policy or position of the Department of Defense or the U.S. Government

17 COSATI CODES			18 SUBJECT TERMS (Continue on reverse if necessary and identify by block number)
FIELD	GROUP	SUB-GROUP	ECM, merchant ships, high frequency sonar, sonar design, ACM

19 ABSTRACT (Continue on reverse if necessary and identify by block number)

The necessity for merchant ship self protection has become more and more obvious during recent years. This thesis will investigate the threat (missiles and mines) and associated counter-measures that might be installed to provide a reasonable degree of protection. The results indicate that it is possible to get protection against a sea-skimming missile with a combination of ECM and ESM deployed aboard the ship. For protection against the mine threat, a sonar is designed in order to give the ship enough warning time to make an avoiding maneuver. The sonar investigation indicates the difficulty in designing a sonar that can fulfill all design objectives year-round in a complex acoustic environment.

20 DISTRIBUTION / AVAILABILITY OF ABSTRACT: ☒ UNCLASSIFIED/UNLIMITED ☐ SAME AS RPT ☐ DTIC USERS	21 ABSTRACT SECURITY CLASSIFICATION: unclassified
22a NAME OF RESPONSIBLE INDIVIDUAL: Robert L. Partelow	22b TELEPHONE (Include Area Code): (408) 484-1551; 22c OFFICE SYMBOL

DD Form 1473, JUN 86 — Previous editions are obsolete. — SECURITY CLASSIFICATION OF THIS PAGE

S/N 0102-LF-014-6603 — UNCLASSIFIED

Approved for public release; distribution is unlimited

Electronic Countermeasures (ECM) and
Acoustic Countermeasures (ACM) Supported Protection
for Merchant Ships Against SSM/ASM Missiles and Mines

by

Bo L. Wallander
Lieutenant Commander, Royal Swedish Navy
Swedish Naval Academy, 1974
Swedish Staff and War College, 1987

Submitted in partial fulfillment of the
requirements for the degrees of

MASTER OF SCIENCE IN SYSTEM ENGINEERING (EW)
MASTER OF SCIENCE IN ENGINEERING ACOUSTICS

from the

NAVAL POSTGRADUATE SCHOOL
December 1989

Author: _____
Bo Wallander

Approved by: _____
Robert L. Partelow, Thesis Advisor

_____
Allan B. Coppens, Co-Advisor

_____
Scott H. Hershey, Second Reader

_____
A.A. Atchley, Chairman,
Engineering Acoustics Academic Committee

_____
J. Sternberg, Chairman,
Electronic Warfare Academic Group

ABSTRACT

The necessity for merchant ship self protection has become more and more obvious during recent years. This thesis will investigate the threat (missiles and mines) and associated counter-measures that might be installed to provide a reasonable degree of protection. The results indicate that it is possible to get protection against a sea-skimming missile with a combination of ECM and ESM deployed aboard the ship. For protection against the mine threat, a sonar is designed in order to give the ship enough warning time to make an avoiding maneuver. The sonar investigation indicates the difficulty in designing a sonar that can fulfill all design objectives year-round in a complex acoustic environment.

TABLE OF CONTENTS

LIST OF TABLES

LIST OF FIGURES

ABBREVIATIONS

ACM	Acoustic Counter Measures
AGC	Automatic Gain Control
AOA	Angle Of Arrival
AGPO	Angle Gate Pull Off
ASM	Air to Surface Missile
CM	Counter Measures
CW	Continuous Wave
CTFM	Continuous Transmitting Frequency Modulation
dwt	Deadweight tonnage
d	Detection index
DIFM	Digital IFM receiver
DT	Detection Threshold
EW	Electronic Warfare
ECM	Electronic Counter Measures
ECCM	Electronic Counter Counter Measures
ESM	Electronic Support Measures
EOB	Electronic Order of Battle
ERP	Effective Radiated Power
FM/CW	Frequency Modulated Continuous Wave
FFT	Fast Fourier Transform
HP	Horse Powers
HOJ	Home On Jam
I&W	Indication and Warning
IFM	Instantaneous Frequency Measurement
LO	Local oscillator
LFM	Linear Frequency modulation
NSL	Noise Spectrum Level
NSL(A)	Ambient Noise Spectrum Level

NSL(S)	Self Noise Spectrum Level
P(D)	Probability of Detection
P(FA)	Probability of False Alarm
PRF	Pulse Repetition Frequency
POI	Probability Of Intercept
PPI	Plan Polar Indicator
PW	Pulse Width
PRI	Pulse Repetition Interval
RO/RO	Roll On Roll Off
RCS	Radar Cross Section
RGPO	Range Gate Pull Off
RWR	Radar Warning Receiver
RAM	Radar Absorbing Material
RPV	Remote Piloted Vehicle
SSM	Surface to Surface Missile
SSL	Source Spectrum Level
SL	Source Level
SLL	Side Lobe Level
SIGINT	Signal Intelligence
TL	Transmission Loss
TS	Target Strength
VLCC	Very Large Crude Carrier
VGPO	Velocity Gate Pull Off
WAM	Window Addressable Memory

I. INTRODUCTION

A. BACKGROUND

The increase in threat technology since world war two has been alarming. A threat of particular concern to world navies is the anti-ship missile. Computer programmed, multi-sensor guided, multi-platform delivered missile systems, aimed at over-the-horizon targets are very effective against the warships for which they are designed.

A second threat, of less sophisticated technology but nevertheless of good effectiveness against warships, is the mine. Mines can be deployed by all kinds of platforms and can also be designed for various purposes. However, as recent events have clearly demonstrated, anti-ship missiles and mines are also devastating against unarmed merchant ships. As a result, countries depending on maritime trade need to enhance their self-protection capabilities.

A merchant ship needs self-protection in two specific situations. First, when transiting through a defined "war zone" area and second, when used for logistic support of a military operation. Both of these situations occurred in the Falkland war in 1982 and again in the Persian Gulf war in 1985 through 1988. If the merchant ships involved in these operations had been equipped with some kind of self-protecting systems, many political, economic and tactical advantages would have been realized.

Over the past 30 years there have been significant changes in the size, appearance and general characteristics of ships engaged in international commerce. The design and construction technology through the period have accelerated this development and given us new types of ships with the ultimate goal of increasing ton-miles per day at maximum

profit. Containerships, barge carriers, RO/ROs (Roll On Roll Off) and liquefied gas carriers are some of the newcomers which are operating worldwide. Few in number, they are relatively large, fast, and employ the latest technology. Tankers and other bulk carriers have been in service for many years and their numbers, size and power have grown dramatically. Although participating in worldwide operations, the immense size of some classes limits them to terminal ports and routes. Oil, or oil derivatives, are a vital product for practically all developed countries so that the transportation of these products has resulted in a large number of ships of all sizes; from small coastal tankers to VLCCs (Very Large Crude Carriers) of over 500,000 dwt.

Figure 1 [Ref. 1] shows the sizes of deep sea tankers by delivery date.

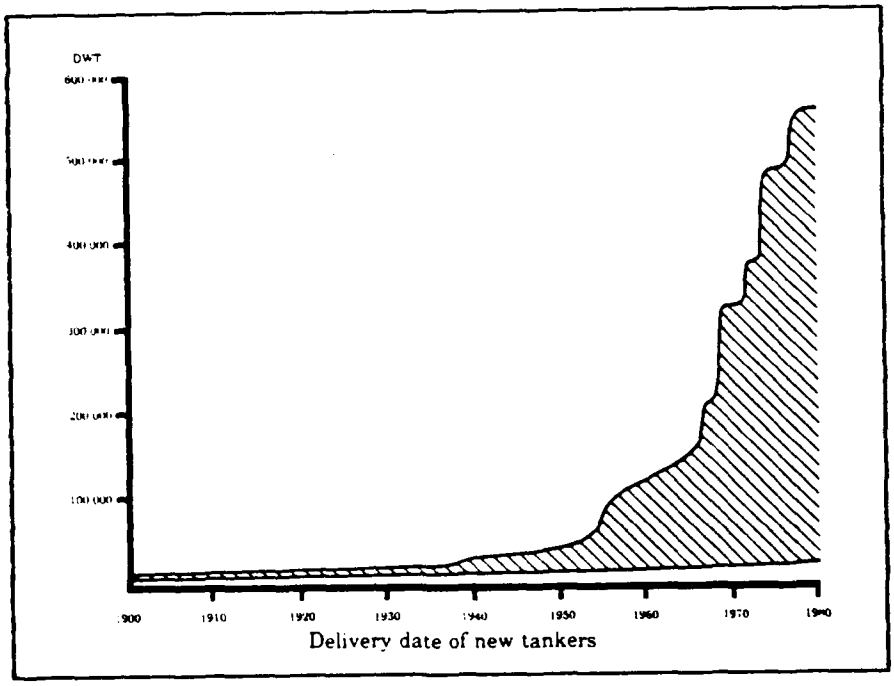

Figure 1. Deepsea tanker sizes by delivery date

The yearly world oil production today (1989) is estimated to be around 3 billion tons and is increasing. Of this, 1 billion is transported in tankers. With an estimated 60% of the world reserves located in the Middle East, the demand for tankers will likely increase.

Today, the tanker fleet consists of 2,500 large ships (over 10,000 dwt) and represents a capacity of 230 million dwt. In addition, there are 280 ships capable of carrying both oil and/or ore and approximately 4,000 small coastal tankers.

B. DISCUSSION

To maximize profits, shipowners are making great efforts to reduce expenditures. The cost of acquiring self-protecting systems for a tanker must be weighed against the potential cost savings. That is, are the costs resulting from loss of life or property versus the cost savings from a reduction in insurance premiums, enough to offset the costs of the self-protection systems?

Considerations other than hardware acquisition will also affect the overall cost of the self-protecting systems. For example, do the self-protection systems need to have an operator or operators? Or is training of current crew members an option? What about maintenance? Portability? Having to hire additional, specially educated and trained personnel to operate and care for the equipment adds a great deal of cost to the life cycle of the systems. Therefore, the systems must be easy to operate and maintain. Since the tanker does not always have to transit "war zones" to get to its destination, and must keep its time in port to a minimum, the necessary equipment should be easily installed and removed.

C. OBJECTIVES AND CONSTRAINTS

The focus of this thesis will be to:

* Examine the use of Electronic Warfare support in reducing the anti-ship missile threat.
* Give design parameters for a mine hunting sonar system in order to reduce the mine threat.

The thesis will first study the threat and merchant ship characteristics. It will then study the EW system(s) possibilities that can provide a degree of protection, and give guidelines and suggestions for further investigations. The thesis will subsequently continue with a mine hunting sonar design procedure, where design parameters will be determined based on outlined mission and technical assumptions and specifications.

In pursuing the objectives, the following constraints will be considered:

* A scenario paralleling the Persian Gulf experiences of neutral shipping, transiting through defined "war zones," will be used.
* The threat consideration will be a "generic" radar guided missile and a "generic" mine.
* The EW support and Mine hunting sonar design characteristics must be relatively inexpensive, easily installed and removed, nearly autonomous or, if not, very "user friendly."
* The merchant ship is operating alone.
* EW protection will be limited to ESM and ECM support.
* The Acoustic Counter Measure (ACM) will be limited to the design of a high frequency mine hunting sonar, mounted on the bow of the ship.
* The sonar hardware design and transducer theory (except beam forming) will not be covered.
* The sonar design environment will be limited to a specific area in the Baltic sea.

II. TARGET SCENARIO

A. TARGET CHARACTERISTICS

Besides the fact that ship sizes have been getting bigger, even the ship proportions have changed significantly. Length to beam ratios are now typically 5.5 to 6.5, where previously they were in the 7.5 range. The draft has also increased and has actually made it impossible for the largest ships to operate normally in almost all ports of the world. Careful planning is necessary to determine how best to accomplish the assigned mission within the unique constraints of each port. In many cases the ship or ships have to be unloaded outside the port by smaller tankers. [Ref. 2]

Although a "standard" tanker will be used throughout the thesis, other tanker dimensions will be considered as appropriate.

The reference tanker has the dimensions shown in Figure 2. [Ref. 2]

Appendix A shows the general arrangement of typical "reference" tanker.

B. OPERATIONAL CONSIDERATIONS

During transit through a "war zone" one can assume that the bridge is manned with at least three persons: one duty officer, one steersman (no automatic steering during war zone transit) and one look-out. The alert level is high at all times. One can also assume that the ship has at least one X band and a C band radar.

The ship cargo tanks and the bow area are unmanned when operating at sea. They are also the most insensitive part of the ship to missile attack. Since crude oil has low

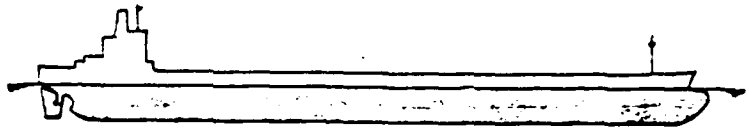

Length in meters	330
Beam in meters	50
Depth in meters	25
Draft in meters	20
Speed in knots	16
HP (horse power)	30,000
Propulsion	Steam
Light ship in tons	30,000
Deadweight in tons	250,000
Displacement in tons	280,000
Length/Depth	12.8
Length/Beam	6.3

Figure 2. Profile of tanker

inflammability, it is unlikely that the oil will be ignited by missile impact. Consequently, if it is impossible to avoid the missile, this is the least vital part of the ship to have hit. The zone extends through approximately three-fourths of the ship's length. If the vital one-fourth can remain relatively undamaged, the VLCC may be able to proceed to the nearest "friendly" port.

Even if a VLCC is capable of withstanding several missile hits without sinking, there are still strong political reasons to protect the ship. The recent situation with United States' involvement in the Gulf War of 1988 is a good example.

In spite of their size, the VLCCs are occasionally operating in narrow straights and close to shore. This leads to a situation where a missile can be launched from the shore. This thesis will look at both the open sea case, whether the missile is fired from an aircraft or a ship, and the shore case.

C. PERFORMANCE

This section discusses ship maneuverability limits and the consequences for missile avoidance. It should be obvious that a VLCC is not designed for fast maneuvers or speed changes. However, the vertical semicylindrical bow shape resulting from a tanker's low speed/length ratio, lowers water resistance and improves propeller efficiency (Figure 2). The resulting ship stability gives the tanker more maneuverability than its size might indicate.

Table 1 shows maneuvering data for the reference target [Ref. 3]:

TABLE 1. MANEUVERING DATA FOR REFERENCE TARGET

Crash stop ahead test (full load condition)	Appendix B
Crash stop astern test (ballast condition)	Appendix C
Modified Zig-Zag test (ballast condition)	Appendix D
Turning test (ballast condition)	Appendix E
Reversed spiral test (ballast condition)	Appendix F

Given a nominal speed, for both open-ocean and in-shore situations, of 16 knots (together with the performance characteristics above), it takes around 20 minutes for a fully loaded tanker to stop. If the tanker is in ballast, it will require only about 14 minutes.

With a maximum rudder deviation (35 degrees port or starboard) and a 16 knot speed, the angular turning velocity is 0.7 degrees/second. Therefore, the time required to turn the ship's head 90 degrees is 2.5 minutes in ballast condition, and is estimated to be 3.0 minutes when fully loaded.

These results indicate that to use "speed changes" to deceive an incoming missile is not effective. However, in some situations, a tanker at full speed can reduce the missile's approach angle significantly, within the missile's flight time, by applying the appropriate full rudder deviation. This is naturally dependent on what kind of indication and warning (I&W) the ship has available.

D. RADAR CROSS SECTION (RCS)

The quantitative measure of the ratio of power density of a radar wave scattered from a target, to the power density in the radar wave incident upon the target, is called the radar cross section (RCS) of the target.

It is assumed that the target is in the far field, i.e., when the target is sufficiently far from the antenna so that the incident wave upon the target is approximately planar. In this case, the radar cross section can be defined as independent of range to the target. [Ref. 4]

The RCS dimensions are generally expressed as unit square meters. This convention will be used throughout this thesis.

To get correct values for a target's RCS is very difficult. There are formulas to calculate theoretical RCS areas for a number of standard shapes, but when the targets

get more complex, such as with aircraft and ships, there are no simple relationships to use.

The RCS of complex targets are further complicated by the viewing aspect and the radar frequency. The target comprises a number of independent shapes and objects which scatter energy in all directions. The relative phases and magnitudes of all the scattering shapes contribute differently at the receiving antenna and give a varying RCS area as the target shifts in orientation, moves or the viewing aspect is changed.

The theoretical approach to defining RCS relates incident to reflected electromagnetic fields and is shown below as [Ref. 4]:

$$\sigma = \lim_{R \to \infty} 4\pi \cdot R^2 \cdot \left[\left| \frac{E_r}{E_i} \right| \right]^2$$

where σ = RCS

R = Distance between radar and target

E_r = Reflected field strength

E_i = Strength of incident field at target

An easier and probably better way of plotting RCS is to measure the real target in the real (at sea) environment.

Another way is to break up a complex target into a number of simple geometrical shapes, for which we know the scattering behavior, and then to compute the sum of their individual contributions to the whole-target RCS.

A VLCC tanker is considered to be a complex target. Unfortunately, there is no reliable RCS data available, using the approaches described above. Therefore, the only option is to use a simple empirical expression. This expression assumes a ship target at a shallow grazing angle, to obtain an average RCS. This means the expected maxima

about the port and starboard sides are averaged downward, and the resulting value is a median (50th percentile) RCS.

The RCS formula to be used is shown below and was derived from measurements made at X, S and L bands for ships from 2,000 to 17,000 tons. If the formula is valid outside this size and frequency range, it will give us the numbers shown below for the X and the K band radars. [Ref. 4]

$$\sigma = 52 * F^{1/2} * D^{3/2}$$

where σ = RCS in m
F = Frequency in MHz
D = Ship's (full load) displacement in kTon

Calculation: for X band radar = 24 million m^2
for K band radar = 33 million m^2

These numbers are grossly in error when compared with collected data from other kinds of ships.

The effective radar cross section for the reference target is finally estimated to be 100,000 sm average value, valid at all aspect angles and under both loaded and unloaded condition [Ref. 3]. This estimation is a compromise of empirical and measured data. This is a very crude picture of the reality. For example, there is a significant RCS difference depending on whether the ship is exposed from the broad side or from the stern. The fact that the maxima are quite narrow in angle, however, makes this a special case that can be utilized by an attacking missile only if the ship is unable to react quickly enough.

As mentioned above, the cross section area of a target in motion is almost never constant. The variations may be caused by meteorological conditions, the lobe structure of the antenna pattern, equipment instabilities or relative

motions of radar and target. The variations due to a complex target's cross section fluctuations with viewing angle are considered to be the most sensitive parameters and must be taken into account.

The easiest and the most economical method for making adjustments for this is to use the Swerling models (Table 2), where it is possible to adjust the detection probabilities is terms of four different fluctuating models of cross section. [Ref. 6]

TABLE 2. FLUCTUATION MODELS

	Slow target fluctuation	Fast target fluctuation
Many reflectors of same size	model 1	model 2
One dominant reflector	model 3	model 4

In our case, model 3 is the most adequate. A tanker is a relatively "clean" target, considering its superstructure (that is, few small reflectors), so the whole ship is basically one dominant reflector. Further, the missile radar is typically a tracking radar where the number of radar returns is large and the RCS area fluctuation is slow.

E. SELF NOISE STUDY

Noise generated by the platform engines and movement through the water, etc., complicates the sonar detection process. This self noise is measured in dB re 1 μ Pa/Hz$^{1/2}$. Self noise is entered in the sonar equation as an equivalent omni-directional noise spectrum level (NSL(A)). The NSL(A)

and NSL(S) are competitive, and if one dominates (over 10 dB) the contribution of the other is negligible. [Ref. 7]

The objective will be to determine the major noise sources of the VLCC tanker and further give an estimation of the NSL(S) at the sonar location. The assumption for the discussion is that the tanker is transiting a war zone with a speed of 16 knots. No measured NSL(S)s for a tanker of this size and high sonar frequencies have been found in the literature.

The most significant noise causes in a ship can be depicted as seen in Figure 3. [Ref. 8]

The general rule is that self noise tends to increase with the increasing speed of the platform. Further, the relative importance of the different noise sources can be seen in Figure 4. The figure shows the areas where the different noise sources are dominating [Ref. 9].

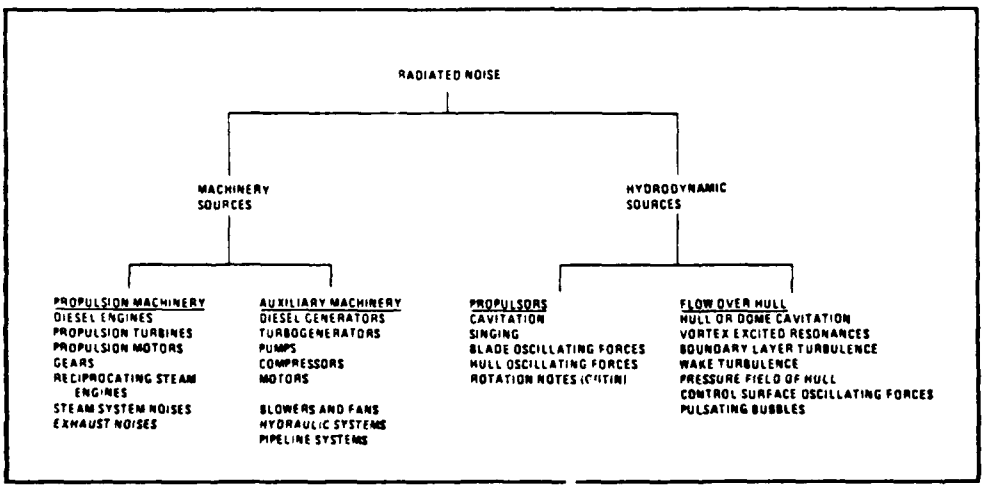

Figure 3. Noise sources in ships

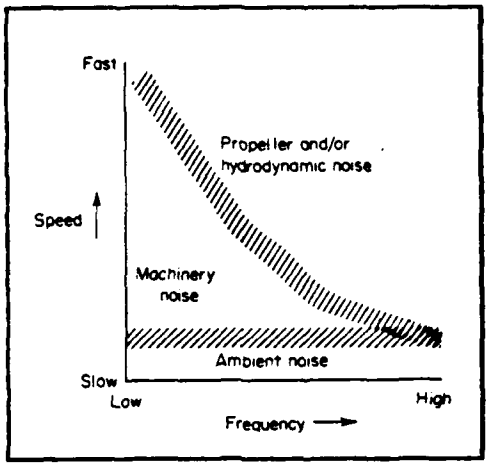

Figure 4. Regions of dominance of the sources of self noise

Other important considerations when estimating the self noise are the location and mounting of the sonar, together with the search sector. The fact that the purpose of the sonar is to detect a stationary mine in a limited sector and in a forward direction reduces the self noise considerably. The sonar is deployed in the front part of the ship and will never point in a direction (astern) where most of the noise sources are located. Further, the high frequency noise spectrum levels in general are relatively low even at high speed.

Self noise can take different paths on its way to the sonar as shown by Urick in Figure 5 below. [Ref. 9]

Path A is a path where the noise is propagating entirely in the hull of the ship. In path B the noise is propagating directly from the noise source to the sonar. Path C is a reflecting path where the noise is reflected to the sonar by volume scatterers in the sea (like reverberation) and finally, path D is a bottom reflecting path. Path B is of minor importance in this case, since the sonar is screened off in all astern directions.

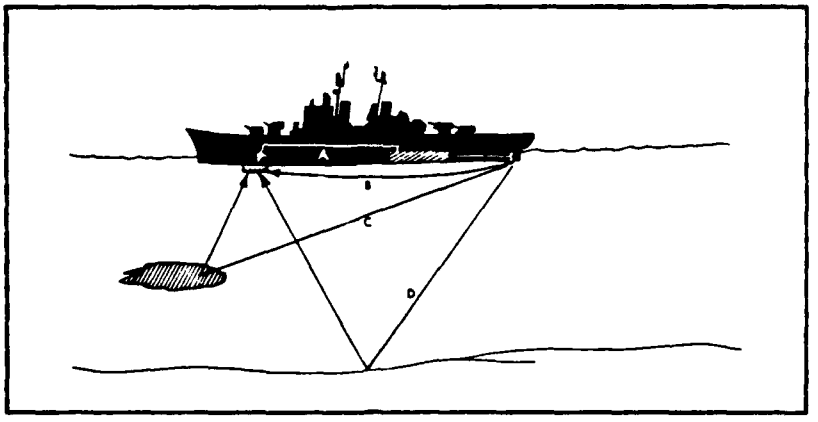

Figure 5. Self noise paths on surface ship

The following three noise contributors are the most significant in this particular sonar application and will be investigated further below.

* propulsion machinery
* propulsors (propeller)
* flow over hull (flow noise or boundary layer turbulence)

1. Propulsion machinery:

The propulsion machinery comprises a steam engine with 30,000 HP, reduction gears, drive shafts and bearings, etc. The noise originates from dynamic unbalances in the systems resulting in oscillating and friction forces. These forces transform into sound and vibrations and are transmitted through the hull into the water and also through the structures (path A) toward the sonar. The sound frequencies are typical narrowband tonals imbedded in a broadband component (see Figure 6). The tonals are caused by the oscillating forces and are occurring at the same rotational frequencies (and their harmonics) of the systems involved. The broadband component is produced by the frictional forces. [Ref. 10]

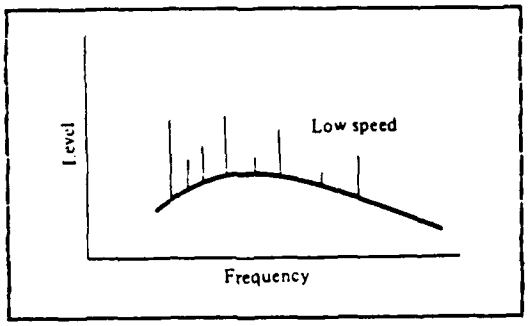

Figure 6. Example of broadband and narrowband components of a ship signature

Sound propagating through the structure of the ship (path A) will be heavily attenuated on its way to the sonar. According to Kohlman and Plunt [Ref. 11], the sound will attenuate on the average of 0.8 dB per frame. For a 300 m path length, containing 125 frames, this gives an attenuation of 100 dB. The source strength in an engine room is assumed to be well below 125 dB re 1 μ Pa based on data regarding noise control in ships [Ref. 8]. Therefore, we can conclude that the sound factor in path A can be excluded from the noise contributors. Sound can still be transmitted through the hull and into the ocean and eventually reach the sonar using path C and/or D. This acoustic energy, however, is typically in the lower frequency range and is more or less overcome by the much more significant propeller noise.

Vibration is a more complicated problem to analyze. The major vibrations originate from the machinery, propeller shaft and propeller, but they also originate when ocean waves strike the ship as it moves forward. The hull is vibrating with vertical, longitudinal, horizontal and torsion vibrations. Other vibrating parts are panels, superstructures, the engine room and the rudder. Vibrations can be reradiated out by the hull and cause noise. It may also cause vibrations on the mounting of the sonar which is a severe problem. [Ref. 9]

To theoretically estimate the impact of vibrations in terms of some kind of noise spectrum level is extremely difficult and will not be attempted in this thesis. It is assumed that the design of the sonar hardware, together with an adequate mounting technique dampens out most vibrations. Using chock suspensions and making the sonar hardware resonance frequency higher than the excited vibration frequencies are some of the actions that can be taken.

2. Propulsors

The major propulsor that produces acoustic noise in the ocean is the propeller (propeller noise). Propeller noise consists mainly of cavitation by the rotating propeller blades and "singing." Cavitation develops when bubbles behind the propeller blades rapidly collapse. This produces a broadband acoustic noise signal. The cavitation noise decreases with depth and increases with propeller rotation speed. The "singing" phenomena is emanating from the vibrational excitation of the propeller blades when water is flowing around them. This builds up tonal components in the broadband cavitation spectrum. [Ref. 10]

The high design frequencies considered and the long path length (300m) from the propeller to the sonar location are factors that, even in this case, help to reduce the noise. Figure 7 shows a typical propeller cavitation spectrum. [Ref. 12]

An estimation of the source level at a distance of 1 m from the propeller in the audible frequency band (100 Hz to 10 kHz) can be made by the following formula:

$$SSL \lesssim K+10 \log(B*D^4*N^3*f^{-2}) \text{ dB re } 1\,\mu\text{bar}$$

where K = 63 (conventional propellers)

D = Propeller diameter in m

N = Revolution rate per second

f = Frequency in Hz

B = Number of blades

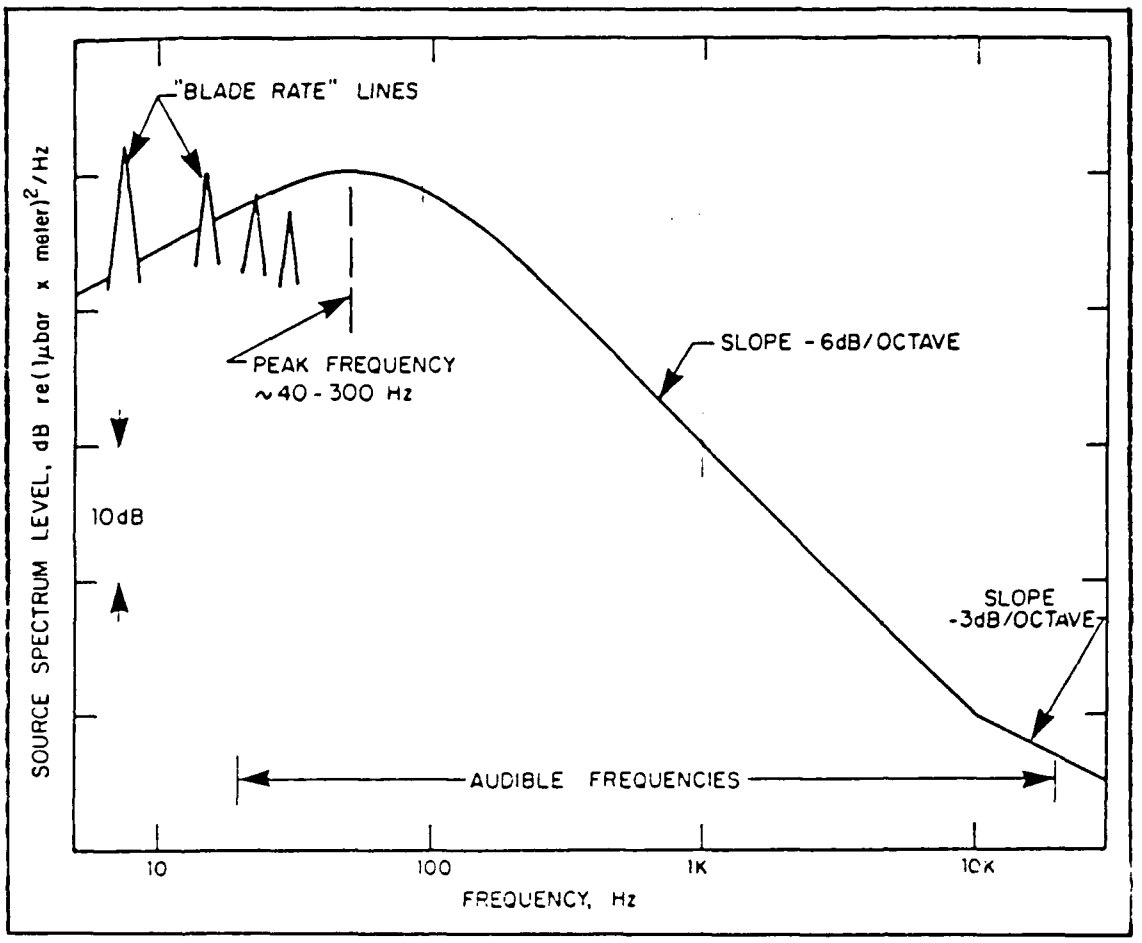

Figure 7. Typical propeller cavitation spectrum

This gives for D = 7 m, N = 3 rev/s, f= 10 kHz (upper limit) and B = 4, an estimated SSL of 37 dB re 1 μ bar/$Hz^{1/2}$. The level is then decreasing with -3 dB per octave which gives

37 -10 dB= 27dB re 1 μ bar/$Hz^{1/2}$

or

27 + 100= 127 dB re 1 μ Pa/$Hz^{1/2}$ at 100 kHz

The transmission loss (TL), with an assumption of spherical spreading, a worst case path length (Path B) of 300 m and an absorption coefficient a=0.02 dB/m gives at the sonar location [Ref. 12]

TL = 20 log R + a*R = 50 + 6 = 56 dB re 1 Pa

The SSL at the sonar location then yields 71 dB re 1 μ Pa/Hz$^{1/2}$. However, even if this is a significant SSL the screened-off sonar makes the noise contribution negligible. The propeller noise will consequently not give a significant noise contribution. The "singing" overtones might still show up in the sonar receiver bandwidth, but it is assumed that this is not very likely to occur. Even if they show up they can easily be removed by using "notch filters."

Cybulski [Ref. 13] shows measurements of the noise spectrum levels (NSL) from a VLCC tanker (dead weight of 271,000 tons) at a speed of 16 knots. The measurements were performed in a low frequency band (2 to 80 Hz), abeam at a distance of 360 meters. At 10 Hz the NSL was measured to about 175 dB re 1 μ Pa/Hz$^{1/2}$. The slope of the measuring curve goes negative at higher frequencies and the fall rate is about -11 dB/octave. This means that the NSL at 100 kHz is estimated to be (13 octaves * 11 dB) 143 dB re 1 μ Pa/Hz$^{1/2}$. This leaves 32 dB re 1 μ Pa/Hz$^{1/2}$ at 100 kHz, assuming the slope rate holds through the entire frequency spectrum. Again, since the sonar is only looking in a very limited angle ahead and never astern, the propeller noise contribution can still be assumed negligible.

3. Flow over hull noise

The most significant "flow over hull noise" source is the "boundary layer turbulence" or "flow noise." Flow noise is generated in the turbulent part of a boundary layer. A boundary layer is developed between the hull and a transitional flow of water when the ship is propagating through the water. It is defined as the region where the fluid viscosity is present and it extends from a zero flow velocity at the hull out to 99% of the free stream velocity. [Ref. 14]

Figure 8 shows a ship model propagating in the water with its boundary layer. Note that the transition point depends on the size of the ship, speed and smoothness of the hull, etc. [Ref. 14]

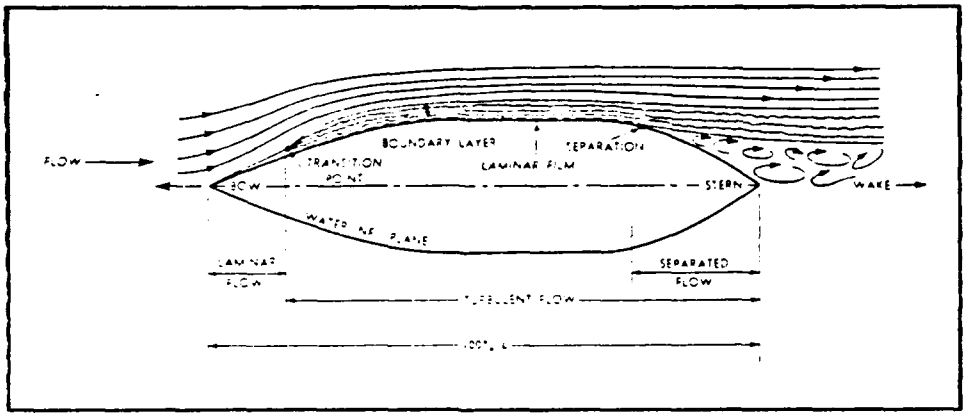

Figure 8. Example of boundary layer on ships

The actual noise is produced by fluctuating pressure patches in the turbulent boundary layer. These give rise to a fluctuating noise voltage at the output of a pressure transducer. [Ref. 9]

The importance of flow noise increases as the speed increases and becomes, in many cases, the major contributor to the self noise [Ref. 15]. In order to reduce the flow noise the following actions can be taken: mount the sonar right at the bow of the ship (this is a stagnation point where the flow separates and the boundary layer is absent); make the transducer size large; and use a dome that surrounds the sonar.

The first two actions are self-evident in this particular sonar design, since the mines are deployed in a forward direction and the beam widths must be narrow (which normally implies a large transducer). Using some kind of housing or dome is a very beneficial action, since a dome reduces the whole self noise picture. It reduces the

turbulent flow and hull cavitation and provides space between the transducer and the flow noise. It is evident that a sonar dome must be used, mounted on the bow of the ship as an extension of the bow-bulb. This limits the flow-noise contributors to the flow-noise surrounding the sonar dome.

Several measurements have been done in the effort to estimate the flow noise NSL of different bodies. Urick [Ref. 6] gives NSL values for a transducer located in a buoyant body and propagating in water at different speeds. According to these measurements, an extrapolated NSL of 30 - 40 dB re 1 μ Pa/Hz$^{1/2}$ is given at 100 kHz. Note that there is a major size and shape difference between the experimental body and the real sonar dome, though.

Skudrzyk and Haddle [Ref. 15] gives measurements from an experiment with a rotating cylinder placed in a so-called "Garfield Thomas Water Tunnel." For a value of $\delta^* = 0.14$ (δ^* = the nondimensional displacement thickness of the boundary layer at 16 knots. The reference indicates that the boundary layer thickness $\delta = 5 * \delta^*$) and f = 100 kHz, these measurements give a NSL of about 60 dB re 1 μ Pa/Hz$^{1/2}$.

There is a significant difference between the results of the two measurements, which is not surprising since the assumptions and experimental configurations are different. However, the experimental set up is more applicable in this case, even if the measured body is different. Hence, the values given by Urick [Ref. 9] are probably more accurate to use in this case.

The NSL in the high frequency part of the spectrum is also highly influenced by the surface roughness and smoothness. [Ref. 15] The more grit and/or rust at the surface, the more noise is generated. Since the sonar system

is only deployed for a limited time, a reasonable assumption is that the sonar dome is always clean and smooth during operation.

5. Conclusion:

The elimination of many noise sources has been possible because of the nature of the design problem. The only noise source that makes a significant impact is the flow noise. Use of a sonar dome to decrease the flow noise is necessary. The design of such a sonar dome is beyond the scope of this thesis, but the design requirements are severe, in order to decrease both the flow noise and the internal losses.

In order to get a specific number for the NSL the measurements by Urick [Ref. 9] are probably the most reliable to use. An upper limit value of 40 μ Pa/Hz$^{1/2}$ is chosen to be the ship's NSL(S) in this particular sonar application. This upper limit value is assumed to take care of the body size scaling in the experiment and also account for other small noise contributions.

NSL(S) = 40 dB re 1 μ Pa/Hz$^{1/2}$

III. THREAT SCENARIO

A. MISSILE THREAT

1.Definition of the threat

As mentioned earlier, the missile threat utilized in this thesis is a surface-to-surface or an air-to-surface missile (SSM/ASM) whose launch platforms include a ship, submarine, airplane or missile batteries ashore. Although both missile types have been available for approximately 40 years, it was not until they had been used in a battle, such as the war between Israel and Egypt in 1967, that their effectiveness was firmly established. As a result of this demonstration and technical development, very cost-effective, capable systems have entered the inventories of almost all countries having military forces.

The most applicable missiles used against a surface target are the "sea skimmers," most threateningly those with long stand-off or over-the-horizon capabilities [Ref. 16]. These missiles are designed to fly just above the ocean surface to make them more difficult to detect, apply ECM or shoot down. To achieve long stand-off distances the missile's trajectory toward the target is usually separated into three phases.

First comes the boost phase where the missile is separated from the host carrier, usually to a high altitude. Then comes the midcourse phase where the missile is guided with some kind of passive navigation system and also descends to low altitude at some point in the phase. In this phase the goal is to avoid any kind of electro-magnetic radiation to prevent detection. The third phase is the terminal guidance phase where the missile utilizes its

tracking radar system to get close enough to the target for proper fuze operation and target damage.

Some of the guidance methods being used are pure inertial navigation, active mapping by radar or just straight dead reckoning. To keep the altitude stable during the terminal phase, some sort of altimetry is used. Since the missile is flying at relatively low altitudes, a low power FM/CW radar altimeter using very short wavelengths can be employed. The FM/CW radar radiates a frequency modulated CW signal having a periodic baseband modulation waveform. Another common altimeter is the pulsed radar with a narrow pulse (0.002 to 0.003 microseconds). Alternatively, a low power laser can also be used, which is jam resistant and more difficult to intercept because of the narrow beam and suppressed sidelobes. A typical missile trajectory is shown in Figure 9 [Ref. 17].

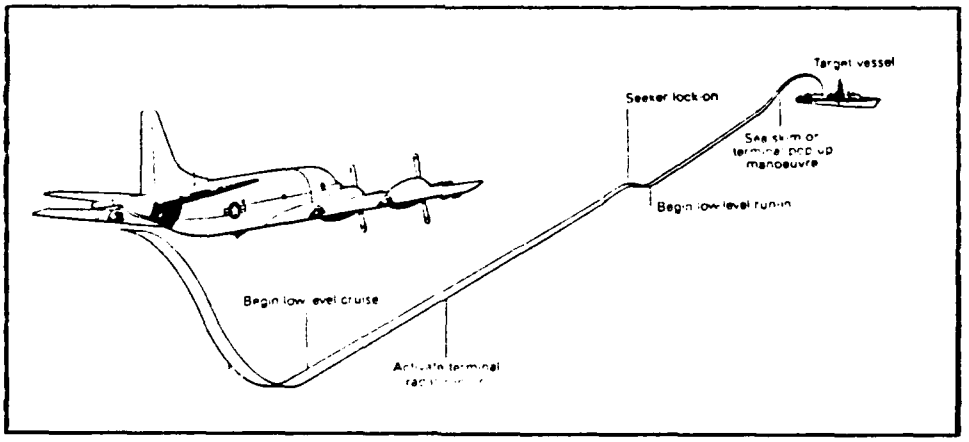

Figure 9. Example of missile trajectory

Prior to the phases described above, the launch platform performs an acquisition cycle where it initially is trying to locate the target. This can be done using external resources or from the platform's own sensors. To draw conclusions during this cycle, such as that a missile launch

against one's ship is imminent, needs both sophisticated ESM equipment and well-trained personnel. Neither are available onboard our reference ship, hence this acquisition cycle will not be further investigated.

2. Design principles

There are many ways of estimating an enemy's threat capability. One method is to determine his electronic order of battle (EOB). This means that enemy targeting-systems capabilities are determined through intelligence efforts. Historically, the intelligence community has been unable to obtain totally objective information on enemy capabilities, resulting in a tendency to underestimate (or overestimate) the threat. Another approach is to assume the enemy has the same capability that ones own country has, and which you therefore know quite accurately. Finally, the third technique is to use a generic design approach, where the optimum theoretical threat parameters are estimated. Both of the latter methods have a tendency to overestimate the threat. Since this is an unclassified thesis, the approach will be a mix of the two latter methods, but the generic method will be emphasized [Ref. 18].

Although many missile seeker configurations are possible, this thesis will only consider a radar guided missile.

Radars, designed for missile seekers, are often a form of specialized tracking radar whose function is to provide high data rate guidance information to the missile's control surfaces. Neither the common tracking nor surveillance radar designs provide the data rates required. Because the missile seeker utilizes a narrow beamwidth antenna, more power is placed on target. The problem with a radar mounted in the nose of a missile is that the size of the antenna aperture must be small, on the order of 12 to 40 cm in diameter, and the capacity to generate high transmitter power is limited.

These design considerations must be traded off with the atmospheric attenuation factors which become more significant as the frequency increases and the flight altitude decreases. In general, at low altitudes, the radar efficiency falls off above X-band at a rate inversely proportional to frequency.

The missile seeker design has significantly improved in the last few years. A modern missile seeker is provided with digital processing, frequency agility, selectable search patterns and modes, target choice logic (to select the most important ship in a ship formation) and considerable ECCM capabilities. [Ref. 17]

The missile seeker ECCM features become vital during the missile terminal phase, when the radar seeker becomes active. At this point,the missile's presence becomes known and susceptible to CM employed by its intended victim. Therefore, different ECCM methods must be considered to get a jam resistant missile. Some of the terminal homing schemes that can be applicable are as follows:

* Active radar with TV scan. The TV scan can be used as a kind of target identification device where a stored target picture is correlated with the real time TV scan.
* ARM. An anti-radiation missile whose mission and design are focused only on destroying specific emitters, according to their signature.
* HOJ capability. This is a missile seeker counter-measure designed to destroy the source of the jamming. It is similar to an ARM but less fussy as to signature identification.
* Command guided missiles. Passive homing on reflected target signals from a radar illuminator or designator in the area.

In future missile designs one can also expect further improvement in seeker systems including multi-guidance modes, multi-sensors and improved target discrimination capability. [Ref. 19]

The missile design characteristics to be considered in this thesis are [Ref. 20]:

* missile dimensions
* missile aerodynamic performance
* seeker performance (power, scan, pulse type, ECCM, etc.).

The following sections in this chapter will determine the parameters of a generic missile that will be used as the threat reference in the thesis. Some of the parameter definitions will be broad in order to provide the opportunity to conduct performance impact analysis.

3. Dimensions and performance

The dimensions of modern sea-skimming ASM/SSM missiles do not vary much between designs. One possible explanation is that the same missile type can be fired from different weapons platforms. Based on unclassified sources, the parametric values for the generic missile discussed in this thesis are listed in Table 3:

The flight profile is shown in Figure 10.

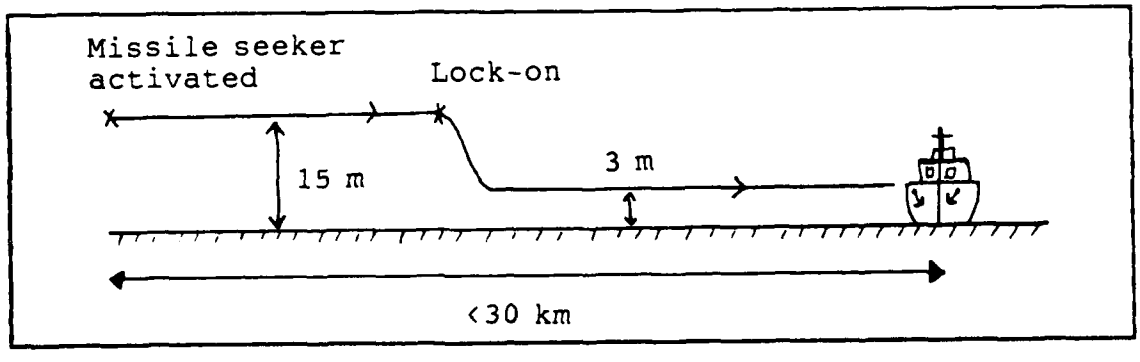

Figure 10. Missile flight profile

TABLE 3. VALUES FOR GENERIC MISSILES

Dimensions:	Length	4.3 m
	Body diameter	0.5 m
	Span	1.4 m
Propulsion:		turbojet
Weight:		600 kg
Warhead:		penetrating/blast with impact/delay and proximity fuzing
Performance:		speed Mach 0.9
Range:		100 km

4. Missile seeker

Potential missile seeker characteristics will be defined as outlined in this chapter's section on design principles. The parameters chosen correspond, in essence, to what is operational today.

The missile seeker has two modes: the search mode and the tracking mode. In the search mode the antenna scans a specified sector while the seeker is trying to decide which echo to track. The seeker processor sorts out the incoming echoes and, based on predetermined logic and inertial measurements, decides which echo is the "best" target choice. Once radar tracking lock-on is achieved, radar tracking data is used to guide the missile to the chosen target. As the missile continues inbound to the target, the antenna continues to scan and provides the processor with updated target position data. New targets in its field of view are evaluated to determine if there is a better target choice. If the processor finds a "better" target choice, it may switch over to the new one, depending on design.

a. Radar search mode:

The missile seeker search mode is by active pulsed radar, utilizing either a fixed frequency or frequency agility operating in the X-band or K-band, depending on the design range of the terminal phase. Having a short terminal phase in future seekers is desirable to reduce the ECM threat. In addition, frequencies above the X-band will improve data accuracy. Short terminal phase also means short reaction time for the target. Future missiles may start their terminal phase at ranges close to 5 km, which results in a reaction time of approximately 15 seconds (assuming a mach 1 missile). [Ref. 16]

The search radar is not designed to have a big tanker as its primary target. It is more plausible to assume that the radar is optimized for a naval combatant such as a destroyer or a frigate. The radar parameters listed in Table 4 are therefore estimated against those targets.

Figure 11 shows the radar beam with range resolution, and Figure 12 shows the missile scan.

b. Radar tracking mode:

The antenna performs a horizontal sector scan as shown in Figure 12. The seeker makes the decision which echo to track in a predetermined way that can be either manually preselected or selected by artificial intelligence. In short, the first echo meeting the programmed target characteristics will initiate the tracking mode.

c. Tracking parameters:

The range tracking technique is a split-gate system that compares the duration of the echo in two times gates. The time difference is a measure of the gate's location compared with the echo pulse. Each time gate is 0.2 microseconds in duration.

TABLE 4. PARAMETERS OF SEARCH RADAR

Radar parameters:	
Radar type:	pulsed, active radar
Frequency:	fixed within 8-10 GHz
Bandwidth:	10 MHz
PRF:	4 KHz ± 400 Hz pseudo random hop
Power:	30 KW
Noise fig:	9.0 dB
Pulse width:	100 nsec
Misc.:	non-coherent detection/integration
Swerling case 3	
P(D):	0.9
P(FA):	10^{-6}
Antenna:	
Type:	Cassegrain, or flat phased array
Aperture:	0.3 m (diameter) nonuniformly illuminated
Scan velocity:	25 degrees/sec
Scan angle:	±10 degrees (azimuth)
Beamwidth:	7.2 degrees (conical lobe)
Gain:	27 dBi
Polarization:	vertical

The tracker is assumed to be centroid, that is, homing is on the central part of the echo pulse. This central part need not be the center of the ship itself. There is almost always a "hot spot" that the seeker is actually homing on.

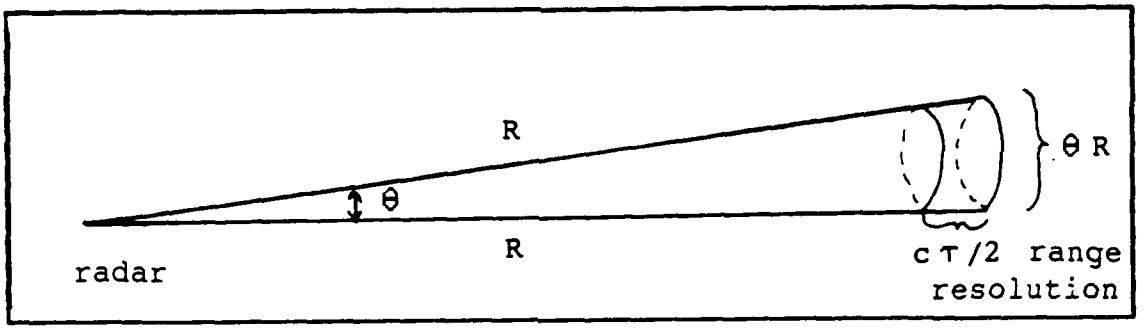

Figure 11. Beam top view

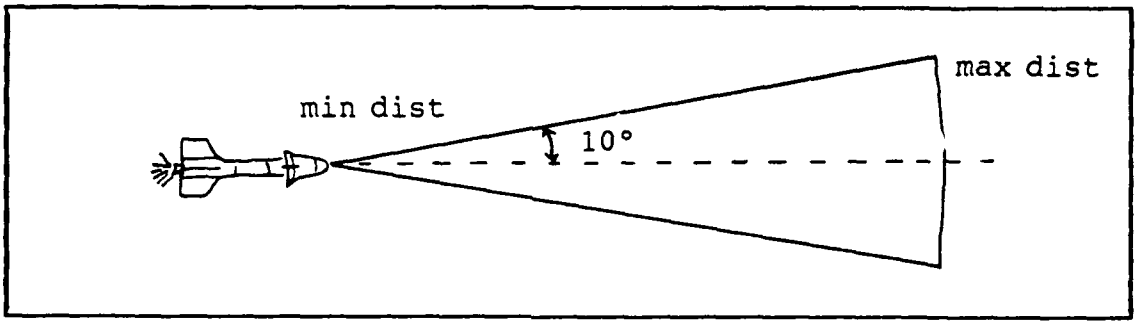

Figure 12. Scan top view

d. ECCM capability

In electronic warfare of today, missile seekers must continue to remain on target in spite of being subject to a number of ECM techniques (RGPO, chaff, etc.). Maintaining the seeker effectiveness in the face of the changing ECM capabilities is a very costly problem for the designers, but it is a price that must be paid. As much as 50% of the total cost of a missile system can be traced to the ECCM features in a well-designed system.

This missile is assumed to be equipped with:

* HOJ (Home On Jam) capability if other ECCM fails against active ECM.
* Automatic gain control (AGC) gates to counter deception ECM.
* "Dickie Fix" receiver to counter against swept spot noise jammer.

B. MINE THREAT

The objective of this section is to determine the target strength (TS) of a "generic" mine. This parameter is similar to the radar cross section (RCS) for a radar target discussed in Chapter 2, and will be an important part in the sonar equations later.

1. Operational considerations

The sea-mine is a very versatile weapon and is used by almost all countries with a sea border. Some of the advantages of mines are:

* They are relatively inexpensive.
* They can be deployed by almost all kinds of platforms (surface ships, submarines, aircraft etc).
* They can be deployed in covert operations.
* They can be tailored to a particular target and environment.
* They are mostly uncontrolled as soon as they are deployed, which implies independence from auxiliary system(s).

The major disadvantage with mines is that it is a relatively slow and stationary weapon system. To sweep mines and redeploy them in another area is both time consuming and dangerous.

Mines are often deployed in large numbers and in a pattern. The area that is sown with mines is termed a mine field. The outer borders of a mine field are normally very carefully determined, since the deploying country, in most cases, wishes to use the water area surrounding the mine field itself. This is not always true, however. There are examples of covert mine deployments, such as in the Persian Gulf, where mines were deployed in ship lanes without any pattern and in vast water areas.

The conclusion is that mines can be used by any nation in a conflict and they can show up almost anywhere in a "war zone."

2. Dimensions and performance

There are a great variety of mines worldwide and their dimensions and performance depend on their purpose, environment and the kind of carrier they are to encounter. This thesis will only consider moored proximity mines since these are the most appropriate in the outlined scenario. The water area considered has a water depth of 100 m which excludes bottom mines that normally must have a water depth of less than 50 m to be effective. Also, contact mines just beneath the surface are very ineffective and seldom used in modern mine warfare. Moored proximity mines are built by many countries and some of the typical shapes with measurements are shown in Figure 13 below. Note that the mine shell can consist of metal, plastic or cellular plastics (for reducing TS).

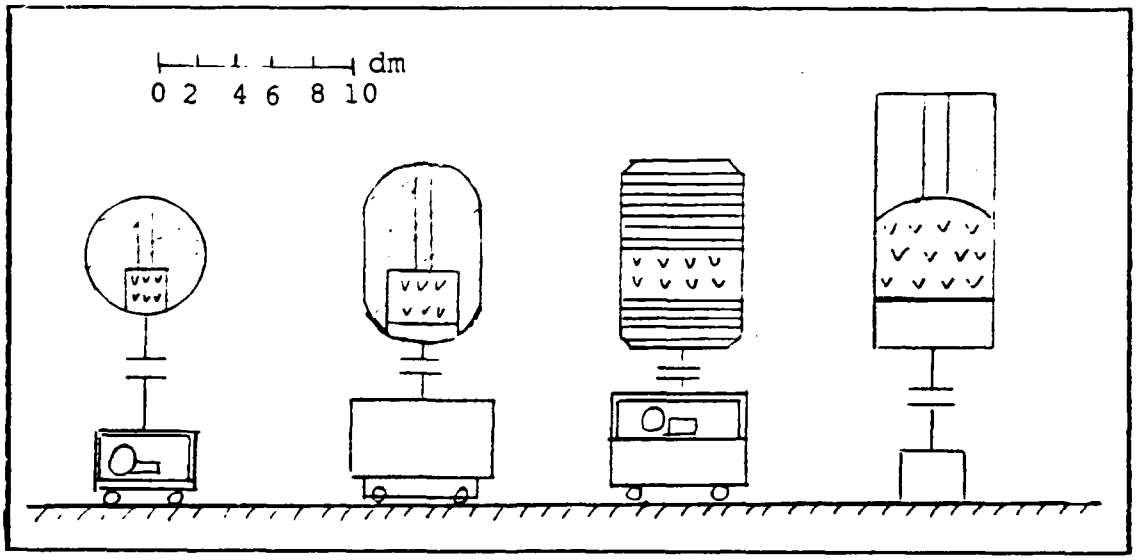

Figure 13. Typical mine shapes and measurements

The figure also shows an inside view of the mine. The mine has a very thin shell and the inside contains a charge, a sensor with electronics and air. The charge weight is normally 200 kg and the total weight can be around 900 kg (with anchor).

Figure 14 shows a deployed moored proximity mine. Note that the mine depth is approximately 20 m and the proximity distance is approximately 20 m. The mine depth is optimized for surface ships.

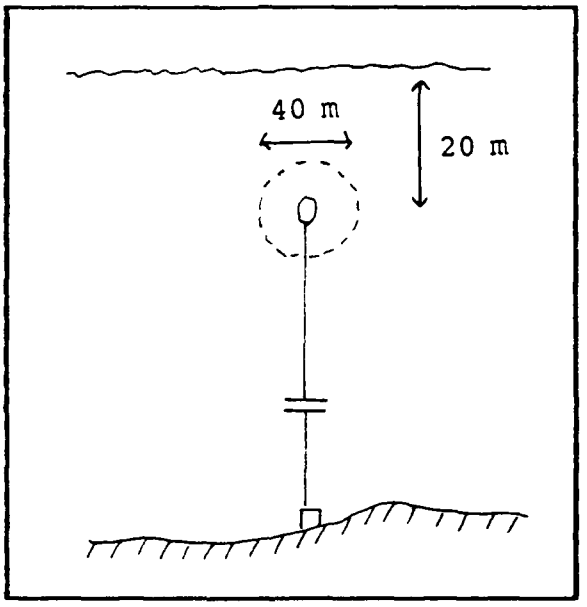

Figure 14. Deployed moored proximity mine

The performance of mines is a highly classified area, but in general, mines consist of multiple sensors with programmable microprocessors to select targets and to resist countermeasures.

An example of how a mine works is; when a ship comes in the vicinity of the mine, say a few nautical miles, an acoustic sensor alerts the mine. If the sound behavior is "correct," the mine activates a magnetic and/or a pressure

sensor. If the response(s) follows certain conditions the mine will detonate.

3. Target strength

When a transmitted sound pulse propagates in the water and impinges on a discontinuity (target) in the water, some portion of the incident energy will be reflected back toward the transmitter. This reflected energy is called the echo and is the signal of interest at the receiver location. [Ref. 7] "The target strength (TS) is defined as the ratio of the reflected intensity (I_r) in the receiver direction, measured 1 m from the effective target center, to the incident intensity at the same point." [Ref. 10: p. 366]

$$TS = I_r/I_i$$

The TS depends on the geometry, size and acoustic impedance of the target. It also depends on the frequency of the incident signal. In order to get correct TS values the most adequate way is to measure the particular target under real conditions. This is not an option in this case, however. Another possibility is to compare the target with simple geometrical shapes where TS has been derived. The problem here is to determine which shape is the most representative to use, among the shapes shown in Figure 13. Urick [Ref. 9] gives computed TS values for quasi-cylindrical mines. These values vary between +10 to -25 dB depending on aspect angle. This indicates at least the range and magnitudes of the target strength for a mine. Further issues that need be discussed to get correct theoretical TS values are: (1) How much of the incident energy is absorbed by the mine? (2) What is the target response if sound is penetrating into the mine? (3) What kind of resonant effects and vibration modes get excited by the incident signal and how do these effect the TS?

In addition, efforts will be made by the deploying country to reduce the target strength of the mine as much as possible. Some of the methods that can be used are listed below [Ref. 9]:

* Anechoic coating
* Viscous absorbers
* Gradual-transition coatings
* Quarter-wave layer
* Active cancellation

These techniques are especially applicable at high frequencies. The frequency choice in this case is in the high frequency region, so consequently the TS reduction techniques must be considered.

The discussion above indicates that to determine a particular TS value for a "generic" mine by theoretical means is not a viable option. Instead, let's handle the problem by assigning a target strength of 0 dB re1 μPa, and then use the target strength parameters in a sensitivity analysis at the end of the design study.

TS = 0 dB re 1 μ Pa

IV. ELECTRONIC COUNTER MEASURES (ECM)

The basic purpose of electronic countermeasures (ECM) is to introduce wave forms into a hostile electronic system which will prevent or hamper the system or its operator from performing their mission.

One way of subdividing the ECM field is shown in Appendix G. ECM includes jamming, deception and tactics. [Ref. 18] Jamming is a deliberate radiation or reflection of energy with the objective of impairing the deployment of electronic devices used by a hostile force. Deception is the deliberate radiation or reflection of energy in an effort to mislead a hostile force. Tactics include what kind of actions the ship commander can perform to support the jamming and deception ECM. Only techniques that are applicable to the active sea skimming missile seeker will be covered.

As mentioned earlier, the seeker has two modes and both can be affected by ECM. In the search mode the missile seeker is activated at approximately 20 to 30 km from the target. Given the 100,000 square meter size of the intended target, the seeker should be able to immediately "lock on" the target, assuming no other similar targets are in the seeker's field of view. It would then switch over to the tracking mode. The time the seeker spends in the search mode is therefore assumed to be very short. Because the missile seeker will spend most of its time in the tracking mode, it is during this part of the flight profile that the seeker is most vulnerable to ECM. The thesis will focus on the ECM considerations in this mode.

The main objective for the VLCC tanker is to get the missile to avoid the target entirely. This includes the case when the missile misses the target but is sufficiently close

to initiate the proximity fuze. If an impact is unavoidable, a secondary objective is to force the missile to impact the ship at a point having the least effect on operations.

The purpose of this chapter is to come up with different ECM support that can be effective for the VLCC tanker described in Chapter 2.

The advantages and disadvantages of the ECM support will be documented along with the support's feasibility. Conclusions will be made at the end of the chapter.

A. JAMMING ECM

1. Noise jamming

a. Description

Noise or "denial" jamming is divided into spot noise jamming and barrage noise jamming. In principle, spot noise jamming focuses a narrow band of noise on the operational bandwidth of the victim seeker. Barrage noise jamming is broadband and will effect the operation of seekers emitting within a wide range of frequencies. Spot noise jamming requires that the seeker operate at one known frequency unless swept spot noise is employed. If the seeker utilizes frequency hopping as an ECCM technique, the jammer must be able to anticipate the seeker frequency changes to be most effective. This jammer capability is only completely effective against seekers using a repeated frequency pattern which can be anticipated by the jammer's frequency programming logic. Pseudo-random frequency patterns will degrade a spot jammer's ability to anticipate and jam. Having a spot jammer capable of following predictable frequency hoppers will be expensive, swept spot jamming can be a good compromise. Barrage jamming can cover the operating frequency range of the seeker, but there is the penalty of a reduction in Effective Radiated Power (ERP). Increasing power has the companion constraints of larger

size and higher costs. General advantages and disadvantages with barrage noise and spot noise jammers are in Table 5.

TABLE 5. EVALUATION OF JAMMERS

	Advantages	Disadvantages
Spot noise jamming	good efficiency; light, small volume; easy to discriminate own frequencies	need good signal-analysis and skillful operator or complex automatic; little effect against frequency agility
Barrage noise jamming	little signal analysis; simple to operate; efficient against frequency agility	low efficiency, large weight and volume; can interfere with own radar frequencies
Swept spot noise	good trade-off on ERP and jamming effectiveness against frequency agility	best trade off of these three against frequency agility

The goal of noise jamming is to raise the noise floor of the missile seeker such that the actual signal is completely submerged by the interference or confused with noise impulses randomly appearing in the receiver. [Ref. 20]

The special case of noise jamming called swept spot jamming, is effectively a combination of barrage noise jamming and spot noise jamming. It utilizes narrow band noise that is rapidly swept over a larger frequency band (Figure 15) [Ref. 6]. Δf can be nearly 1 GHz and T approximately 1 microsecond.

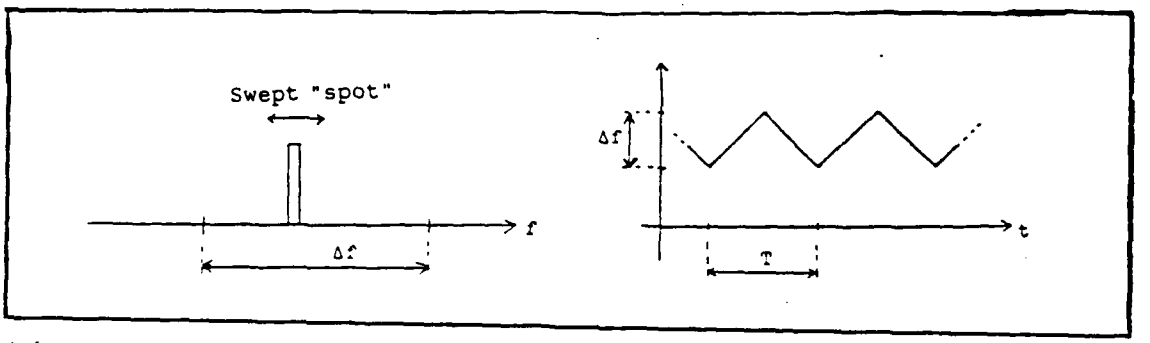

Figure 15. Wave form for swept spot jamming

The advantage with this method is that many seeker frequencies can be jammed at the same time. The disadvantage is that the jamming pulse is received intermittently, and at a lower rate than the seeker's received echo pulse and is therefore less then 100% effective. This kind of jamming can be substantially degraded by incorporating "Dicke Fix" in the seeker receiver.

b. Analysis

The target has several ways of utilizing noise jamming. Some examples are shown below, together with approximate calculations. All of the values are based on the reference target seeker in Chapter 3.

The following assumptions are made:

* free space propagation (no multipath)
* no atmospheric attenuation
* no lobe divergence

Further, a new reacquisition cycle, that is, when the seeker is changing target, takes approximately one second. If the seeker loses information only in one coordinate (i.e., in range), or is acquiring a new target, the reaction time is on the order of milliseconds.

One part of evaluating the effectiveness of noise jamming is to mathematically predict burnthrough distance, power requirements, etc. Figure 16 is used throughout this section of the chapter [Ref. 6].

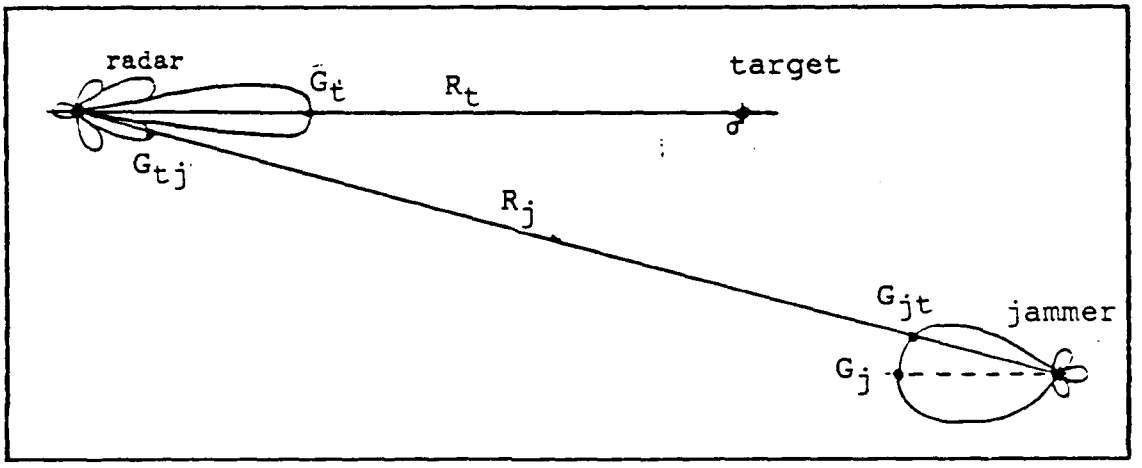

Figure 16. Typical jamming situation

Abbreviations that will be used for jamming calculations are.

P_t : radar transmitted power
G_t : radar maximum antenna gain
G_{tj}: radar antenna gain in jammer direction
d_t : G_t/G_{tj} antenna side lobe ratio
B_t : radar bandwidth
P_j : jammer power
G_j : jammer maximum antenna gain
G_{jt}: jammer antenna gain in radar direction
d_j : G_j/G_{jt} jammer side lobe ratio
B_j : jammer bandwidth

d_s : B_t/B_j bandwidth ratio

σ : target radar cross section area

R_t : distance radar to target

R_j : distance radar to jammer

λ : wavelength

Return power at the pulse reflected from the target into the radar receiver (when the main lobe is pointing on the target) is:

$$S = \frac{P_t \cdot G_t}{4\pi \cdot R_t^2} \cdot \frac{\sigma}{4\pi \cdot R_t^2} \cdot \frac{G_t \cdot \lambda^2}{4\pi}$$

Jammer power in the receiver (within the receiver bandwidth) is:

$$J = \frac{P_j \cdot G_{jt}}{4\pi \cdot R_j^2} \cdot \frac{G_{tj} \cdot \lambda^2}{4\pi} \cdot d_s$$

The general formula for signal to jamming ratio becomes:

$$S/J = \frac{P_t \cdot G_t \cdot \sigma \cdot R_j^2}{4\pi \cdot R_t^4 \cdot P_j \cdot G_{jt} \cdot G_{tj} \cdot d_s} = \frac{P_t \cdot G_t \cdot \sigma \cdot R_j^2 \cdot d_j \cdot d_t}{4\pi \cdot R_t^4 \cdot P_j \cdot G_j \cdot d_s}$$

Assume that the required signal to jamming ratio (for given values of P(D) and P(FA)) is S/J min. Assume further

that this is achieved at the "burnthrough" distance R_b, that is (S/J)=(S/J) min for $R_t = R_b$.

(1) Case 1: Selfscreening jamming. This is the case when the jammer is located on the target or very close to it. The case is explained in the analysis graph, Figure 17. The location of the jammer is a very important issue since the missile, if equipped with HOJ capability, probably will be guided to that location.

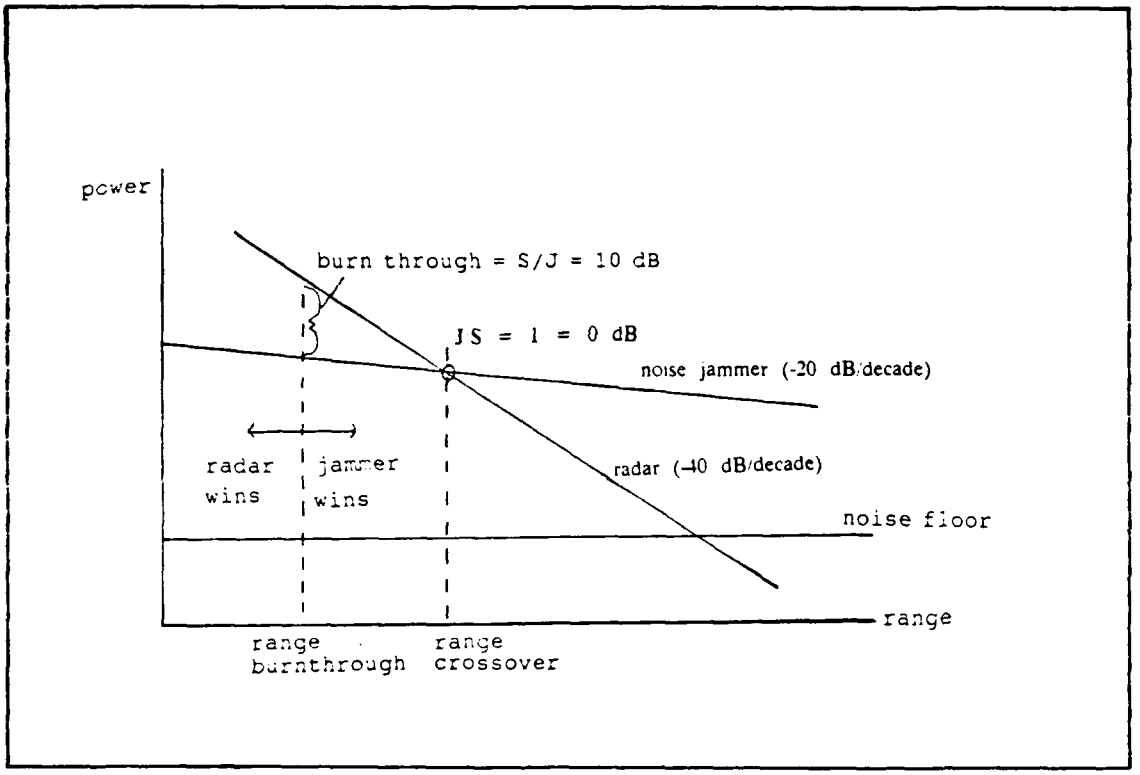

Figure 17. Selfscreening jammer analysis graph

Assume a jammer with an antenna gain of 10 dB and that an (S/J) min ratio of 10 dB is required.

Then the jammer power required for a burnthrough distance of 600 m (worst case, based on missile reacquisition cycle and maneuvering capability), and for the barrage noise jamming becomes:

$$P_j = \frac{P_t \cdot G_t \cdot \sigma_t}{4\pi \cdot (S/J)_{min} \cdot G_{jt} \cdot d_s \cdot R_b^2} = 66 \text{ KW}$$

(Since this is selfscreening jamming, $R_j = R_t$ and the $G_{tj} = G_t$, that is $d_t = 1$.) It also assumes:

$$d_s = \frac{10 \text{ MHz}}{200 \text{ MHz}} = 0.05$$

The jamming power required for spot noise jamming with the same values as above becomes:

$P_j = 3.3$ KW, where $d_s = 1$

(2) Case 2: Side lobe jamming. In this case the jammer is external but with approximately the same range to the missile as the target ($R_j = R_t$).

With the same assumptions as above, but with $G_{tj}=G_t$, $d_t=1$ and the seeker side lobe ratio of 15 dB gives:

For the barrage noise case, with $d_j=1$ and $d_t=15$ dB

$$P_j = \frac{P_t \cdot G_t \cdot \sigma \cdot d_j \cdot d_t}{4\pi \cdot (S/J)_{min} \cdot G_j \cdot d_s \cdot R_b^2} = 2.1 \text{ MW}$$

For the spot noise case, $P_j = 106$ KW

The small aperture and the low average transmitted power in the missile seeker generally results in strong sidelobes. This makes the missile seeker more vulnerable to sidelobe jamming. [Ref. 18]

The requirements in both cases described above are fully achievable with today's techniques.

As shown in Chapter 3, the range tracking system generates two gates. They are 0.2 μ s in duration (that is 60 m) each. The angle tracking resolution (width) depends on the range to the target and the relationship @ * R, where @ (the lobe angle) is expressed in radians. This relationship gives the following gate sizes shown in Table 6:

TABLE 6. TRACKING SYSTEM GATE SIZES

Range (km)	Length (m)	Width (m) (cross range)
30	60	3,780
20	60	2,520
10	60	1,260
5	60	630

When these numbers are compared with the target, it is clear that the reference VLCC tanker, which measures 330 m in length and 50 m in width, can easily fill the gate's length.

c. Discussion

As stated in Chapter 1, the ECM system must meet the basic parameters of simplicity, reliability, effectiveness and low cost. Noise jamming is a very effective and inexpensive way of denying the missile seeker target data. Based on information theory, white Gaussian noise injected into the receiver system provides for the

most effective jamming. It is statistically impossible for the seeker to distinguish between this jamming noise and the noise generated by the receiver itself. So, if the seeker is exposed to enough high quality, high power noise jamming, seeker "break lock" is possible. [Ref. 18]

The major problem with any kind of noise jamming is that the missile seeker, in almost all cases, is equipped with HOJ capability (that is, it homes on the jamming signal). This ECCM technique can be utilized by the target to guide the missile to a dummy target or to an insensitive part of the target itself. One solution is to tow a jammer mounted on a small craft behind the ship. There might be a problem keeping the craft in position due to the wind, currents and weight of the tow line, etc. A more fundamental problem is how far behind the target must the craft be towed to effectively lure the missile from the ship? The technique can be used both in main lobe and side lobe jamming depending on the length of the tow line. Another serious problem arises when the missile is approaching within 45 degrees of the bow or stern. According to the maneuvering data discussed earlier, there is not enough time to turn the ship sufficiently to present the craft mounted jammer to the missile. This situation is natural counter countermeasure that the launching platform can use against the target.

In the selfscreening jamming case, the jammer is located on the target, that is, on the ship itself. One approach is to mount the jammer in a location that is prepared for the impact. For example, one tank section in the front part of the ship can be kept empty with the jammer mounted on the deck above it. The intent is to attract the missile so it will do the least amount of damage. However, the bow/stern missile approach still remains. But, since the aft section is considered to be the most important part of the ship, missile impact here must be avoided.

Ship maneuvering might have an effect in the selfscreening case. It is probably sufficient to turn the ship 45 degrees either way to get enough bearing resolution for the missile to distinguish the jamming section of the ship. To turn the ship 45 degrees takes approximately one minute. In this time the missile has flown 18 km. So, given enough warning, say when the missile is still between 20 to 25 km from the ship, a ship maneuver could solve this problem.

Given the advantages and disadvantages of noise jamming discussed above, for a ship with lots of space and no power restrictions, the choice of which system design to choose is more a matter of cost. Whether a simple radar warning receiver (RWR) together with a barrage noise jammer or a more complex and sophisticated ESM receiver together with a spot noise jammer is chosen depends on one's assessment of "cost benefit."

Noise jamming together with a ship maneuver can be an effective way of solving the main objective.

If the missile seeker is not equipped with HOJ capability, the missile will get no target information and will, with very high probability miss the target. Further, if HOJ capability exists, the missile is deliberately guided by the jammer to a expendable dummy target or to a "prepared" section of the ship.

2. Radar Absorbing Materials (RAM)

Different methods have been investigated in the effort to decrease the RCS area for ships, airplanes, missiles, etc.

The most important and least expensive method is to initially construct the ship for a low RCS area. Large metal surfaces with interior orthogonal corners (corner reflectors effect) must be avoided. Large RCS areas can also be obtained from openings such as ducts that create resonance

effects. Convex spherical and cylindrical shaping of major surfaces is desirable. The idea is to make the ship into a scatterer and not a reflector, i.e., produce divergent reflections for impinging EM waves.

These construction guidelines can be useful in new ship construction if they don't increase costs to a point greater than the benefit to be achieved.

Another method used to decrease the RCS area is to cover the metal surfaces with RAM. This material can be used for an absorbing or an interfering technique. This could be used, for example, on surfaces or structures which are retroreflective. [Ref. 21]

The absorbing coating can be based on rubber, plastic or ceramic compounds and mixed with absorbing material such as ferrite or graphite (Figure 18). In the coating, the incoming electromagnetic radiation energy is transformed into heat. A one cm thick layer decreases the RCS area to 1% from the K band to the L band.

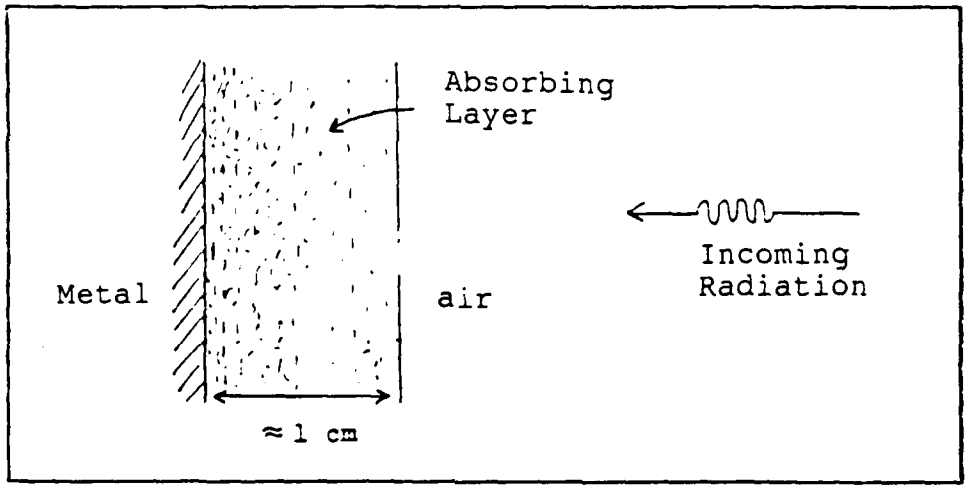

Figure 18. Example RAM (absorption)

The method is expensive and the ship will gain a considerable weight if all surfaces are coated. There is a problem with the strength and durability of these coatings. [Ref. 6]

The reflecting damping material can also be of an interfering type. The metal surfaces are painted with a semi-transparent 1/4 wavelength layer, reflecting half and transmitting half of the energy. The reflected energy is 1/2 wavelength out of phase with the transmitted energy causing destructive interference shown in Figure 19 [Ref. 6]. The layer can be designed for any frequency from 400 MHz to 40 GHz and the absorption is around 99%. However, the bandwidth is narrow and the effect depends on the angle of incidence. The material is also affected by the sea environment so that its lifetime is limited. Like the previous method, this is an expensive technique if a whole ship is to be coated. In addition, the surface of the ship has to be specially prepared to accept the coating.

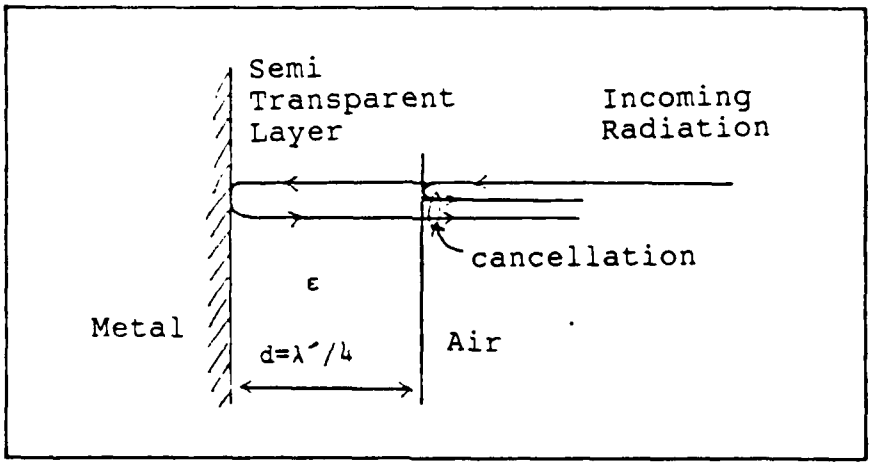

Figure 19. Example RAM (interfering)

B. DECEPTION ECM

1. Repeater jamming

a. Description

Repeater jamming takes a received radar signal, amplifies it, delays it, amplifies it again and finally retransmits it. The enhanced echo or "cover" signal received by the victim radar represents a credible target. The repeater jammer can be approximately the size of a sonobuoy (5 inches in diameter, 30 inches long) while the false target presented can be the size of a ship (the size of the target depends on how far the jammer is from the victim radar). A block diagram of the technique is shown in Figure 20 [Ref. 6].

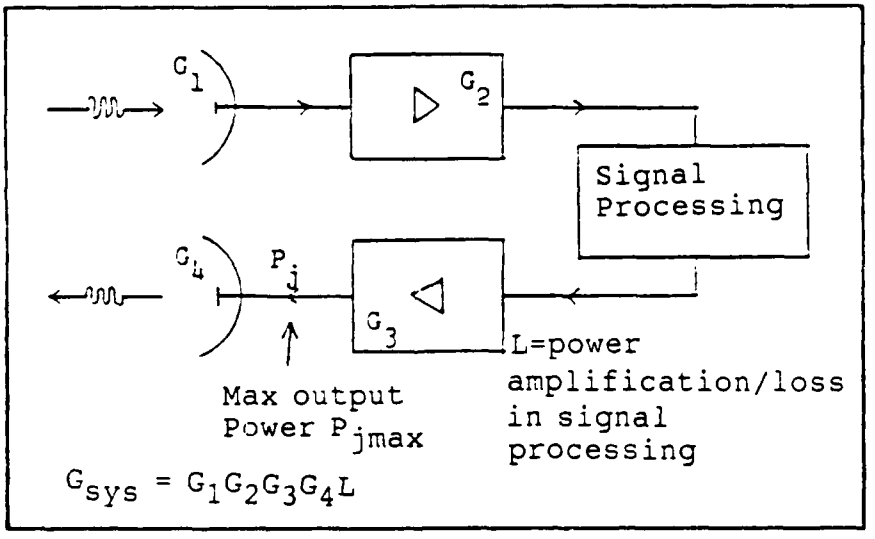

Figure 20. Example repeater jammer

The advantages with deception jamming are:

* no signal analysis required
* the jamming procedure can be done automatically
* simple operation (jamming signal is the amplified received signal)
* the equipment can be made small and light

The disadvantages are:

* easy to saturate by other transmitters
* hard to get sufficient isolation between the transmitting antenna and the receiving antenna.
* unable to reproduce complex wave forms (chirp, monopulse, e.g.), except when the repeater is incapable of range deception.

The repeater jammer is more complex [Ref. 18] than the noise jammer and needs a greater amount of processing power for its implementation.

The three repeater jamming techniques are:

* velocity gate pull off (VGPO)
* angle gate pull off (AGPO)
* range gate pull off (RGPO)

The range gate pull off (RGPO) is the most useful technique in this case. VGPO is mainly useful against radars using doppler or CW techniques. AGPO techniques can only be applied when angle gates are being used in the missile seeker.

The RGPO technique is effective against pulse radar and the goal is to create a false echo that arrives at the seeker a little later than the real target echo. The distance between the missile and the target is then changed to a false value.

The RGPO technique initially repeats the received echo with a minimum delay time. The amplitude of the repeated echo is increased slowly but still with minimum time delay. This causes the radar automatic gain control (AGC) to adjust to the stronger echo by reducing the gain. The real echo amplitude is reduced, causing the seeker to capture the strong repeated echo instead.

Now, the jammer begins to increase the amount of time delay in the repeated signal and the range gate circuitry gradually "walks off" the real target echo. When

the jamming signal stops, the tracker has no "skin" data in its range gate and must do a reacquisition cycle.

Since deception is only in range and not in angle, target reacquisition may be very rapid, in a matter of milliseconds since the angle information may still be available.

The best result is achieved with a combination of the repeater techniques above causing the reacquisition cycle to be accomplished in seconds, but combining the techniques is very hard to achieve.

A special case of repeater jamming (blip enhancer or repeater) is when the signal is intercepted and amplified as above but is not delayed. This will create a return echo similar to the target echo and hence, can be used as a decoy.

b. Analysis

An estimate of the feasibility of using repeater jamming includes calculations of the system gain and power requirements. The assumptions and notations made in Table 4 and Figure 16 are used.

The jammer in this chapter is assumed to be on the target, i.e., the ship. The jammer retransmitted power is (Figure 16, p. 40):

$$P_j = \frac{P_t \cdot G_t}{4\pi \cdot R_t^2} \cdot \frac{G_1 \cdot \lambda^2}{4\pi} \cdot G_2 \cdot L \cdot G_3$$

It will be assumed that $P_j < P_j$ max, where P_j max is the maximum power achievable before the amplifier gets saturated. The missile seeker then receives the following power from the jammer:

$$J = \frac{P_j \cdot G_4}{4\pi \cdot R_t^2} \cdot \frac{G_t \cdot \lambda^2}{4\pi}$$

The seeker receives the following power from the RCS area of the target:

$$S = \frac{P_t \cdot G_t}{4\pi \cdot R_t^2} \cdot \frac{\sigma}{4\pi \cdot R_t^2} \cdot \frac{G_t \cdot \lambda^2}{4\pi}$$

The J/S ratio after the antenna of the missile seeker becomes:

$$(J/S) = \frac{4\pi \cdot P_j \cdot G_4 \cdot R_t^2}{P_t \cdot \sigma \cdot G_t}$$

The condition for the jamming to succeed is:

$J/S > (J/S)_{min}$

where $(J/S)_{min}$ is the smallest jamming signal ratio necessary to deceive the missile tracker. $(J/S)_{min}$ depends on what kind of jamming is utilized and what kind of receiver it shall be used against. The $(J/S)_{min}$ is a very difficult parameter to estimate.

The following two equalities must be fulfilled for successful jamming (where G_s = system gain):

$$G_s \geq \frac{4\pi \cdot \sigma \cdot (J/S)min}{\lambda^2} \; ; \; P_{jmax} \geq \frac{P_t \cdot G_t \cdot \sigma \cdot (J/S)min}{4\pi \cdot R_t^2 \cdot G_4}$$

If the distance between the jammer and the missile becomes smaller, the missile radar looks through the jamming independently of increasing G_t.

For calculations assume the following additional values:

(J/S)min = 10 dB

G_4 = 10 dB

λ = 0.03 m

Calculation yields:

$G_s \geq 100$ dB

P_{jmax} (at R_t = 670 m) $\geq$ 265 KW

The values above indicate that deception jamming is a possible technique to use.

c. Discussion

As mentioned earlier, the most effective deception jamming method is RGPO, due to the generic missile description chosen for analysis. Since only range deception can be applied, the effectiveness of the technique is doubtful when used alone. The reacquisition process becomes very short and the radar will quickly "lock on" to the target again after being pulled off.

Another consideration is that the target in this scenario presents a very high freeboard, especially when unloaded. Since the missile is programmed to fly continuously at a very low altitude, if the missile does not do a "pop up" during its final approach, the range gate pull off has no direct effect since the boresight is still aimed at the target.

2. Chaff

a. Description

Chaff is a passive radar countermeasure. The "jamming" effect that chaff makes in the radar receiver is caused by the reflected energy of the active radar transmitter itself. Chaff is still the most widely used countermeasure and was first introduced in World War Two.

The material used for chaff today consists of aluminized glass fibers with a diameter of approximately 0.1 mm. They are easy to disperse, the fall rate is low (0.6 m/s) and the blooming time is fast (in the order of 3-6 sec). [Ref.16]

There are three methods in using chaff to protect ships against sea skimming missiles. They are:

* the deception method
* the lock-on or dilution method
* the break-lock method

The deception method involves trying to confuse the search and target acquisition radar by increasing the number of credible targets in the vicinity of the target. This method can lead to an initial tactical advantage, but the "real" target will sooner or later be discriminated from the chaff clouds. This is not a recommended method to use since the personnel aboard are limited in their ability to handle the interception and classification of search and acquisition radars. Also, the great target size together with long transiting time and large number of acquisition radars in the environment makes the method very costly and impractical to use.

The lock-on or dilution method uses a number of chaff clouds deployed in a specific pattern around the target in order to distract the missile seeker ideally causing it to lock on the chaff cloud (false target) instead of the real target. This method is appropriate in the

missile seeker's search mode. The search mode in this case though, is assumed to be very short. Together with the great target size and the same practical problems encountered with the deception method above, the lock-on method is a poor choice as well.

In the break-lock method, the missile has already locked on to the target and the goal is to seduce the seeker to lock on to a large chaff cloud deployed within the seeker's field of view. Once the seeker has locked on to the chaff cloud, the ship can maneuver out from the cloud (if the warning time is enough) or use the cloud as an extension of the ship in order to ensure a "close" miss by the missile.[Ref. 16]

Because the break-lock method is the only viable choice, it will be further investigated. It is shown in Figure 21. [Ref. 16]

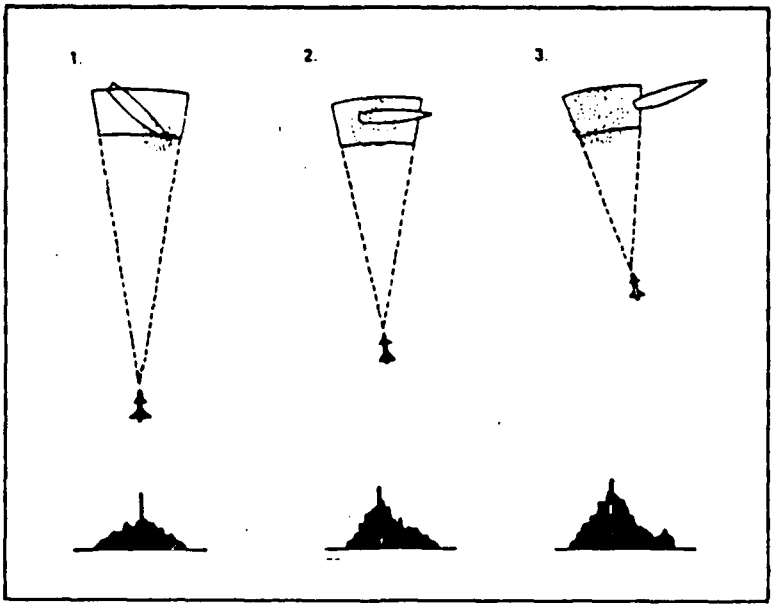

Figure 21. The break-lock method

b. Analysis

The length of the chaff depends on what frequency band they are supposed to be used against. The largest RCS area is achieved if the chaff length is around half the wavelength ($0.45 - 0.48\lambda$). Their resonance bandwidth is approximately ±10% of the resonance frequency. The RCS area is also dependent on the incident angle of the electromagnetic radiation. Since the chaff is randomly oriented when deployed, an average value for the RCS of each chaff fiber is [Ref. 6]:

$$\sigma_1 = k * \lambda^2$$

where k depends on the tendency of the chaff to stick together when released. The k factor is usually between 0.1 to 0.3, and is in this case estimated to 0.15.

The number of chaff fibers necessary to achieve a particular RCS area is:

$$n = \sigma / (k * \lambda^2)$$

Assume that a chaff cloud of 100,000 m^2 is necessary to get the seeker operating with centroid tracking to barely miss the target. This means that the large number of 741 million chaff dipoles must be deployed. This can be achieved by, for example, chaff grenades dispersed in a specific pattern. The blooming time can be made very short and a reasonable value is around 4 seconds.

This means that a sufficient chaff cloud both in geometric size and RCS area, can be deployed well in advance of the missile to adjust its centroid tracking point to a position just outside the boundary of the real target. Consequently, the break-lock method is possible to use.

c. Discussion

The special case of the lock-on method described above is a fast, reliable and fairly inexpensive method to use.

The problem with chaff, though, is that the wind

direction and velocity have an impact on the effectiveness of the chaff cloud. To counter this, two systems can be deployed: one in the fore and one in the aft of the ship. It also accounts for the possibility that the chaff cloud moves in over the target due to the wind. The chaff can be dispersed by grenades, for example, or some other launching arrangement. The chaff can be dispersed, taking wind direction and missile bearing., etc., into consideration. One chaff grenade might contain chaff for a 100 m^2 RCS (Philax system). This means that 1,000 such grenades must be launched from the fore or aft each time there is an indication of a missile tracking radar. This is practically impossible to pursue since it will be very expensive in both launchers and projectiles and there will be a serious problem of reload. Shipborne launchers capable of producing 20,000 m^2 clouds per shot exist (NATO SEA GNAT) and represent an alternative approach.

A considerably smaller RCS area could be acceptable if one considers the same option as in the jammer case, where an impact in an insensitive part of the ship is acceptable. The fact that the missile seeker prefers a "hot spot" to home on implies that the chaff cloud still must be significant.

In an effort to reduce the chaff cloud, a combination ECM technique with RGPO, chaff and ship maneuver can be considered. This technique, however, is based on ships with relatively high maneuverability and is therefore not viable in this case.

C. DECOYS

Decoys are mostly thought of as a special kind of expendable countermeasure used to create false target echoes or to enhance the signature of a low value target. Decoys can be deployed by remotely piloted vehicles or simply launched from the ship. [Ref. 22]

Decoys can be equipped with jamming and/or deception ECM features. A selection of the most interesting techniques, as they apply to this thesis, will be investigated below.

1. Towed craft

This kind of decoy has been mentioned earlier in the chapter but will now be further investigated. One way of getting the missile to home on the craft instead of the real target is by getting the craft to look like the real target to the missile radar. That is, to increase the RCS area as much as possible.

It has been reported [Ref. 22] in the press that towed barges with corner reflectors have already been used in, for example, the Persian Gulf War. The purpose was the same then as it is now: to get the attacking missile's centroid tracker to "slide off" the real target.

The maximum RCS obtained from a corner reflector (Figure 22) on the symmetry axis is given by the following formula [Ref. 22]:

$$\sigma_{\Delta\,max} = \frac{4\pi a^4}{3\lambda^2}$$

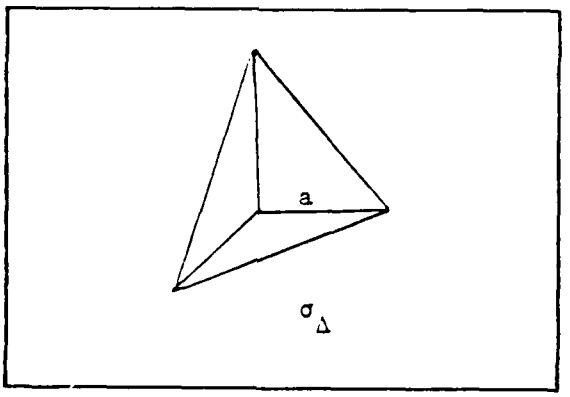

Figure 22. Corner reflector

A corner reflector with a side (a) equal to 2.1m gives an RCS of around 90,000 m^2 (around its symmetry axis). Consequently, a number of corner reflectors would easily achieve a sufficient RCS area to exceed the real target RCS. There seem to be both practical and electronic problems with this approach. Although there are no directly accessible reports available, some problems can be assumed based on shiphandling experience. For example, the huge corner reflectors mounted on the barge deck act like sails, making the barge very wind sensitive and unstable. Even with different kinds of anchors to keep the barge in position, there will still be many problems. This has the consequence that the ship has very little influence on where the barge is positioned when the missile is attacking. This is not satisfactory for the ship commander.

Instead of a corner reflector, one can use Luneberg lenses. The formula for RCS is given by the formula [Ref. 6]:

$$\sigma_{max} = \frac{\pi}{4} \cdot \left(\frac{d}{\lambda}\right)^4 \cdot 2^3$$

where d is the diameter of the lens.

To get the same RCS area as above, a Luneberg lens of 1.8 m in diameter is required. This will take care of some of the "sail" effect discussed above, but there is another problem with Luneberg lenses. They must be kept quite clean from salt and other particles if their high performance is to be maintained. They are also much more costly.

Another alternative is to put a deception jammer or a repeater jammer on the barge instead. This has been discussed previously and gives both a sufficient simulated RCS area and is also a more practical solution due to the

environment. Probably the best solution is a combination of corner reflectors and some kind of jammer, but then the problem with the large reflectors remains.

The advantages with utilizing a towed craft are:

* No power limitations if supplied from the ship.
* The craft is easy to launch when transiting a war zone.
* The distance between the craft and the towing ship is easy to adjust to get maximum "slide off" effect by the missile tracker. This must be considered together with shiphandling matters like the tow line, weight, etc.
* The raft is operational until it is hit.
* The corner reflectors can be replaced with smaller Luneberg lenses.
* The detection distance of the missile can be very short because of the fact that the decoy is already in position and it is just a matter of directing the jamming device (if not omni-directional) and turn it on.
* Inexpensive technique, since the craft is not wasted until the missile hits the craft (missile centroiding extends the craft's lifetime).

The disadvantages are:

* The craft can be very wind and sea state dependent, especially if huge corner reflectors are being used.
* Problem with maintaining high performance with Luneberg lenses close to the water surface.
* There might be a problem if the missile is approaching within 45° of the bow of the ship and there is not enough time to maneuver.
* If there is an option (not possible in the reference missile) for the missile launching platform to choose between centroid tracking or left/right edge tracking, once the ECM technique with craft is known, it is easy to change the tracking mode as a counter countermeasure.
* The missile launching tactics can easily be adapted to the new situation by changing the launch direction.

2. Buoys

Expendable buoys equipped with a repeater jammer are currently under development by contractors in the United States. These consist of a floating device with a jammer

mounted on top. A number of buoys are launched when a threat appears and they immediately start to enhance and repeat incoming signals while in the water. When the batteries are discharged, they self scuttle and sink to the bottom.

Since the buoy is very small compared to the craft discussed above, sea state is an additional environmental factor to consider. For example, there can be a signal direction problem due to high wave crests.

The advantages of buoys are:

* Buoys can be easily and quickly launched from the ship.
* Individual buoys are inexpensive, but if the threat duration is long, the costs can be high.
* A number of buoys can be used to simulate false echoes in the missile search mode.

The disadvantages with buoys are:

* The missile intercept and warning must be long enough to give the target enough time to launch and activate the buoys.
* As mentioned above, it might be an expensive solution.
* Tactical placement relative to threat and target is important.

3. Rocket decoy

A rocket decoy comprises a rocket with a repeater jammer. The rocket is launched from the ship in a relatively high elevation angle. When the highest altitude is reached, a parachute is unfolded and while the rocket is slowly descending toward the ocean surface, the repeater jammer is active and hence, acts as a false-target decoy. Figure 23 shows the "Siren" rocket decoy developed by Marconi Defence System in the United Kingdom [Ref. 23].

The rocket decoy alternative is very similar to the previously discussed buoy alternative. The major difference is that the rocket decoy is very wind sensitive and that the operating time is limited to the time duration of descent. The wind factor is particularly significant in this case

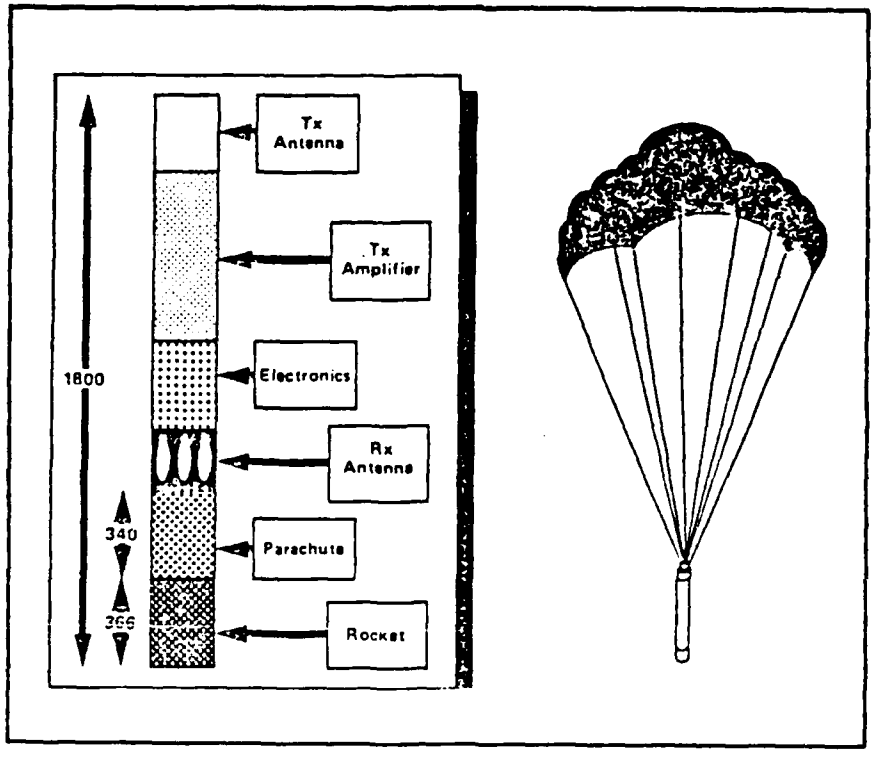

Figure 23. The "Siren" rocket decoy

since the wind speed and direction varies with altitude. The decoy behavior after being launched is therefore very unpredictable.

4. Remotely piloted vehicles (RPV)

A small radio controlled drone can be used as an RPV. It can be launched from the ship deck and after the mission is completed, land in the ocean to be recovered by the crew. After recovery, it can be cleaned up and prepared for the next mission. With a number of drones aboard at least one can be in the air continuously while the ship is transiting a hostile area.

A drone can measure around 3-4 m in length and be propelled by a jet engine or an ordinary propeller engine. Each drone can carry a ECM payload of say 15 kg.

The RCS area of the drone itself is very small, from 0.01 m seen from the nose and the tail, to 10 m from each broadside. [Ref. 23]

The uses of drones are as follows:

* Carry radar beacons (expendable or mounted on the drone) to deceive the missile radar in search mode.
* Disperse chaff for deception, lock-on or break-lock purposes. This is not a viable alternative in this case, though, since the payload must be very big to simulate 100,000 sm RCS area.
* Carry jammer (noise) in applications discussed earlier in this chapter.

The advantages are:

* The drone can be operating far from the ship and can be moved quickly to an optimum location.
* Different kinds of ECM can be loaded into the drone, depending on the situation.

The disadvantages are:

* The payload (15 kg) is very small.
* A special organization is needed aboard the ship to take care of the drone.
* Special guiding equipment is needed.
* It is a very expensive system.

D. TACTICS ECM

Tactics ECM is a matter of what the ship commander can do with the ship in an effort to deceive the missile and/or combine ship tactics with other ECM.

The most viable tactic in this case is to use ship maneuvers in combination with another ECM. This has been discussed in the chapter above.

One way to "hide" the ship using only ship tactics is to operate the ship so closely to the coast that the coast line and the ship itself is within the seeker's resolution cell. However, this tactic is terrain and navigation dependent.

One obvious consideration for the ship commander is, of course, to choose the less hostile transiting path through the war zone. This includes collecting information about hostile forces and missile batteries ashore, etc.

E. ECM CONCLUSIONS

All of the ECM support techniques described above are more or less possible to pursue. This section of the chapter will decide which technique or combination of techniques is the most viable against the reference missile. To do this, the expected performance criteria will be defined and then compared to the available techniques. The technique(s) selected will provide a new set of options to be evaluated in a similar manner. The evaluation will be done in four levels:

* Very high
* High
* Medium
* Low

Comments will be made for each choice of level.

The evaluation is the author's own judgement and is based on theoretical guidelines and naval experience since no performance data is readily available.

The following is a list of performance criteria given in priority order:

Operational effectiveness. This will answer the overall question: "Over a given period of time, how well does the alternative achieve the objective of protecting the ship from a missile attack?" [Ref. 24] The period of time is in this case the time the ship is spending in the "war zone."

Risk. This is the risk that vital parts of the ship, including the crew, will be influenced by the missile impact.

Life-cycle cost. This will include:

* research and development cost
* production and construction cost
* operation and support cost (like personnel and ESM support)

Reliability. The reliability can be defined as the probability that the alternative will perform when needed. "When" is, again, during the war zone transit. Other considerations include:

* geographic location of the war zone
* day and/or night capability
* weather and sea conditions

Supportability. The supportability includes the following issues:

* number of personnel needed to maintain a developed system
* education level of the operating personnel
* training of personnel
* human factors

Transportability. The transportability will include issues like:

* size and weight
* ease of installation and removal

The main ECM alternatives discussed in the chapter are listed below. The alternatives are not entirely comparable but this approach will simplify the decision process. Combining techniques will be discussed when appropriate.

A. Selfscreen noise jamming (from the ship itself)
B. Deception jamming, RGPO from the ship
C. Chaff in a lock-on method
D. Decoys (includes using part of the ship as a decoy)
E. Radar Absorbing Materials (RAM)

Alternative A will be excluded from the decision process since this is not a viable alternative due to the reference missile being equipped with HOJ capability.

Details are shown in Tables 7, 8, 9, 10.

TABLE 7. EVALUATION OF SELFSCREENING REPEATER JAMMING

Criteria	Evaluation level	Comments	
Operational effectiveness	Medium	Positive: *	The same jammer can be used all the time through the war zone
		*	Effective against radars with no human operator involved
		*	Manage to deceive more than one incoming missile
		Negative: *	With only RGPO the reacquisition time can be very short
		*	The jammer can be saturated by other transmitters
		*	Doubtful technique since the boresight is aimed at the target
Risk	High	Negative: *	The jammer is located aboard the ship
Life-cycle cost	Low	Positive: *	State of the art technique
		*	Inexpensive system to operate and support
Reliability	High	Positive: *	The technique has been tested and operable for many years
Supportability	High	Positive: *	The system can be operated autonomously
Transportability	High	Positive: *	Low size and weight

TABLE 8. EVALUATION OF CHAFF IN LOCK-ON METHOD

Criteria	Evaluation level	Comments	
Operational effectiveness	Medium	Positive: *	Chaff can be made for broad bandwidth
		*	Manage to deceive more than one incoming missile
		*	Easy to combine with other ECM technique
		*	Very good historical experience with chaff
		Negative: *	Practical problems to achieve sufficient RCS area for the reference target
		*	Problems to reload and aid launchers
		*	Needs relatively long warning time
Risk	Medium	Negative: *	Chaff cloud is dispersed close to the ship itself
Life-cycle cost	Medium	Positive: *	State of the art technique
		*	Chaff grenades themselves relatively inexpensive
		Negative: *	Launching technique can be expensive
		*	The chaff technique will be expensive if many "false alarms" and long transition distance for the ship
Reliability	Medium	Positive: *	Well established technique
		Negative: *	Chaff fibers can bundle together
		*	Chaff is sensitive to wind in combination with the ship heading
Supportability	Medium	Negative: *	Need a special organization aboard for reloading the launchers, etc.
Transportability	Low	Negative: *	The amount of chaff grenades that are needed together with launching equipment that must be mounted and aligned in different pattern, etc., makes the transportability low.

TABLE 9. EVALUATION OF DECOYS

Criteria	Evaluation level	Comments:
Operational effectiveness	Medium	Positive: * Can in some cases use combined ECM techniques Negative: * Usually power limitations * Usually warning time necessary
Risk	Low	Positive: * Usually decoy deployed far from vital parts of the ship
Life-cycle cost	Medium to high	Evaluation depends on the technique chosen
Reliability	Medium	Negative: * Decoys can be (very) sensitive to weather and sea condition
Supportability	Medium	Evaluation depends on the technique chosen
Transportability	Medium	Evaluation depends on the technique chosen

TABLE 10. EVALUATION OF RADAR ABSORBING MATERIAL

Criteria	Evaluation level	Comments
Operational effectiveness	Medium	Positive: * No warning time necessary Negative: * Limited bandwidth
Risk	Medium	Negative: * Even if the absorbing efficiency is high, the large ship size can, despite this, give a significant RCS area
Life-cycle cost	High	
Reliability	High	
Supportability	N/A	
Transportability	N/A	

Alternative D is also divided into different kinds of decoys. They are:

A. jammer aboard spec prepared ship section (JS)
B. towed craft
C. buoy
D. rocket
E. rpv (drone)

The decision process continues further (Tables 11, 12, 13, 14, 15) with the same criteria definitions areas previously outlined.

TABLE 11. EVALUATION OF JAMMER

Criteria	Evaluation level	Comments	
Operational effectiveness	High	Positive: *	Easy for the seeker to change to new "hot spot" on the ship
		*	No power limitations
Risk	High	Negative: *	The missile is deliberately guided to the ship (close to the crew and other vital parts)
Life-cycle cost	Low		
Reliability	High		
Supportability	High	Positive: *	The system can be made autonomous
Transportability	High	Negative: *	Needs certain preparations aboard

TABLE 12. EVALUATION OF TOWED CRAFT

Criteria	Evaluation level	Comments
Operational effectiveness	High	Positive: * No warning time necessary * Easy to use combined ECM support * No power limitations * Craft is operable until destroyed by missile impact Negative: * Easy to make tactical adaption by the hostile force
Risk	Low	Decoy is separated from ship
Life-cycle cost	Low	
Reliability	Low	
Supportability	Medium	Negative: * Weather and sea sensitive * Maneuverability problem
Transportability	High	Need personnel for launching, etc.

TABLE 13. EVALUATION OF BUOY

Criteria	Evaluation level	Comments
Operational effectiveness	Medium	Positive: * Easy to use tactically Negative: * Too small for combined ECM * Power limited * Warning time necessary
Risk	Low to Medium	Dependent on warning time
Life-cycle cost	Medium	Buoys expandable
Reliability	Medium	Can be sea-state sensitive
Supportability	High	Can be made autonomous
Transportability	High	

TABLE 14. EVALUATION OF ROCKET

Criteria	Evaluation Level	Comments
Operational effectiveness	Medium	Positive: * Easy to use tactically Negative: * Too small for combined ECM * Power limited * Warning time necessary * Radar coverage problem
Risk	Low to medium	Dependent on warning time
Life-cycle cost	Medium	Decoy expendable
Reliability	Medium	Wind sensitive
Supportability	High	Can be made autonomous
Transportability	High	

TABLE 15. EVALUATION OF REMOTE PILOTED VEHICLE

Criteria	Evaluation Level	Comments
Operational effectiveness	Medium	Negative: * Needs warning time * Limited pay-load and power
Risk	Low to Medium	
Life-cycle cost	Very High	RPV is a sophisticated decoy
Reliability	Medium	Weather dependent
Supportability	Low	Needs specially-trained personnel for both launching, maintenance and operation
Transportability	Medium	

The towed craft and the buoy alternatives are the two most interesting of the options. The buoy and the rocket alternative are very similar to each other, but the buoy alternative is preferable in this application (due to the wind problem). The towed craft has both high efficiency and low risk. The problem is that it is not a very practical alternative since it must be towed behind a ship. This also allows the enemy to easily adapt to the countermeasure. The buoy alternative is comparable to the towed craft but has poorer performance since its power is limited. It is also dependent on a defined reaction time, since the bucys need to have been just launched from the ship. This problem can be alleviated with a proper warning and launching equipment. Both alternatives are currently being developed by companies around the world. [Ref. 23]

The buoy alternative is chosen, mainly because it is more practical and flexible for a merchant ship's particular needs.

The decoy buoy can be equipped with one of the following:

* noise jammer
* repeater (beacon)

The requirements for the jammer are:

* small size
* high power
* omni-directional
* inexpensive

The repeater best meets the requirements above. The noise jammer needs very high power to be efficient in an omni-directional jammer technique.

The conclusion is that expendable buoys with a repeater jammer technique is the ECM choice for the reference ship.

The buoys should be launched autonomously in predetermined directions. The warning must be early enough to give the activated buoys time to be effective against the missile.

V. ECM RECOMMENDATIONS

Given the discussion above, the most appropriate ECM support for the reference tanker is the expendable, omni-directional, repeater jammer buoy.

This chapter will expand the buoy alternative further and discuss the kind of support requirements needed. The chapter will not include buoy patterns and other tactical considerations.

The general requirements for an operable buoy ECM system are as follows:

* the system must be easily installed and removed
* the system must be nearly autonomous, or if not, very user friendly
* the buoys must be launched to at least a few hundred meters from the ship in any direction.
* the buoys must be activated within 30 sec (10 km) from the first detection of the missile and stay active for at least two minutes.

The following topics will be covered in the chapter:

* repeater jammer operational characteristics
* general buoy description
* ESM support

A. REPEATER JAMMER

The objective of the repeater jammer is to create a credible false target close to the ship in order to deceive the missile seeker. Given the specifications discussed earlier, a repeater jammer can be made small (dimensions) and light (weight) as mentioned in Chapter 3.

To create a credible false target, the jammer must repeat an incoming signal that corresponds to 100,000 sm RCS area. The following calculations will determine the necessary system gain and power requirements.

For unity J/S ratio, the required system gain is given by [Ref. 23]:

$$G = 1.4 * 10^4 * A\,(F)^2$$

where A is the target cross section in square meters and F is the operating frequency in Megahertz.

This gives for A = 100,000 sm and F = 10 GHz a required gain of approximately 90 dB.

For unity J/S ratio and an omni-directional jamming antenna the required "electronic" power output is given by [Ref. 23]:

$$P_j = \frac{P_t \cdot G_t \cdot \sigma}{4\pi \cdot R_j^2}$$

where P_t = output power in watts (radar)
G_t = antenna power gain (radar)

This gives (P_t = 30 KW, = 100,000 sm and G_t = 27 dB in the mainlobe) the ranges shown in Table 16.

This shows that the earlier the jammer buoys are launched and activated, the less power is required to simulate a false target with 100,000 sm RCS area. On the other hand, in order to deny the missile the ability to change target from the buoy to the ship during its approach, the jammer must keep the high RCS return to a very close distance, which implies the need for the very high output peak power requirements calculated above. This will also assure that the missile target seeker will initially "lock on" the buoy.

TABLE 16: RANGE AND POWER REQUIREMENTS FOR JAMMER BUOY

R=	P= (peak power)
300 m	1.3 MW
1 km	119 KW
5 km	4.8 KW
15 km	530 W
25 km	190 W
30 km	130 W

The power requirements are an important parameter in the design since the jammer must have power supplied by batteries. One way of decreasing the high output power requirements is to launch the buoys toward the approaching missile. However, if the buoys are launched too far from the ship, the missile can start a new reacquisition cycle after passing the buoys, and still hit the ship. Hence, the optimum buoy pattern must focus on first, trying to keep the ship in the missile seeker's sidelobes in order to decrease the power requirements and second, denying the missile a reacquisition target. A complement to lowering the power requirements is to decrease the RCS (skin return) of the ship. There are several approaches to accomplishing this, including metal nets and RAM.

The antenna is assumed to be omni-directional because of the buoy size and cost considerations. If only one antenna is being used (which is advisable on a small buoy) it has to work both as a receiving and a transmitting antenna. This implies time gating in the jammer design. Further, some kind of modulation of the output signal can also be introduced in the repeater in order to better simulate a "real" target (echo fluctuation, etc.).[Ref. 23]

One approach of designing a repeater jammer is shown in Figure 24.

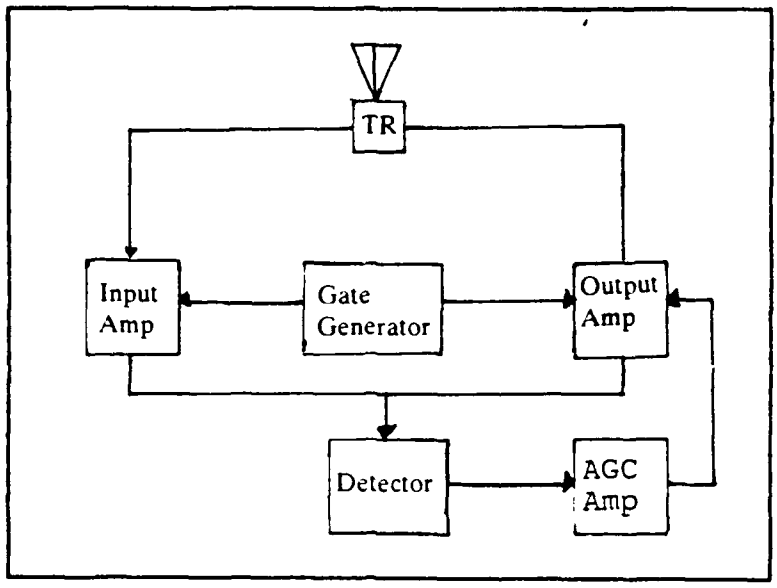

Figure 24. Example of a repeater jammer design

To get the high gain, several TWTs (Travelling Wave Tubes) cascaded together are required. The TWT bandwidth should be adjusted to the frequency band of interest in order to prevent saturation of the jammer.

The duty cycle of the missile seeker radar can be relatively low. This fact, together with a short operating time (2 minutes), makes the required energy storage quite reasonable. This implies that batteries (sea-water activated and/or lithium) are possible to use.

B. GENERAL BUOY DESCRIPTION

The purpose of this section is to give an example of how the general features of the buoy can be designed. In the introduction to Chapter 5 some of the operational buoy requirements are listed. To fulfill these requirements the buoy must be launched from the ship in some way. This implies that the size, shape and weight, etc., of the buoy must be designed accordingly. In Chapter 3 the repeater jammer is described as being the size of a sonobuoy (5

inches in diameter, 30 inches long). Why not use the well-developed and thoroughly-tested sonobuoy concept and adapt that idea here? This leads to the following general buoy philosophy:

The buoy(s) should be delivered folded aboard the ship in some kind of container, ready to be launched. The containers should be mounted on the ship deck in such a way as to cover a number of launching bearings from the ship.

When the buoy is launched from the ship and hits the water surface, it should unfold itself and begin jamming immediately. After the active phase (i.e., when the batteries are out of energy) the buoy should lose its buoyancy and sink to the sea bottom.

The deployed unfolded buoy is depicted in Figure 25. [Ref. 26]

Taking advantage of proven techniques keeps the life-cycle cost of the system down. Also, many other requirements, such as the supportability and transportability questions, etc., would already be satisfied.

There are two launching technique options: 1. using a rocket to deliver the buoy in position, or 2. using some kind of catapult. There are advantages and disadvantages with both of these techniques. The rocket can deliver the buoy faster and to a greater distance from the ship than the catapult. On the other hand, the catapult technique gives lower acceleration stress and is much safer to handle. Tactical considerations will determine the most applicable technique.

C. ESM SUPPORT

In order to launch the buoy in time to be effective, sufficient warning of an incoming missile is needed. This can be accomplished in from one to three ways: optically, radar or ESM. The ESM way is probably the most reliable

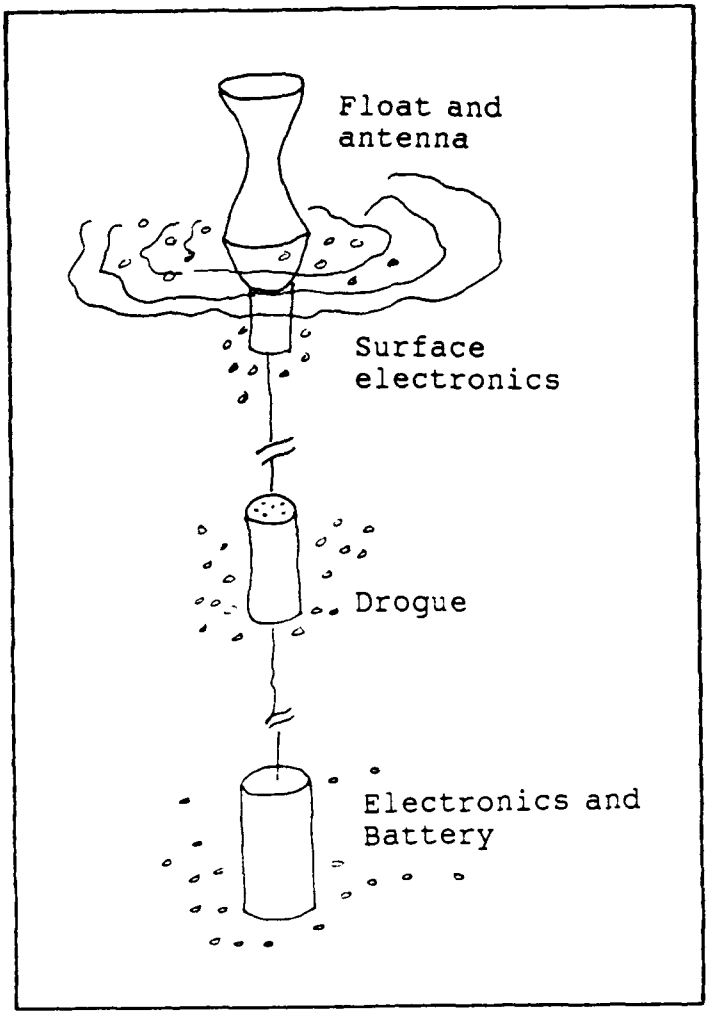

Figure 25. Example of an unfolded ECM buoy

method, considering the personnel constraints aboard a merchant ship. But given an ARM threat, it might be an advisable tactic to stop ship radar transmission.

The different kinds of signals associated with a missile launch are:

* prelaunch targeting radar
* signals for fuze ignition
* altimeter signals
* terminal phase guidance signals

To receive as much warning time as possible, the most viable alternative appears to be detecting the signals radiated from the missile in its terminal phase and signals from prelaunch targeting radar. The detection of the signals radiated from the missile in its terminal phase is estimated to be the most important and least ambiguous.

The following ESM issues will be treated:

* signal environment
* receiver
* signal processing
* user interface

The general requirements for the ESM system are:

* Real time operation. The threat missile must be intercepted, detected and classified as soon as it starts radiating.
* Omni-directional coverage. The assumption is that while there may be a preferred direction of attack, the system must be designed for attacks originating from any direction.
* Easy to operate. The system would be operated by non-military people who probably would not spend much resources on training to use the system. As such, the system must be easy to operate with minimal training.

  This translates into a requirement for a high degree of automation.
* Relatively inexpensive system.

The main objective for the receiver is to intercept and determine the lethality of incoming signals as quickly as possible.

Since the threat in this case is something quite specific, one design approach for making the system response faster would be to filter out unwanted signals as early as possible, in order to keep low the amount of data that needs to be processed.

The mode of operation would be to let the system receive signals from the environment and search for the specific missile threats that the operator deems to be significant for the particular war zone through which the ship is transiting. After having detected and classified the threat missile, it would alert the operator and pass threat information to some kind of ECM processor that computes launching data for the buoys and also issues maneuvering recommendations to the bridge operator to increase the probability of countering the threat successfully.

1. Signal environment

The assumption is that the emitters in the environment, in the frequency band of interest, are from civilian or military ships and coastal radars. A pulse density of about 90,000 pulses per second is estimated from assumptions about the maximum PRF arising from unambiguous range requirements. (See Appendix H)

The merchant ship itself will have its own transmitters that may, because of the short distances involved, get into the ESM system. These signals have to be screened out to prevent false alarms.

2. ESM receiver

The receiver in this ESM system must be some kind of Radar Warning Receiver (RWR). An RWR is characterized as a simple, rugged and relatively inexpensive receiver. A simple RWR system block diagram is shown in Figure 26 [Ref. 6].

There can be a number of integrated antennas and receivers to cover all azimuth angels and frequency bands.

The performance of an RWR is usually discussed in terms of sensitivity, dynamic range, probability of intercept (POI) and throughput rate.

Short definitions of the different terms are given below. [Ref. 27]

The sensitivity of a receiver is a function of the ratio of RF bandwidth and video bandwidth.

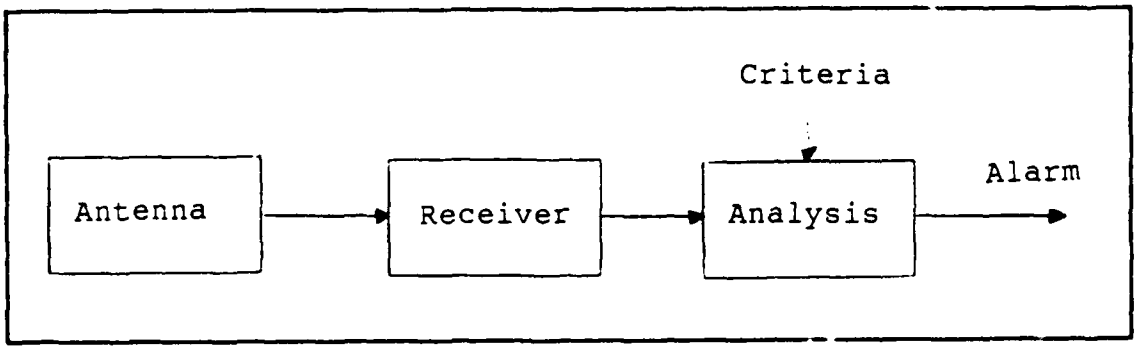

Figure 26. Simple RWR block diagram

The dynamic range is used to indicate the input signal amplitude range that the receiver can process properly. The lower limit of the dynamic range is the sensitivity of the receiver.

The POI is used to tell the percentage of pulses the receiver will collect in a certain signal environment.

The throughput rate is applicable when the signals are pulsed and tells the maximum pulse rate the receiver can process.

One important missile seeker parameter to be determined by the RWR is the antenna scan pattern. The fact that the missile seeker is scanning in a sector, which means that the dwell time on the target is relatively long, makes this parameter very significant.

Other significant parameters are Angle Of Arrival (AOA), Pulse Repetition Interval (PRI), Pulse Width (PW), Frequency and Signal Amplitude.

The following discussion about the required performance parameters for the receiver can be made:

* The receiver sensitivity need not be extremely high since the seeker radar is quite powerful and the distances considered are relatively short (5 - 30 km).

* The receiver must have wide dynamic range to be able to handle both strong and weak signals.
* The probability of intercept must be as high as possible.

The different kinds of RWR receivers (state of the art) that can be considered are:

* the crystal video receiver
* the instantaneous frequency receiver (IFM)
* the superheterodyne receiver
* the wideband YIG-tuned superheterodyne receiver

The most important features of the techniques are summarized below.

RWR often use a crystal video receiver, which means that the mixer, local oscillator (LO) and the IF amplifier are missing. A block diagram of the receiver is shown in Figure 27 [Ref. 18].

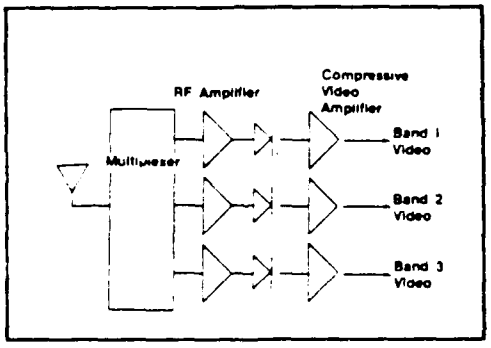

Figure 27. The crystal video receiver

The receiver is relatively simple, low in cost, lightweight and small in size. It is used for wideband detection (2 - 18 GHz) of low duty cycle signals but can also be modified for CW detection.

The disadvantage with the receiver is that it cannot closely determine the frequency of the incoming signal.

Another disadvantage is that the key threat signals can be masked by other signals and noise jamming.

The sensitivity of the receiver is relatively low, between -50 dBm and -60 dBm. It has a high probability of intercept and a large dynamic range.

The IFM receiver is essentially a crystal video receiver but is provided with a delay line which makes it possible to measure frequency. The RF bandwidth is wide, sometimes up to more than one octave. The weakest point in the IFM receiver is that it can be captured by a strong CW or jamming signal. There are ways of getting around this problem, [Ref. 27] by using a frequency rejection technique for the offending emitter. The POI can be made to approach 100%. The dynamic range and the sensitivity are moderately high.

Modern IFM receivers are mostly digitized (DIFM), which gives the ability to detect intrapulse frequency agile emitters. Some typical DIFM values for X-band interception are a sensitivity of -65 dBm and a dynamic range of 70 dB.

A typical block diagram of an IFM receiver is shown in Figure 28 [Ref. 18]. IFM/DIFM receivers are mostly used in SIGINT applications.

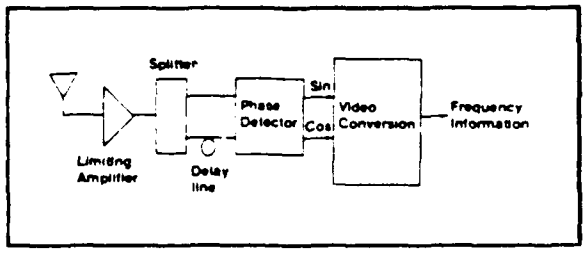

Figure 28. The IFM receiver

A superheterodyne receiver has a very high sensitivity, excellent selectivity and frequency resolution. Superheterodyne receivers use a mixer, LO and filter to get

an IF frequency which can then be processed further. To get the receiver to intercept more than one frequency signal, the receiver must scan a frequency band. The YIG technique is used most frequently, but it gives a relatively narrow bandwidth. A scanning receiver gives a poor POI and also has a problem intercepting emitters with scanning antennas. The superheterodyne receiver is used primarily in SIGINT or to complement another faster receiver, in order to get the fine grain information.

A block diagram is shown in Figure 29 [Ref. 18]:

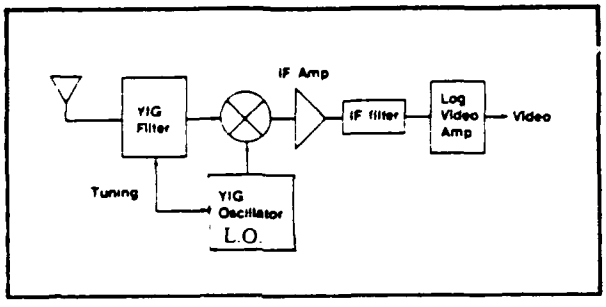

Figure 29. A superheterodyne receiver

A special case of the YIG tuned narrowband superheterodyne receiver is the "wideband superheterodyne receiver." This gives very good detection of wideband radars such as frequency agile and pulse compression radars. It can also be designed with switchable filters that can be tuned to frequency bands of interest. As a result the scanning procedure can now be made very fast (in the order of microseconds).

A block diagram of the wideband superheterodyne receiver is shown in Figure 30 [Ref. 18]:

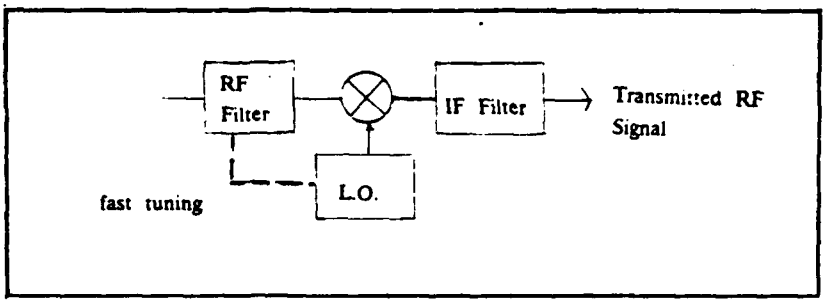

Figure 30. The wideband superheterodyne receiver

As indicated above, the most common receiver in RWR applications is the Crystal Video Receiver. However, it must be complemented with another receiver (i.e., a superheterodyne receiver) to measure frequency, and this takes time. Further, the wide bandwidth capacity is not a requirement for the receiver in this application. It is, rather, a disadvantage since only very specific signals in a limited frequency band need to be detected.

Another alternative might be to consider a wideband superheterodyne receiver. The receiver would be stepped to a particular frequency band of interest where it then sweeps through this band continuously. It would consequently spend less time scanning, resulting in a higher POI.

In this way unwanted frequencies will be filtered out, since they are outside the band of immediate interest, and the downstream processing need not cope with these signals, which will speed up the processing rate. The penalty of using some kind of scanning receiver is always that the POI goes down, even though the frequency band is limited and the scanning rate very high.

To fulfill the requirements of AOA, a number of matched receivers can be arranged in a certain configuration (i.e., four receivers, one in each quadrant). The intercepted signal's amplitude and/or phase is then compared between the receivers.

3. Signal processing

In order to get high throughput rate, further filtering can be applied before the actual pulse parameter measurements in the preprocessor. The main processor could be in parallel with auxiliary processors. To process the signals in real time, window addressable memory (WAM) can be used to assist in the pulse deinterleaving and pulse train matching. The display console should also be "smart" in order to offload the main processor. E.g, keyboard scanning and interpretation should be done by the display console itself.

4. User interface

In order to be an autonomous system the user interface must be provided with an automatic mode. When the processor finds a lethal match, i.e., an incoming missile, launch data should go directly to the buoy system and to the maneuvering display, via some kind of "ECM processor." The ECM processor should calculate the necessary launching and maneuvering data, due to the ship's RCS variations, maneuvering data and wind conditions, etc.

Even though the system can be put in an automatic mode, an operator must be able to manually operate the system and provide it with necessary initial values. The user interface can consist of a pictorial display, a numeric keypad and some hard and soft keys. The soft function keys can have descriptions written on the display and a menu selection method can be used for prompting and obtaining operator commands. The pictorial display must show the threats (with azimuth and estimated range) and the maneuvering recommendation.

VI. ACOUSTIC ENVIRONMENT STUDY

A. INTRODUCTION

This chapter will give a general description of the Baltic Ocean characteristics and will provide specific detail of the water volume of interest in the sonar design.

B. THE BALTIC OCEAN

The Baltic Ocean is a sub-sea to the Atlantic Ocean and is delimited by the Scandinavian peninsula and the Danish Islands (see Appendix I). The area is 366,000 km^2 and the average depth is 65 m. [Ref. 28] The Baltic is in some sense an inland sea, since it has very narrow and shallow connections to the North Sea and the Atlantic in the west. The water balance can be described with Figure 31 below. The large amount of water from the many rivers makes the Baltic a brackish sea, and the salinity can vary considerably depending on geographical location and depth (Figure 31).

Figure 31 shows that the Baltic works more or less like a gigantic mouth of a river [Ref. 29].

The sea-bottom conditions vary both in roughness and consistency, depending on the geographical location. The sea bottom in the specified water volume will be described later in this chapter.

The density of water depends on salinity, pressure and temperature. Low density water is lighter and is layered on top of high density water. Fresh water supplies from the rivers, wind and temperature variations help to destroy or maintain established water layers. How the salinity in the Baltic varies is shown in Figure 32 [Ref. 29].

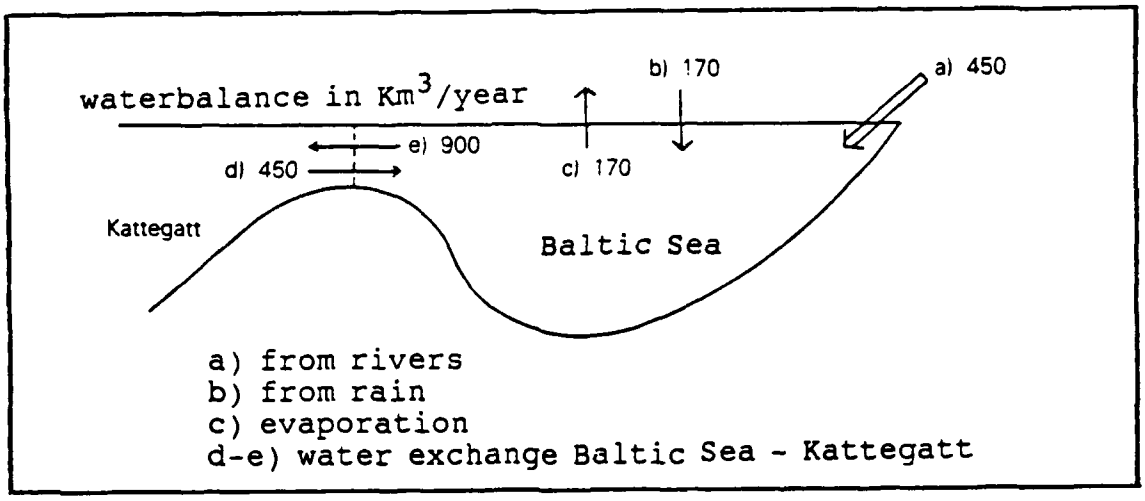

Figure 31. Water balance in the Baltic Sea

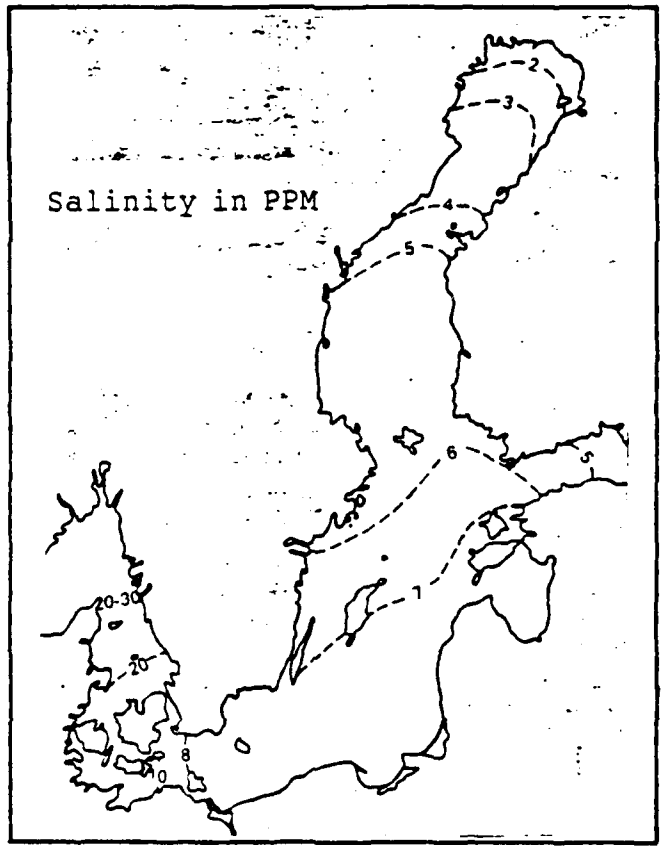

Figure 32. Salinity variations in the Baltic Sea

1. Salinity

Salinity in the middle of the Baltic is 6.5 - 7.5 PPT, in a layer from the surface down to 60 - 80 meters depth. In deep water regions, salinity increases to 10 - 12 PPT.

2. Currents

The sea currents are created and maintained by the following forces:

* wind
* horizontal water density differences
* slope of the sea surface
* tide
* air pressure differences

The wind influences mainly the water closest to the sea surface and the effect decreases rapidly with depth. Water volumes can have different densities which creates pressure differences and hence, currents. If the water surface is slanted, this also causes pressure differences. Tide always implies currents, but since the tide in the Baltic is negligible, the contribution is small. The air pressure forces the sea surface level to go higher and lower which also creates currents. The velocities of the deep sea currents are shown in Figure 33 [Ref. 29].

Depth (m)	Wind (m/s) 1	5	10	20	30
0	0,1	0,2	0,5	1,0	1,5
1	0,0	0,1	0,2	0,4	0,5
5	0,0	0,1	0,1	0,2	0,3
10	0,0	0,1	0,1	0,2	0,2
15	0,0	0,0	0,1	0,2	0,2

Figure 33. The velocity of the deep sea currents in the Baltic Sea

3. Wind and Waves

The wind direction is in general to west or south`west the whole year around (open sea). The average wind velocity can be estimated to be approximately 8 - 10 m/s. In order to determine the wave height, the diagram in Appendix J can be used, with the wind velocity as the input value. Average wave heights at the Almagrundets lighthouse and two other locations are given in Table 17 according to the month of the year.

TABLE 17. WAVE HEIGHTS AT ALMAGRUNDETS LIGHTHOUSE (METERS)

	jan	feb	mars	april	maj	juni	juli	aug	sept	okt	nov	dec
Almagrundet	1.15	0.45	1.00	0.50	0.60	0.45	0.45	0.65	0.80	1.05	1.25	1.20
Glanossodragrund	1.45	1.25	1.40	0.70	0.60	0.55	0.80	0.75	0.95	1.25	1.70	1.60
Trubaduren	0.50	0.40	0.65	0.50	0.60*	0.60*	0.55	0.60	0.95	0.90	0.95	1.05

The average wave height for the whole year is then 0.8 meters. The wind and waves causes the water surface layer to be stirred down to approximately 10 meters, depending on the time of year and the weather conditions. This creates a layer of air bubbles under the sea surface that will highly affect the surface reverberation level.

4. Speed of sound

The speed of sound is mainly influenced by the water temperature in the Baltic. The salinity has almost no effect at all. It is therefore sufficient to determine the speed of sound profile by simply measuring the water temperature as a function of depth. The temperature differences are largest from the surface down to around 40 meters. Below 40 meters the temperature is almost constant. At these depths the higher salinity (10 - 12 PPT) cause the speed of sound to increase slightly. During the summer the surface water is

warm and the underlying water cold. This implies a sharp negative gradient and the sound is strongly refracted toward the bottom. Together with the slightly positive gradient at deeper depths this creates a sound channel, very much like the SOFAR channel in the deep oceans. During the winter the surface water gets colder than the underlying water which makes the gradient iso-speed or positive. A positive gradient makes the sound bend toward the surface. Further, it is quite normal to have iso-speed water from the surface and down to 1 - 10 meters due to the stirring effect.

An assumption is that the speed of sound profile is range independent out to a radius of approximately 1,000 meters. [Ref. 30]

5. Absorption

The absorption of sound in water increases with frequency and decreases with salinity. The diagram in Appendix K shows the absorption in dB/km vice frequency, for both the Baltic and the Atlantic ocean. For example, in the Baltic the absorption is 9 dB/km at 100 KHz compared with 30 dB/Km in the Atlantic Ocean. This means that higher frequencies are more favorable in the Baltic, which also implies that smaller and lighter transducer dimensions may be used.

C. DESCRIPTION OF THE WATER VOLUME

The location of the water volume, that will be the reference for the sonar design calculations, is shown in Appendix L. The speed of sound profiles for different months, together with ray tracing results are shown in Appendix M. The typical sea bottom condition is shown in Figure 34 [Ref. 31].

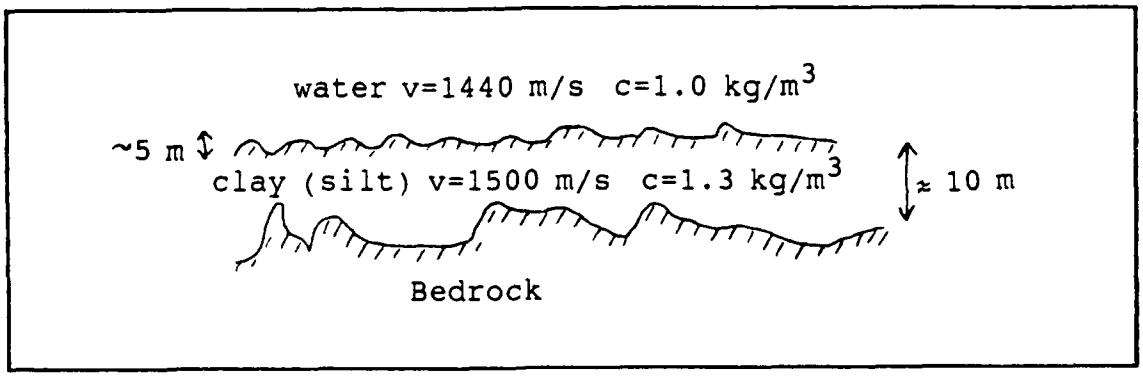

Figure 34. The reference sea bottom

D. AMBIENT NOISE STUDY

The ambient noise is the noise existing in the environment in the absence of both the sonar platform and the target [Ref. 7]. The objective in this section of the chapter is to determine the Noise Spectrum Level (NSL(A)) in dB re $1\mu Pa/Hz^{1/2}$ for the reference water volume described above.

The ocean is never quiet. The lower limit for the noise is the thermodynamic noise, which is created by the molecular movements in the water. In addition to this, sea waves, surf, animals in the sea and ship traffic make contributions depending on the geographical location and the sea state. The only contribution to the NSL in this case, besides the thermodynamic noise, is the noise from waves [Ref. 30]. The NSL(A) values for the sonar design can therefore be taken from Knudsen curves shown in Appendix N. The NSL falls off toward higher frequencies with 5 - 6 dB per octave, until approximately 100 kHz. Then the thermo-noise takes over and increases the NSL at higher frequencies.

VII. SONAR DESIGN STUDY

A. INTRODUCTION

This introduction will determine the sonar specification and give a more detailed picture of the design objective. It will also explain the design method that will be used in pursuing the objective.

As indicated in Chapter 1, the main goal of using a sonar system is to give the ship sufficient time to detect, classify and avoid a proximity mine in its path. In order to write the sonar specification the following questions must first be answered:

1. Which ship maneuver is effective in avoiding mines?
2. At what range and angles must the mine be detected and classified to ensure effective ship maneuver?
3. What are acceptable probabilities for detection and false alarm in the detection process?

In answering the first question, there are two kinds of maneuver options: crash stop or a sharp turn. When using a crash stop the ship will stop at an ahead distance of 3,000 m and slide 300 m in side (Appendix C). When using a sharp turn instead, the ship will make a 90 degree turn at an ahead distance of 850 m and slide 650 m in side. The difference between the two maneuvers, besides the distances, is that the sliding effect in the latter case is more controlled by the ship operator. If the maneuvers could be done without the sliding effect, this would be a great advantage. This is because there is usually not just one single mine ahead, but instead some kind of a mine field. Since a deployed mine field pattern by an enemy is usually unknown, the sliding effect in both maneuvers can cause the ship to activate additional mines while doing the avoiding

maneuver. Accordingly, the best maneuver is to make a crash stop with no sliding and with a short stop distance and then back out in the ship's own wake. Since this is not an option in this case, due to the maneuvering data in Appendices C and E, the second best alternative is to perform a controlled maneuver with as little sliding and ahead distance as possible. So, the answer to the first question is to use a sharp turn maneuver.

Question 2 is answered with Figure 35 below.

In order to pass the mine at a safe distance (in this case 30 meters), the mine must be detected at an ahead distance of 700 meters. This distance is determined from the turning test data in Appendix E and includes an estimated decision time for the ship operator of 30 seconds (or 240 meters at 16 knots) before the maneuver is ordered. If this time can be made very short, say 5 seconds (or 40 meters with 16 knots), the required detection distance decreases to 500 meters. This is the absolute minimum distance for an avoiding maneuver to be successful. During the avoiding maneuver, the sonar must search a forward sector of at least ±10 degrees in order to indicate an approaching mine threat at 700 meters and to keep track of a detected mine down to 500 meters.

An answer to question 3 determines under what conditions the mine must be detected. The determination of the two probabilities is a matter of the cost of making an incorrect decision. To set the values of the probabilities is a very difficult task. They vary with tactics, strategy and environmental factors. In most cases a combination of experience, intuition and sonar tests have to be used to determine them. [Ref. 9] The probabilities are used in the sonar design to determine a threshold value in the detection process. A typical value for the probability of detection P(D) is 50%, when consulting the literature. Also, some

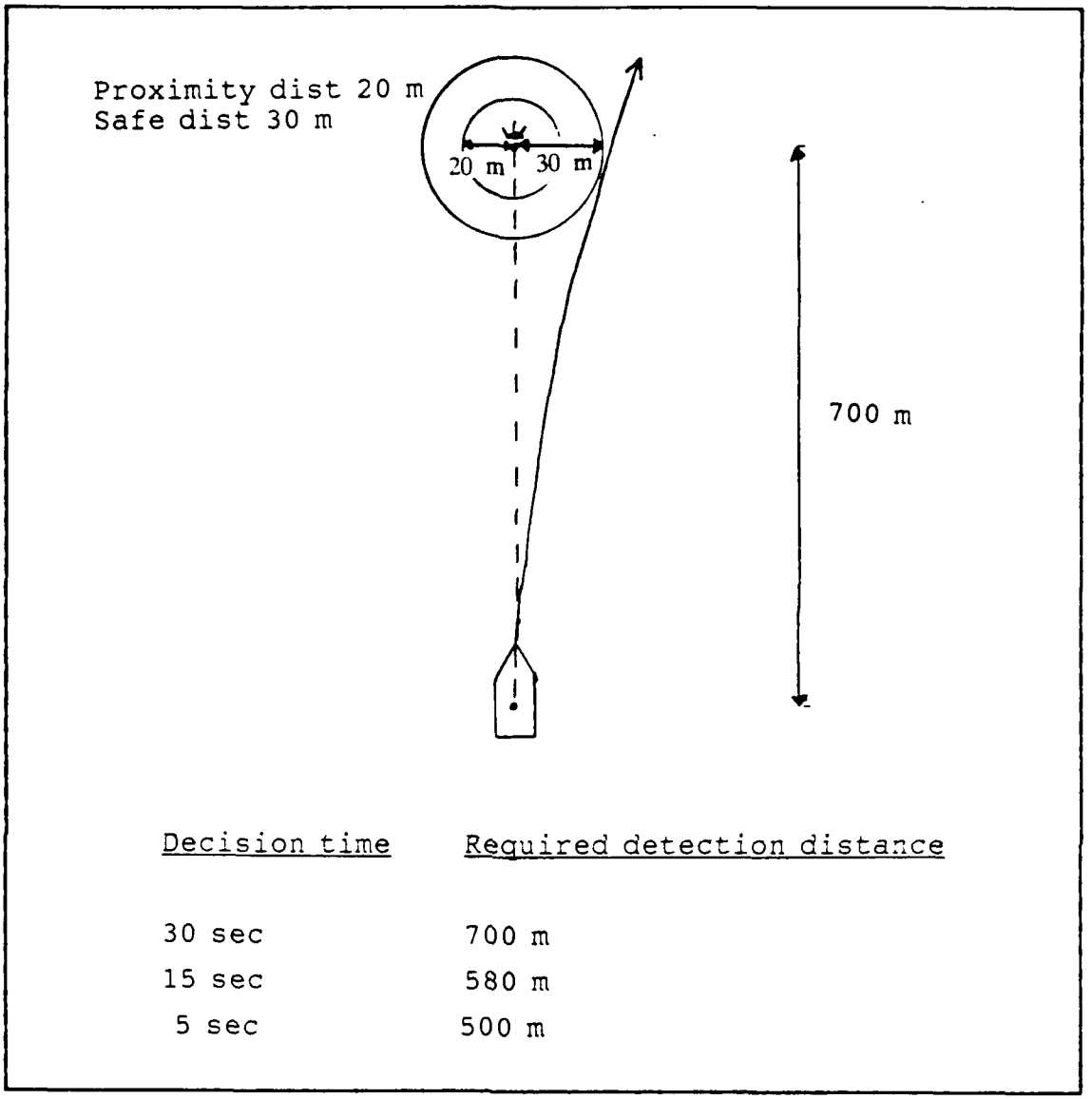

Decision time	Required detection distance
30 sec	700 m
15 sec	580 m
5 sec	500 m

Figure 35. Determining the minimum detection range and search sector

books actually define the detection threshold with the P(D) set to 50%. [Ref. 32] The probability of false alarm P(FA) is defined as the probability of getting a false alarm in the same interval of time as the signal duration. [Ref. 9] It is already now quite obvious that a very narrow sonar beamwidth will be necessary in order to minimize the

reverberation element. This implies that very few false alarms for each transmitted pulse can be accepted. There are approximately 1,000 range increments in one beam (Figure 35), using a pulse length of 0.8 ms (to be explained in a later section on sonar design) and a max distance of 700 meters. Hence, there are 1,000 range intervals examined for each pulse, and with the assumption that no more than one of those will be registered as a false detection, gives a P(FA) of $1/1000 = 10^{-3}$. [Ref. 7]

The sonar concept comprises, in this case, an active, high frequency sonar. In most cases an active sonar implies a reverberation limited performance. This will be the assumption even in this case. A stationary target, like a mine, produces no Doppler shift in the returning echo signal. The echo spectral density and the reverberation spectral density will therefore be essentially identical in their form, when intercepted by the receiver. Based on the discussion above, the sonar specification is stated as follows:

The sonar must be able to detect a generic proximity mine with a P(D) of 50% and a P(FA) of 10^{-3}, in a sector of ± 10 degrees from the ahead direction, in a range gate extending from 500 meters out to 700 meters.

The design objective is to determine the following sonar parameters:

* frequency
* power
* wave form
* beamwidth and beamform
* sonar depth

Figure 36 shows a block diagram of the design method. After calculating the indicated parameters in the active sonar equation, the reverberation level will be determined.

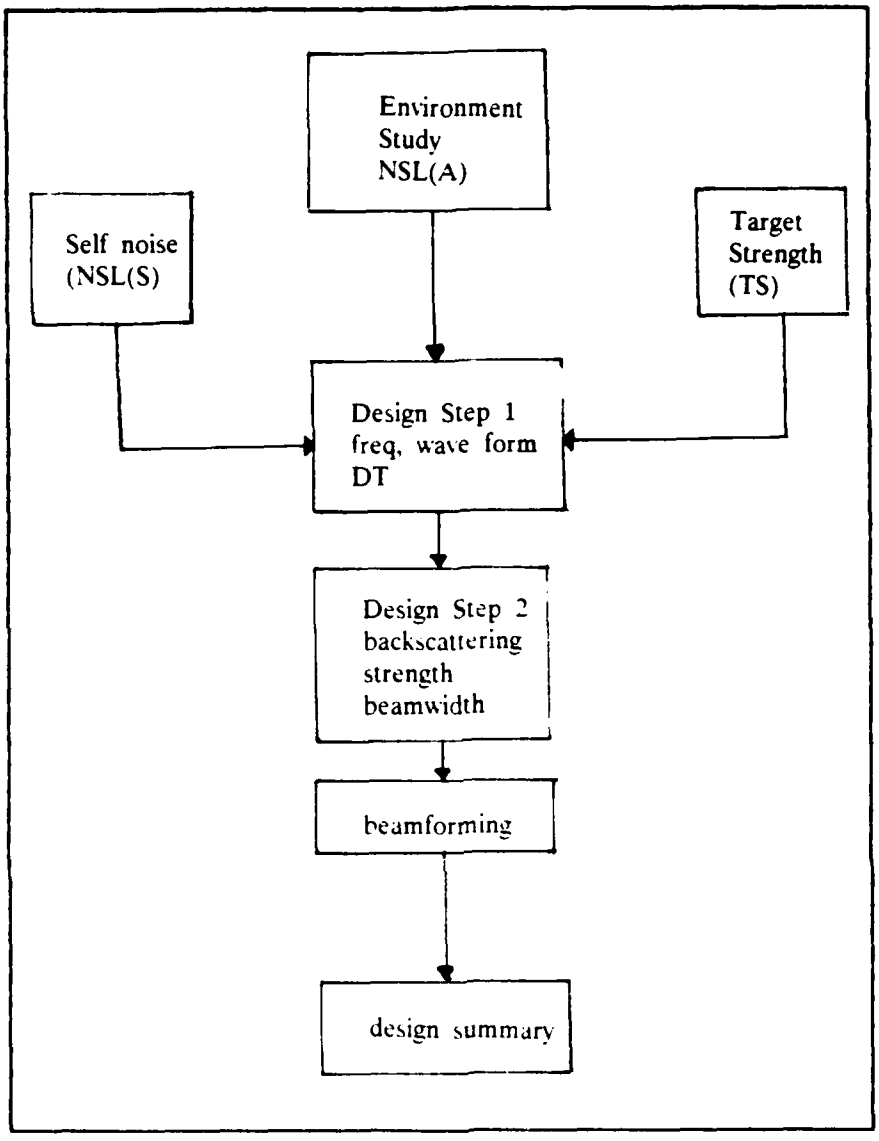

Figure 36. Sonar design method

Since we want to use as low a power as possible in the system, the noise floor (ambient noise and self noise) will decide the reverberation level. The situation is illustrated in Figure 37 [Ref. 32]. Increasing the power level further will have no effect on the sonar range. After the necessary beamwidth is calculated, a discussion about beam forming and beam steering will follow.

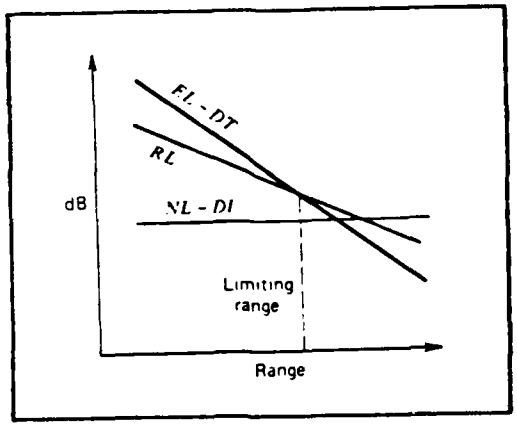

Figure 37. Reverberation limited performance of a sonar system

B. SONAR DESIGN: STEP 1

1. Carrier frequency

The choice of carrier frequency is a very important step, because it involves trade-offs among many interacting parameters. In general, a long range "surveillance" sonar implies low frequencies and short range "classification" sonar implies high frequencies.

The following issues must be discussed before a frequency choice can be made:

* upper limit wavelength to detect the target
* resolution versus transducer size
* absorption
* ambient noise and power dependence

Starting with the first issue, the wavelength must be smaller than the target size in order to make a detection (in a non-resonant case). The smaller the wavelength the more information about the target can be revealed in the detection process. Since the target in this case is a mine with a minimum size of 0.6 meters, it is clear that high frequencies (above 10 kHz) must be considered.

The second issue shows the very strong relationship between resolution and transducer size. This is not always true though, since modern signal processing techniques can overcome that relationship to some degree. The general relationship between the resolution and the transducer size is that the (3 dB) beamwidth gets smaller when the transducer size gets larger, for a fixed frequency. This relationship often limits the smallest design beamwidth, since the transducer size must be designed according to the ship size and because the costs increase with large transducers. Different transducers and beamforming techniques will be discussed later in this chapter. In order to make feasibility calculations and comparisons in the following design steps, a reference transducer will be determined. The sonar carrier is in this case a VLCC tanker, with the sonar design constraints given in Chapter 1. The fact that the sonar is mounted on the bow of the ship and must be removable, implies that the size and shape must be designed according to this. Since the transducer is kept within a streamlined dome and mounted as an extension of the bow bulb, a circular transducer aperture or array is preferable. The maximum possible transducer diameter is taken to be 1 meter, considering practical handling and the problem of getting a smooth and strong bonding between the ship hull and sonar dome. The normalized far-field directivity function for a circular piston is [Ref. 33]

$$D_N = 2 \cdot \frac{J_1\left[\frac{2\pi \cdot a}{\lambda}\right] \cdot \sin\theta}{\frac{2\pi \cdot a}{\lambda} \cdot \sin\theta}$$

where a = radius

θ = polar angle in spherical coordinates

$J_1(.)$ = first order Bessel function of the first kind

From this an approximate expression for the 3 dB beamwidth can be derived [Ref. 34]:

$$BW \text{ (in degrees)} \approx \frac{65\lambda}{d}$$

where lambda is the wavelength and d is the transducer diameter. A simple calculation indicates that to achieve a beamwidth of less than one degree (conical beam) the carrier frequency must exceed 100 kHz. Since the target is relatively small in size, it will be necessary to use very narrow beams, probably fractions of a degree. This implies that carrier frequencies of 100 kHz and above must be used.

The third issue counteracts the usage of high frequencies due to the increasing energy absorption at higher frequencies. The absorption depends mainly on the salinity in the water, which gives an advantage of using high frequencies in the Baltic vice the Atlantic Ocean (see Chapter 6). However, even in the Baltic the absorption will be very significant, when using frequencies above 100 kHz, as can be seen in Table 18.

The fourth issue indicates that the ambient noise and transmitting power must be considered before determining the frequency. As can be seen in Appendix O, the declining ambient noise with frequency has a break point around 100 kHz and will then increase with frequency. This ambient

TABLE 18. ABSORPTION RATES

freq (kHz)	absorption (dB/km)
100	10
200	20
300	30
500	100

noise is due to molecular movement in the water. In order to keep the NSL down, frequencies in the lower region, around 100 kHz are preferable. The power limitation works the opposite way. Higher frequencies allow higher power levels to be transmitted into the ocean. This is due to cavitation effects on the sonar surface and will be further treated later in this chapter.

A target's resonance region for spheres is determined by the factor ka, where $k = 2\pi / \lambda$ and a is the target radius. The resonance region is usually in the ka interval 2-30. Hence, if the speed of sound is 1500 m/s the target's resonance frequency can be found in the interval [Ref. 35]:

$$f = \frac{1500}{\pi \cdot a}, \frac{22500}{\pi \cdot a} \quad (Hz)$$

In this case a = 0.6, so the resonance frequencies must be somewhere between 796 Hz and 12 kHz. A transmitted signal with a frequency in this interval could trigger the target's resonances. As mentioned in Chapter 2, this can enhance the target strength (TS) but it can also lower it, if the target has high internal losses or if the reradiated sound is radiated in directions other than the specular direction. [Ref. 9] In order to utilize the resonance

phenomena, experiments must be performed to first determine the resonance frequencies for the particular target and then measure how the target strength varies. Since in this case the target can have many different shapes and these shapes are practically always unknown, the technique has many disadvantages and can probably not be utilized. Further research and experiments must be performed to investigate this.

To determine an optimum frequency is not an obvious thing to do. Especially since the assumption is that of reverberation limited performance, where the frequency dependent absorption coefficient is essentially the same for the echo and for the reverberation background [Ref. 6]. There must be a trade-off decision with the parameters above as input values. One conclusion is that with the detection range requirement stipulated in the introduction to this chapter, the frequency range must be within 100 - 500 kHz, mainly in order to balance transducer size and absorption.

In order to make comparisons and facilitate the final decision, it is advisable to carry along both limiting frequencies, 100 and 500 kHz, in the design.

2. Transmission loss (TL)

To detect a target, transmitted energy (sound wave) from the transducer must find a path to the target and back to the transducer. Since the speed of sound, with which the energy is propagating, is a function of salinity, pressure and the temperature of the propagating medium, different speeds of sound will occur at different locations. The speed of sound differences have the effect of refracting the energy in a direction dependent on the gradient. In this case the most significant speed of sound differences occur as a function of water depth. If the required detection range had been greater than 1,000 meters, the speed of sound differences in azimuthal distance had also been important.

The energy propagation or sound field can be described with rays which obey "Snell's laws" of refraction, and a ray tracing diagram can be produced for a specific speed of sound profile. There are a number of limitations in the ray tracing concept, since both boundaries (surface and bottom) are assumed to be flat and rigid. Further, no estimation of energy scattered into shadow zones is indicated. A ray tracing program [Ref. 36] has been used in Appendix M, to show the propagating sound field for monthly average speed of sound profiles and different source depths. After discussing the sonar concept with different references [Ref. 30, 36] the conclusion is that there must be a direct path between the transducer and the target, in order to achieve reliable detection criteria. Ray reflections from the boundaries can cause multipath effects and disturb the direct ray echo return. This will be further investigated later. When examining the ray diagrams in Appendix M, direct ray paths can be found for all months except June, July and October, with the source at 10 meters depth. The summer is a difficult season, due to the very strong negative gradient, which causes the rays to strongly refract toward the bottom and create a sharp shadow zone. The shadow zone is not completely dark, however. Some sound energy exists in the zone and measurements have been done at 24 kHz that gave TL values between 20 to 70 dB/Kyd close to the boundary. [Ref. 9] Sound waves propagating in the ocean normally get delayed, distorted and weakened during their transition. This is due to the nature of boundary layers, absorption and the geometrical spreading of the sound field. These phenomena can be taken together in a transmission loss (TL) factor, which is defined as the weakening of sound between a point 1 meter from the source and another point at a distance in the sea. [Ref. 9]

Since at this stage only the direct sound path is considered, and because of the short range requirements, only absorption and geometrical spreading will influence our TL factor. In a sound channel the sound is first spread spherically out to a transition range, which can be estimated by the following formula, valid for a mixed layer with a positive speed of sound gradient near the sea surface [Ref. 7]:

$$r_t = 105\sqrt{\frac{D^2}{D - Z}}$$

where Z = source depth

D = depth of mixed layer

Beyond this range the spreading will become cylindrical and if the two boundary layers are accounted for, something in between spherical and cylindrical will occur. The TL formulas for the two spreading forms are [Ref. 32]:

Spherical spreading: TL = 20 log r

Cylindrical spreading: TL = 10 log r

Using the formula above and comparing with the speed of sound profiles in Appendix P, the transition range will exceed 1,000 meters for all months, and since 700 meters is less than that, only spherical spreading needs to be used. Adding the absorption loss to the spherical spreading gives the following expression [Ref. 32]:

TL = 20 log r + ar (Equation 1)

where a = absorption

r = range

The absorption at different frequencies is found in Table 18 above and the TL for the two carrier frequencies and range limits are shown in Table 19.

TABLE 19. TL FOR CARRIER FREQUENCIES, RANGES

	100kHz	500 kHz
TL at 500 m	59 dB	104.0 dB
TL at 700 m	63.9 dB	126.9 dB

An estimation of the geometrical TL factor can also be performed by using ray diagrams. For two rays with a separation of Δh meters, the transmission loss expression at range r is given by:

$$TL = 10 \cdot \log\left[\frac{r \cdot \Delta h}{\Delta\theta}\right]$$

where r = range

Δh = vertical ray separation at range r (meters)

$\Delta\theta$ = initial ray separation (radians)

For example, in January, where two rays are clearly distinguishable (with Δh = 12 meters, $\Delta\theta$ = 0.0175 radians (1 degree) and r = 700 m), TL = 56.82 dB. This should be compared with a spherical geometrical spreading of 20 * log 700 = 56.9 dB. The comparison verifies the spherical spreading assumption.

A Swedish defense agency [Ref. 30, 37] has, in its model for TL (layered medium), adapted spherical spreading up to a distance of 500 meters. For distances exceeding 500 meters, cylindrical spreading is used together with a frequency dependent loss that is composed by the absorption and an additional leakage loss. The expression for TL when r > 500 meters yields:

$$TL = 10 \log r + (\alpha + \alpha_1) r + 27 \qquad \text{(Equation 2)}$$

where 27 dB is the TL up to 500 m

α = absorption coefficient

α_1 = leakage coefficient

The leakage coefficient decreases with frequency and is linear in a logarithmic scale. The expression for the leakage coefficient (32 Hz - 8 kHz) yields:

$$\alpha_1 = 1.88 - 0.42 \log f$$

With the assumption that this relationship holds even for higher frequencies (100 and 500 kHz), the leakage coefficient will become zero and Equation 2 will become the same as the original TL Equation 1 above.

The following conclusions can be made based on the results above:

* The source depth must be at approximately 10 meters, in order to get most direct paths to the target.
* The spherical spreading with absorption (Equation 1) expression can be used as the TL term in the active sonar equation.
* "Safe" ship operation will not be possible the entire year.

3. Resolution, waveform and target detection

The resolution of a sonar system can be defined by either its measuring precision or its detection capability and depends on:

* the pulse length
* the beamwidth
* the target strength (TS)
* the angle of incident upon the target
* the display and recording technique

The pulse length choice has three important implications. First, it determines the range resolution of the system. Second, it determines how much of the total target strength can be utilized. Third, it determines the reverberation element in length. The pure range resolution

is of minor importance in this case, since it is very unlikely that two mines are deployed very closely together. Of more importance is to minimize the reverberation element as much as possible. Further, in order to get full usage of the target strength, the pulse width must fully ensonify the target [Ref. 10]. For this latter reason the following expression for pulse width must be used:

$$\tau = \frac{\Delta r \cdot 2}{c}$$

where Δr = resolution in meters
c = speed of sound

A Δr of 0.6 meters and c of 1500 m/s gives a pulse width of 0.8 ms. The expression for range resolution is

$$\frac{\text{Pulsewidth} * C}{2}$$

which gives a range resolution of

$$0.8 \text{ ms} * \frac{1500}{2} = 0.6 \text{ meters}$$

This means that if two mines are deployed with less than 0.6 meters between them (which is very unlikely), the echo return will contain both targets and they cannot be distinguished. Hence, the combination of utilizing the full target strength, together with getting minimum reverberation element in length, yields a pulse duration of 0.8 ms.

The return pulse will be stretched out in time by 2*L/c seconds, where L is the target range dimension [Ref. 7]. Using L = 0.3 (since spherical or cylindrical mine

shape) the returning echo will be 1.2 ms long. The fact that the ship is moving toward the mine, with a speed of 16 knots (8 m/s), counteracts this pulse stretching. Using Ziomek [Ref. 33:p. 200], a time-compression`stretch factor can be calculated using the expression (for this case only):

$$s = \frac{(1 - b)}{(1 - c)}$$

where b = - 0.0053 and c = 0.0053 s is then equal to 1.011. Comparing this (reciprocal value) with the pulse length 0.8 ms, gives a pulse compression effect of 0.01 ms. The conclusion is that the time compression, due to the ship speed, has only a minor impact on the returning pulse. The returning pulse will consequently be 1.2 ms - 0.01 ms = 1.19 ms long. This determines the receiver bandwidth to be at least 1/T = 840 Hz.

The angle of incidence upon the target has very little effect in this case, because the shape of the mine is spherical or cylindrical. The angle of incidence would be of more importance, though, if the mine had been deployed on the bottom.

The last issue above, the display and recording device, will not be covered in this thesis. It is assumed that these devices are chosen to present the resolution necessary to fulfill the sonar objective.

The detection threshold (DT) of a sonar system is defined as the input minimum signal-to-noise power ratio, within the bandwidth of the system, that; after all processing (mental analysis) of the received stimulus (signal plus noise) is completed; will guarantee a given probability of detection (P(D)) for a specified probability of false alarm (P(FA)). [Ref. 7] The detection threshold expression depends on the detection index, that is the value

determined from the probabilities P(D) and P(FA); the signal wave form and the choice of detection technique. There are two different detection techniques that will be discussed later. The first is a coherent detection, where the signal is exactly known; and the second is an incoherent detection where the signal is unknown. A coherent receiver is a crosscorrelator, where the signal plus noise is correlated with a noise free replica of the known signal. The crosscorrelator is optimal for a background of Gaussian noise. The incoherent receiver is an energy detector that considers only the amplitude modulation of the signal. Two different transmitting wave forms will also be discussed; the continuous wave (CW) pulse and the linear frequency modulated pulse (LFM). The CW pulse is just a sinosoid that is turned on and off and is therefore very simple and inexpensive to implement. The LFM pulse is a more complicated waveform that needs to be explained a little further. LFM means that the transmitting signal frequency varies linearly *during* the pulse length. A pulse modulated like this is normally much more effective against a target having no or very little Doppler effect. The advantage of utilizing LFM pulse instead of CW pulse is described in Figure 38 [Ref. 37]. A short CW pulse has a large bandwidth and the reverberation is spread out over that same bandwidth. A stationary target is then located entirely in the reverberation. A long CW pulse has a small bandwidth but a wider range gate. In this case very little Doppler is needed to lift the target out of the reverberation. The echo from a LFM pulse is stretched out both in time and in frequency and only a part of the reverberation is added to the target echo. The signal processing then makes the reverberation part of the pulse very short.

Figure 39 shows the difference between a CW pulse and LFM pulse on a PPI (Plane Polar Indicator) display [Ref. 37].

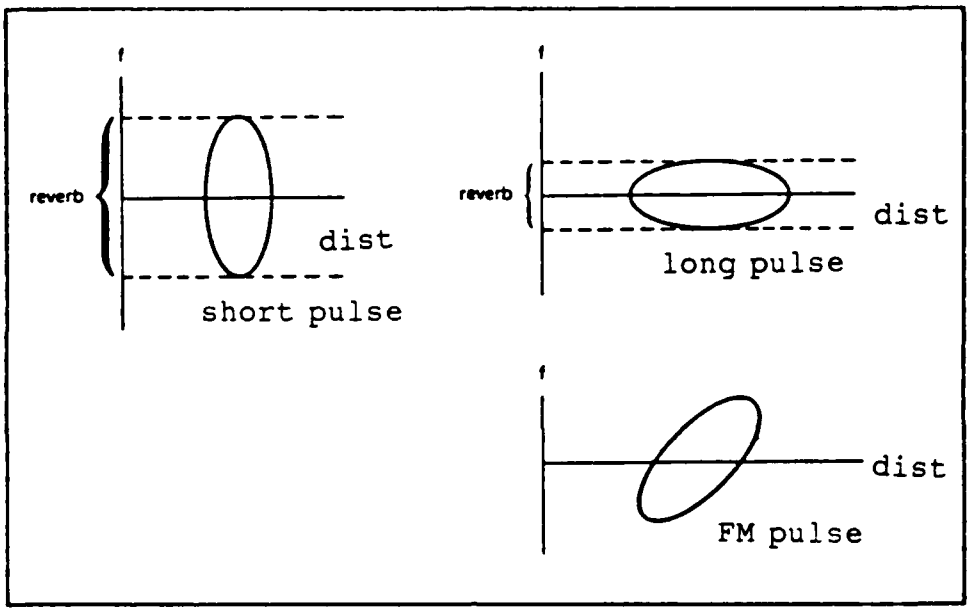

Figure 38. The LFM waveform advantage

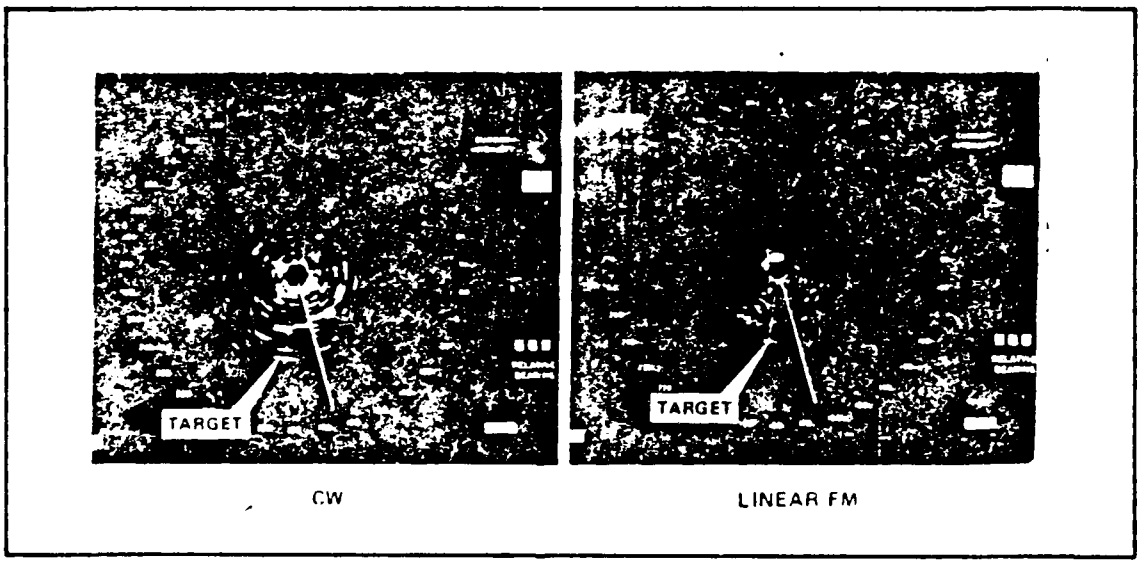

Figure 39. Difference between an LFM pulse and a CW pulse on a PPI.

A variation of the pulsed LFM modulation is the Continuous Transmission Frequency Modulation (CTFM). The frequency modulated signal is continuously transmitted and the different frequencies of the outgoing and incoming signal are determined. This frequency difference is a

measure of the target distance. CTFM sonar gives very good audio information of the echo structure of the target, which can be used for detection and classification [Ref. 37]. The major disadvantage with a CTFM sonar is that two apertures or arrays must be used and there must be good isolation between the two. Due to the practical disadvantages with such a system and the increasing costs, this modulation type will be of minor interest.

The DT expressions for different detection techniques and wave forms will now be discussed. DT expressions from three different references will be covered, since there are differences between them. The pulse duration will be the same for both pulse forms in the calculations in order to obtain a comparison. The design criteria for swept bandwidth and pulse length is found in Ziomek [Ref. 33] and yields:

$$\frac{4\pi}{|b|\,T^2} \lesssim 1$$

where $|b|$ = phase deviation constant (rad/sec^2)

T = pulse length

With a return pulse length of 0.8 ms and the inequality set to one, the swept bandwidth must be 5 kHz. By setting the inequality to 1, the range resolution will decrease to 0.3 meters, when not considering the pulse stretching discussed above. Since the carrier frequencies are up in the 100/500 kHz range, a swept bandwidth of 5 kHz still makes the signal to be "narrowband." In all the calculations below, a return signal pulse length of 1.2 ms will be used. For detection index and the "delta" calculations, the curves in Appendix P will be used.

a. Incoherent detection

Urick assumes in his book [Ref. 9] that the reverberation is "noise like" and describes a "rule of thumb" expression for the DT as follows:

$$DT = 5 \cdot \log\left[\frac{d \cdot w}{T}\right] - 10 \log w' + \Delta \qquad (1)$$

where d = detectivity index (from ROC curves in Appendix P)

w = receiver bandwidth

w' = reverberation bandwidth

T = pulse length

= compensation factor for small bandwidth products (Appendix P).

Urick refers to a paper by Kroenert [Ref. 38] for information about different DT expressions. Kroenert's expressions are based on Urick's assumptions and yield:

$$DT(CW) = 10 * \log (T * \sqrt{d}\ ) + \ - 10 * \log T \qquad (2)$$

$$DT(LFM) = 5 * \log (d * T/w') + \ - 10 * \log T \qquad (3)$$

The third reference is from Burdick's book [Ref. 7] and he assumes that the target signal and the reverberation have the same spectral shape and no processing advantages, with different filter techniques, can be gained. The DT expression, derived in this book, is directly related to this application, with a stationary target and reverberation limited performance. The DT is then a function depending only on the detection index.

$$DT = 5 * \log d \qquad (4)$$

where d is obtained from the ROC curves for a unity time bandwidth product (d = 75).

The numerical values for the above expressions are:

Using Equation 1 with:

d=detectivity index (from ROC curves Appendix P)=11

w = receiver bandwidth = 833 Hz

w'=reverberation bandwidth=5 kHz with LFM, 833 with CW

T = pulse length = 1.2 ms

Δ= (from Appendix P) 1.5 for LFM and 3 for CW yields:

DT(CW-pulse) = 8.3 dB

DT(LFM-pulse) = - 0.6 dB

Using Equations 2 and 3 with the same values as above yields:

DT(CW-pulse) = 8.2 dB

DT(LFM-pulse) = 3.3 dB

Using Equation 4 with d = 75 yields:

DT(CW-pulse) = 9 dB

b. Coherent detection:

Only Kroenert's paper gives expressions for DT with a coherent receiver.

DT(CW-pulse) = 10 * log (d * T/2) - 10 * log T

DT(LFM-pulse) = 10 * log (d/ (2 *w')) - 10 * log T

Using the same values as above yields:

DT(CW-pulse) = 7.4 dB

DT(LFM-pulse) = -0.4 dB

In conclusion, since a coherent detection technique is optimized for Gaussian noise (which is not the case here), an incoherent detection technique must be the most appropriate in this design. Later in the chapter it will also be concluded that the impact of multipath interference supports a choice of an

incoherent receiver technique, especially in an active sonar application. Using an incoherent detection technique gives a number of DT choices as shown above. An LFM waveform gives the lowest DT in all cases, as expected. The problem with using LFM is that it is a much more sophisticated technique, which implies higher costs both for purchase of the sonar and for maintenance. These are not desirable factors when considering the main objective of the design. This implies, that if the detection goal can be fulfilled with a CW pulse, this must be a preferable waveform. Therefore, a CW pulse is chosen to be the main alternative, and a "worst case" DT of +9 dB is adopted for the further design.

The returning carrier frequency will be shifted up in frequency due to the ship's speed (Doppler effect). The returning pulse length will also be stretched from 0.8 ms to 1.19 ms. This makes the necessary receiver bandpass filter decrease from 1250 Hz to 840 Hz. The bandpass filter must be centered due to the Doppler shifted carrier frequency, that is at 101.1 kHz for a 100 kHz transmitted frequency and at 505.3 kHz for a 500 kHz transmitted frequency. In order to make the receiver susceptible to changeable ship speeds, a parallel filter solution can be considered. This will increase the cost, though.

C. SONAR CONCEPT

The main objective of the sonar is to detect a target, i.e., a mine. A refinement of this objective is to include a classification of the detected target. This would discriminate against "false targets" and avoid unnecessary ship maneuvers. This part of the chapter will investigate whether it is possible to design such a sonar for this application or not. It will be shown that only a conventional "classification" sonar design is possible to pursue.

A classification sonar must comprise a very high resolution and give a TV-like picture of the target.

Classification sonars are mostly designed as side-looking sonar, where a towed linear array can be utilized. This facilitates the sonar design, since different kinds of synthetic aperture array techniques can easily be implemented.

The requirement for a classification sonar is to obtain a resolution element on the order of 1/10 of the object size, for a reliable classification. [Ref. 39] This means that a mine, with a minimum diameter of 0.6 meters, must have a resolution element of 0.06 meters. Taking this value and evaluating the horizontal beamwidths for the ranges 500 and 700 meters gives:

At 500 meters -- 0.0014 degrees

At 700 meters -- 0.00098 degrees

Using these required beamwidths as a reference, some design concepts will now be discussed.

1. Case 1: Using ordinary beamforming with a circular piston

The approximate formula was given on page 100 for a circular piston.

The aperture diameter necessary to achieve the required beamwidths above are shown in Table 20.

It can be clearly stated that this technique is impossible to pursue.

TABLE 20. APERTURE DIAMETERS

	100 kHz	500 kHz
at 500 meters	4,062 meters	812 meters
at 700 meters	5,687 meters	1,138 meters

2. Case 2: Using beam focusing

The idea is depicted in Figure 40 [Ref. 34]. The target is located in the transducer's nearfield and is focused at a particular distance, using complex phase weights or by simply using a curved aperture. The resolution at the focal point then depends on the diameter of the Airy disc. The Airy disc's minimum resolution element follows the relationship [Ref. 40]:

$$L_{min} = \frac{1.22 \cdot f \cdot \lambda}{D}$$

where L_{min} = limit of resolution

f = focal length

λ = wavelength

D = aperture diameter

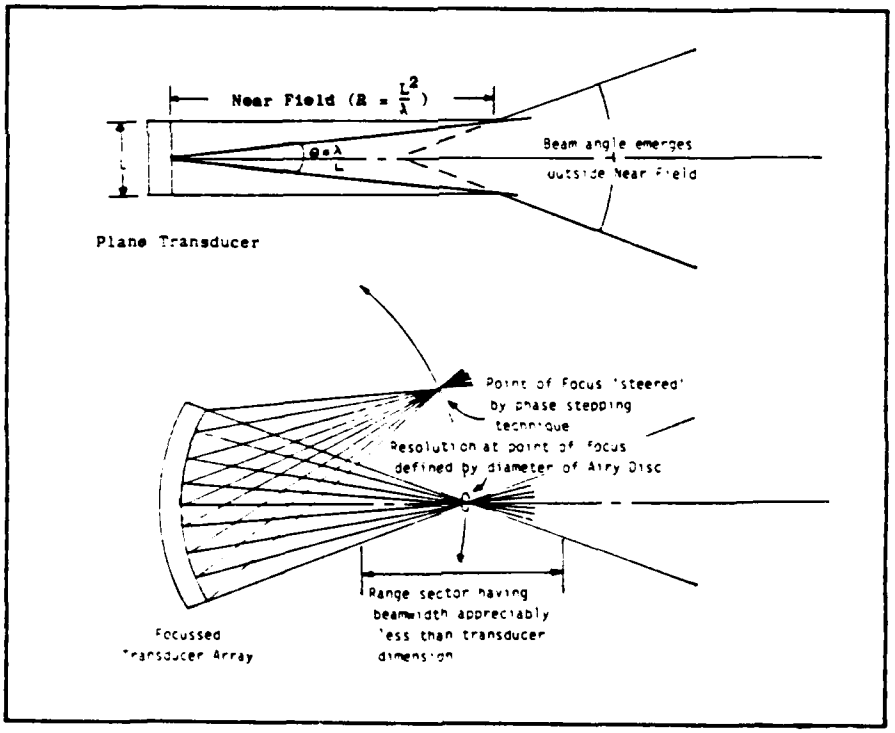

Figure 40. The near-field characteristics of an unfocused beam (top) and a steerable focused beam (bottom)

In order to focus the aperture, the target must be in the nearfield. To achieve this the target must be at a range less than

$$\frac{\pi \cdot R^2}{\lambda}$$

where R is the radius in this case.

Calculating the aperture radius for these values yields the figures in Table 21.

TABLE 21. APERTURE RADIUS

	100 kHz	500 kHz
at 500 meters	1.55 meters	0.7 meters
at 700 meters	1.83 meters	0.82 meters

To achieve the required resolution due to the Airy disc yields the aperture radius in Table 22.

TABLE 22. APERTURE RADIUS

	100 kHz	500 kHz
at 500 meters	76 meters	15 meters
at 700 meters	106 meters	21 meters

Even if it is possible to achieve a near field solution, the impact of the Airy function makes the technique impossible to pursue.

To achieve high resolution, in this application, is not an obvious and easy task. Even with different kinds of traditional array shading techniques, beamwidths like 0.0014 degrees are impossible to get. Maybe new signal processing techniques, like the frequency domain adaptive beamforming technique can narrow down the beamwidth to what is required. The conclusion is that the design must be restricted to a traditional classification sonar, and the necessary beamwidth will be decided using the reverberation limited active sonar equation.

D. MULTIPATH PROPAGATION STUDY

Multipath propagation originates with a single sonar induced by pulses whose reflected paths arrive at the receiver at different times due to sound bending in the water and reflections from the sea surface and the sea bottom. Multipath propagation occurs primarily with ducted propagation and in shallow water. The major multipath propagation effects are:

* signal fluctuations in amplitude and phase
* signal distortion
* signal decorrelation in amplitude and phase
* frequency broadening

The signal fluctuation can cause fading effects, which means that the target detectability decreases. Signal distortion degrades coherent detection. Decorrelation adversely effects the beam forming properties of multi-element arrays. Finally, frequency broadening implies that a wider receiver bandwidth must be used, which increases the noise and reverberation in the detection process. Therefore, multipath propagation is a very unwanted phenomena. It will be shown that multipath is not a major problem for this design due to the short wavelength and rough boundaries. [Ref. 9, 41]

There are essentially three propagation paths, excluding the direct path, that can cause multipath effects in this application.

* the surface reflecting path
* the bottom reflecting path
* paths due to the thermal microstructure in the water

Figure 41 shows the theoretical multipaths to the target, based on the geometry, that can occur in this case.

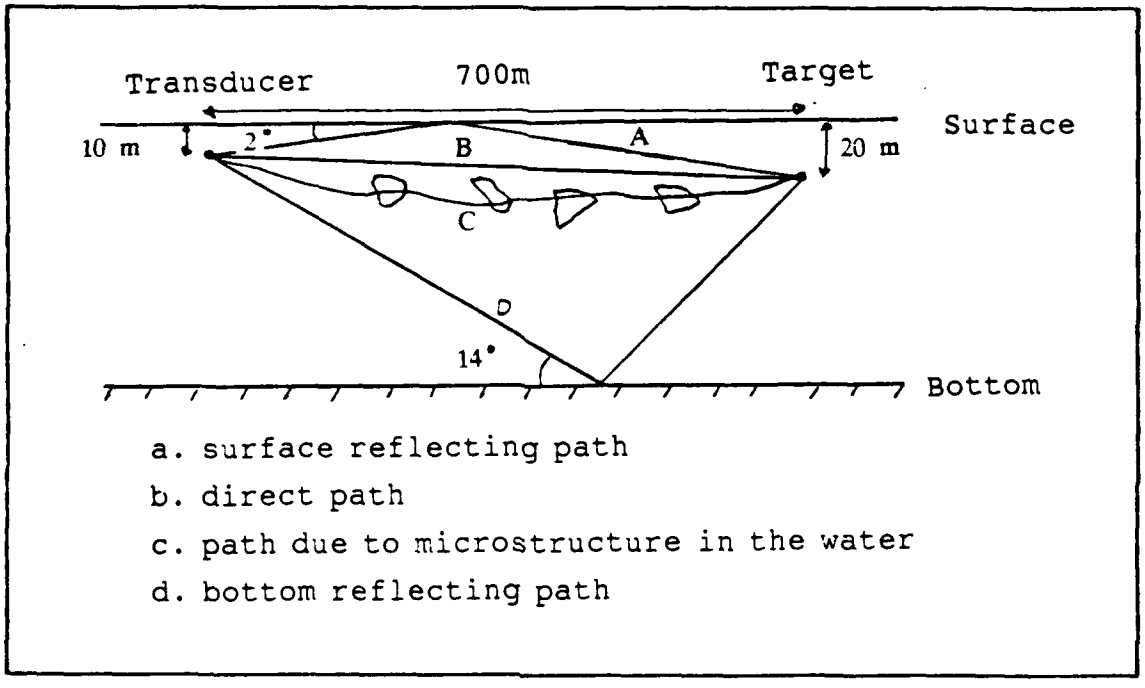

Figure 41. Propagation paths between transducer and target

The surface reflecting path is particularly important to consider when the source and target lie at a shallow depth. Because the path difference between the direct and reflected wave path is small, the target is in the image interference field where, depending on path differences, both waves' intensities constructively or destructively interfere with each other. This phenomena is very significant when the surface is smooth and the incident grazing angle of the

sound field is small. The surface then acts like a perfect reflector. At increasing sea roughness and decreasing wavelengths, the surface turns more and more to a scatterer, which sends out the incident energy incoherent and in all directions [Ref. 9].

The criterion for surface roughness is taken from Clarence and Herman [Ref. 42]

$$R = \frac{2\pi \cdot H \sin\theta_i}{\lambda}$$

where R = Rayleigh parameter

H = average wave height measured from peak to trough

θ_i = incident angle measured from the horizontal

With H = 0.8 m (from Chapter 6), the incident angle 2 and 4 degrees and the wavelengths for 100 and 500 kHz yields the data in Table 23.

TABLE 23. RAYLEIGH PARAMETERS FOR SEA SURFACE

	R (700 m)	R (500 m)
100 kHz	12	23
500 kHz	58	117

If $R << 1$, then the surface acts like a reflector and if $R >> 1$, it acts like a scatterer. There is no doubt that in both cases the surface acts like a scatterer.

The amplitude reflection coefficient of a rough surface is

$\mu = e^{-2R^2}$ [Ref. 43]

For the values of R above, the amplitude reflection coefficients will all be approximately zero.

The conclusion is that there will be no measurable effects at the target by the surface reflecting path.

The effects on a sea bottom reflected path are similar to the sea surface reflection path, but more complex since the sea bottom often consists of multilayered sediments, together with a certain roughness.

The bottom profile with all its data was given in Chapter 6. In order to estimate the specular reflection, a reflection coefficient diagram for this particular bottom is developed in Appendix Q. When only considering the geometrical bottom reflecting path (as shown above in Figure 40), incident grazing angels of 14 degrees (700 m) and 23 degrees (500 m) are found. Comparing these results from the diagram in Appendix Q, a reflection coefficient of 1 is found for 700 m range and 0.3 for 500 m range. The next step is to examine how much the bottom roughness effects the reflected wave. The bottom diagram gives an average height between crest and trough of 5 meters. Calculating the Rayleigh parameter R as above yields the figures in Table 24.

TABLE 24. RAYLEIGH PARAMETERS FOR SEA BOTTOM

	R (700 m)	R (500 m)
100 kHz	507	818
500 kHz	2,533	4,091

Since R>>1 in both cases, the surface is determined to be very rough. Hence, the same expression for calculating the reflection coefficient as given on page 121 is valid. With the R squared factor in the expression, the conclusion is that, even in this case, the multipath effect from a bottom reflection path at the target location can be neglected. A comparison, with the results above, can be done by using Lambert's law for a very rough bottom. [Ref. 6] When using this relationship no frequency dependence has been observed for frequencies over 30 kHz. By using Figure 42 [Ref. 9], the following equation for the scattering intensity can be shown:

$$I_s = \mu I_i \cdot \sin\lambda \cdot dA$$

where I_i = incident sound (intensity)
I_s = scattered sound (intensity)
dA = small surface area

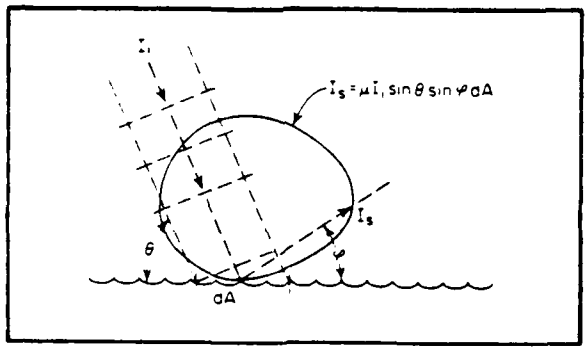

Figure 42. Lambert's law for a scattering surface

It can also be shown by integration that μ is $1/\pi$, if all the incident acoustic energy is scattered into the upper medium and no energy is lost by transmission into the bottom (as in the 700m case) [Ref. 9]. This gives a specular

surface reflection coefficient of 0.019, taking both incident and reflecting angle to be 14 degrees. This result supports the conclusion above that the bottom reflecting path is negligible.

The third multipath cause to consider is due to the lack of homogeneous sea temperatures that constantly change the index of refraction. These temperature changes occur like cells in the direct path between the source and target. Each cell bends the sound ray differently, depending on the launch angle. As a result, when they converge at the target, multipath effects occur. Different equations estimating the cell sizes and sound velocity deviation and their impact on the transmitted pressure pulse are developed by Urick [Ref. 9, 41]. There are no data available in order to do estimations in this case.

In conclusion, the multipath results above support the assumption that only the use of a direct sound path between the source and the target is reliable in making a target detection. Even if the interacting sound at the target happens to be small, it is recommended that the vertical beam pattern be minimized as much as possible to reduce both the multipath and the back scattering (reverberation) effects. When studying the ray diagrams in Appendix O, the depression angle must be on the order of 10 degrees to ensure the propagation of all direct rays. If no direct rays can be found, the chances of detecting the target are very small, despite some scattering into the shadow zones.

E. SONAR DESIGN: STEP 2

1. Back-scattering strength study

In active sonar systems, the returning echo signal comprises both reflections from the target and reflections from the sea surface, the sea bottom and from the water volume. The undesired echo contribution is called

reverberation and is a kind of noise, since it contains no information. The reverberation is a fluctuating, non-stationary process and an amplitude variation of 20-30 dB is common after transmitting the signal. The reverberation amplitude is Rayleigh distributed and the spectral shape is almost identical to the target signal shape. Figure 43 shows an example of how a narrow band signal can vary as a function of time [Ref. 44].

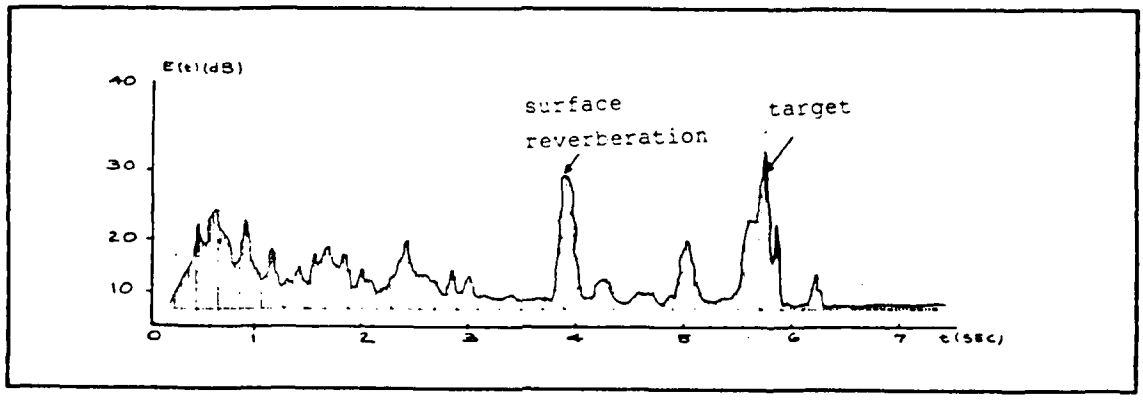

Figure 43. Reverberation and target echo after transmitting a 500 m^2 pulse

The reverberation level depends, among other things, on the scattering strength and the resolution element. Only scattered sound in the resolution element, arriving at the same time as the echo in the receiver, contributes to the reverberation level. The back scattering strength is defined (in dB) as the ratio of the intensity of sound scattered by an area of 1 m^2 or a volume of 1 cubic cm and the intensity of the incident wave. It is important to investigate what regions in the ocean contribute to the total scattering strength. In this case the back scattering situation can be depicted as in Figure 44. This is taken to be the worst case (in January, when multiple regions are involved) [Ref. 9].

The following back scattering regions will be further investigated:

* Surface scattering: surface reflection and bottom reflection
* Surface scattering by a layer of volume scatterers: air bubbles down to 3 meters depth and fish density down to 40 meters depth

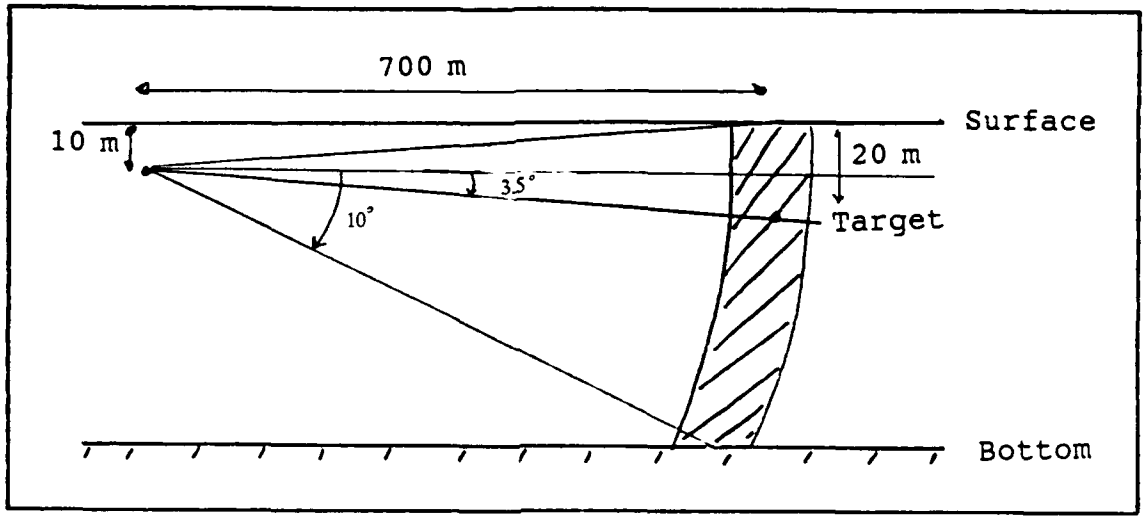

Figure 44. The back scattering regions

The surface scattering for both the sea surface and the sea bottom, has already been investigated in this chapter. The fact that the surfaces are very rough compared to the wavelengths, makes them "scatterers" and the sound is scattered out in all directions incoherently. The sea surface reflection coefficient gives unmeasurably small values when using the Rayleigh scattering model above. The conclusion is that, when using this model, the back scattering contribution is negligible. The Rayleigh model gives the same small reflection coefficient for the sea bottom which also implies negligible back scattering there.

Using the Lambert's Law model instead gives the following equation:

$$S_B = 10 \log \mu + 10 \log \sin^2 \theta$$

where $\mu = 1/\pi$ [Ref. 9]

For a grazing angle of 10 degrees, the scattering coefficient becomes -20 dB.

Urick [Ref. 9] gives values for bottom scattering strengths vice grazing angles that are based on many measurements and frequencies up to 100 kHz (Figure 45), but does not indicate bottom roughness.

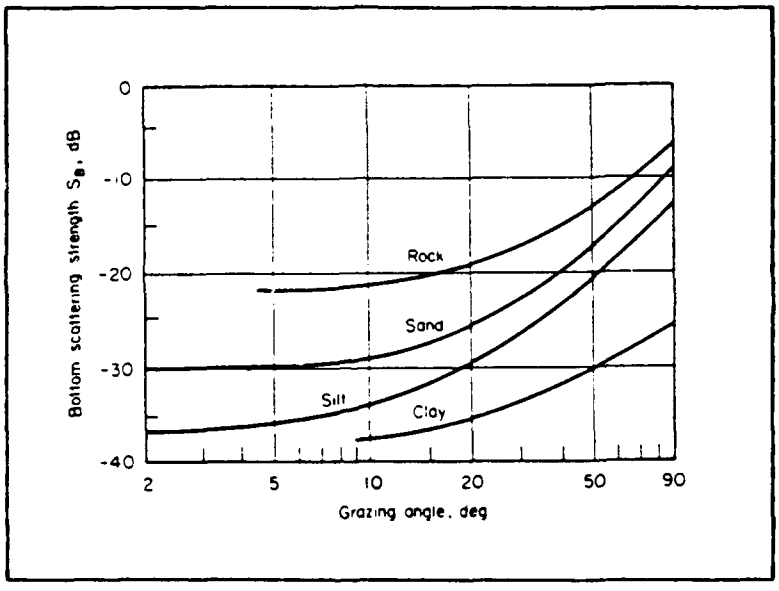

Figure 45. Bottom backscattering strength as a function of grazing angle

A 10 degree grazing angle gives S_B = - 38 dB for clay.

The values above are quite far from each other. Since the speed of sound gradients, during most of the year, are negative, the sound waves are most often bending down toward

the bottom. Hence, the bottom scattering region is more important to consider than the sea surface. Therefore, a worst case value of -20 dB will be assigned as the total back scattering from both surfaces.

"Surface scattering with layer of volume scatterers" models can be used when there are scatterers in layers, such as bubbles and fish. However, instead of calculating a volume scattering situation, the finite layer concept makes it possible to use a surface scattering model. The surface scattering strength S_S is then:

$$S_S = S_V + 10 * \log H \text{ [Ref. 9]}$$

where H = layer depth

Air bubbles are most frequently located in a layer near the surface, and their sizes and numbers depends on the agitation of the sea surface (wind and waves) and the water (fresh water, ocean water, coastal water, etc.). No measured values of bubble sizes and densities have been available for the Baltic, so an estimation must be made. Clarence and Herman [Ref. 42:p. 173] show a figure that summarizes bubble content in water determined by experiments.

For coastal waters there is an average of 10^3 bubbles per cubic meters at 3.3 meters. Their sizes reach from 1 m to 40 m, so an average size of 20 m will be used for the calculations. The bubbles' back scattering can be computed as follows [Ref. 9]:

$$S_V = 10 \cdot \log\left[\frac{n\sigma_s}{4\pi}\right] \qquad (1)$$

where σ_S = scattering cross section

n = bubbles /yd^3 [Ref. 9]

To find the scattering cross section, the following equation applies:

$$\sigma_s = \frac{4\pi \cdot a^2}{\left[\left[\frac{f_r^2}{f^2} - 1\right]^2 + \delta^2\right]} \qquad (2)$$

where f_r = bubble resonant frequency

δ = damping constant [Ref.9]

Further, the bubbles' resonance frequency must be calculated according to the following equation:

$$f_r = \frac{326}{a} \cdot \sqrt{1 + 0.03\, d} \qquad (3)$$

where d = depth in feet [Ref.9]

To compute the scattering cross section in Equation 2, the damping constant of air bubbles in water must be determined. This damping constant is a measure of the dissipation process in the bubbles and is the reciprocal of the bubbles' Q (Quality factor). Figure 46 gives the theoretical damping of resonant bubbles in water [Ref. 9].

Using Equation 3 with the values for bubble radius and the depth indicated above, the bubble resonant frequency is 186 kHz. Then calculating the scattering cross section for both frequencies (100 and 500 kHz) together with a damping constant of 0.1 gives:

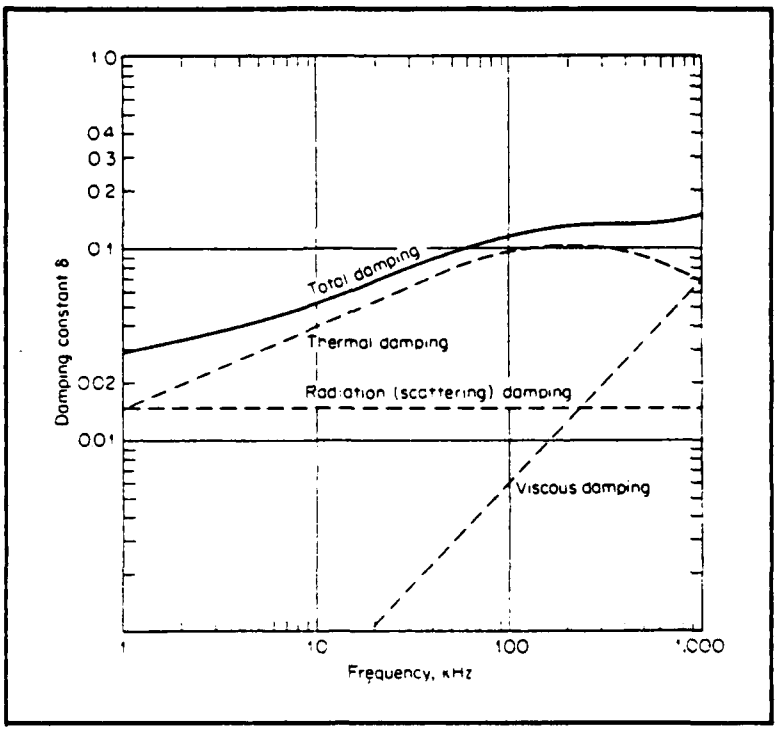

Figure 46. Theoretical damping of resonant air bubbles in water

For 100 kHz $\sigma_s = 8.3 * 10^{-6}$

For 500 kHz $\sigma_s = 6.7 * 10^{-5}$

Finally, using Equation 1 to calculate the scattering strength yields

100 kHz $S_s = -31.8$ dB

500 kHz $S_s = -22.7$ dB

Converting these values into a surface scattering case gives:

For 100 kHz $S_a = -31.8 + 10 \log 3.3 = -26.6$ dB

For 500 kHz $S_a = -22.7 + 10 \log 3.3 = -17.5$ dB

The scattering strength for fish population can be computed in the same way as above by using Equation 1. No measured values for the fish average size and population density in the Baltic have been found, so even in this case an estimation must be made. In Lake Michigan in the United

States, fish density samples have been taken for various depths and locations. An average fish density of 5.7 * 10^{-3} fishes per cubic meter has been computed for this lake. [Ref. 42] Even if the Baltic has brackish water and Lake Michigan has fresh water, this is the best estimation we have. Using the diagram in Urick [Ref. 9:Figure 9.19], the target strength (TS) for a particular fish length and transmitting frequency is given. The transmitting frequency dependence on the TS is very weak, compared to the size of the fish. The Baltic has no really big fish as in the deep oceans. Cod, salmon and herring are some good representatives of the population. Based on this, an average fish size of 7 inches is adopted. Using the diagram in the reference for 100 kHz gives a TS of -40 dB per fish. Using Equation 1 and noting that

$$TS = 10 \cdot \log \frac{\sigma s}{4\pi} \qquad \text{yields}$$

$S_v = 10 * \log 5.7 * 10^{-3} + (-40) = -62.4$ dB

Assuming this fish density is true in the whole water column (100 m) gives:

$S_s = -62.4 + 10 \log 100 = -42.4$ dB

No TS value for 500 kHz is indicated in the reference.

In conclusion, the scattering regions in Table 25 will be taken into account:

TABLE 25. SCATTERING REGIONS

Bottom region	-20 dB for both frequencies
Bubble region	-26.6 dB for 100 kHz
	-17.5 dB for 500 kHz
Fish region	-42.4 dB for 100 kHz

In order to get a total backscatter level, these values must be adjusted in a diagram like the one in Figure 47 [Ref. 37].

This gives the final back scattering strengths:

S_s (100 kHz) = -19.1 dB

S_s (500 kHz) = -15.5 dB

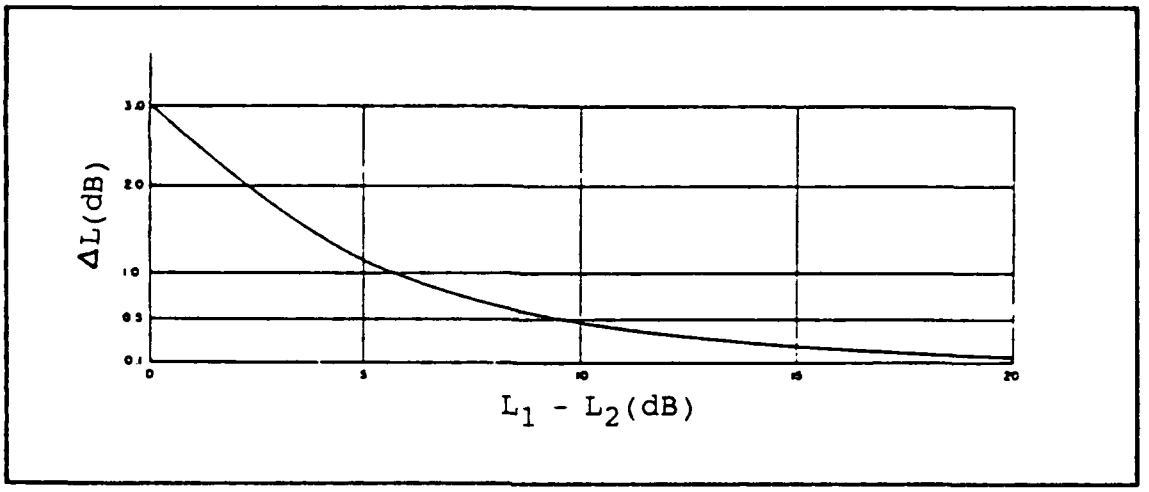

Figure 47. Curve for summation of levels. L_{tot} = L1 + ΔL where L1 > L2

2. Beamwidth calculation

This section will utilize the sonar parameters determined above and first calculate the horizontal beamwidth and then the required transducer size. The reference transducer (circular and 1 meter in diameter) will still be used in the initial calculations, but after a sensitivity analysis regarding the target strength (TS) has been performed, other transducer sizes and shapes will be discussed.

The active sonar equation with surface reverberation limited performance yields [Ref. 32]:

$$RL = SL - 2TL + 10 \log r + S_a + 10 \log (\theta c \tau/2)$$

where θ = horizontal beamwidth

τ = pulse length

The equation will be solved for θ, after determining the reverberation level according to Figure 36 on page 99. Then the following equation will be used for the sensitivity analysis [Ref. 32]:

$$TS = S_a + 10 \log r + 10 \log(\theta c \tau /2) + DT$$

where TS is the target strength of the mine.

A best choice of sonar parameters will be determined under the calculation process. The goal is to come up with rough values for a transducer size and shape that fulfills the major sonar objective. All calculations are carried out in Appendix Q and only the results will be shown here. The first step is to calculate the noise floor level (NL - DI), where DI is the directivity index for the reference transducer. The noise floor level yields:

for 100 kHz 23.6 dB

for 500 kHz 9.6 dB

These noise levels are now taken to be the required reverberation levels (according to Figure 36 on page 99.)

The second step is to calculate the necessary source levels in order to get the required detection ranges and to calculate the required horizontal beamwidths as shown in Table 26.

TABLE 26. DETECTION RANGES AND BEAMWIDTHS

BW (in degrees)	Range	Frequency (kHz)
1.888	500	100
1.397	700	100
0.787	500	500
0.556	700	500

Noting that the reference transducer gives horizontal beamwidths of 1.397 degrees for 100 kHz and 0.556 degrees for 500 kHz we can conclude that satisfying the sonars required range, is possible. In addition, given the decrease in sonar size requirements, other objectives, simple logistics and low cost, for example; become possible once the carrier frequency is determined. Since 100 kHz gives beamwidth values that makes the transducer sizes reasonable, this lower frequency is preferred from a hardware point of view. Further, since the primary goal is to detect a mine at a distance of 700 meters, a 1.397 degrees beamwidth is acceptable.

The third step is to vary the target strength versus beamwidth, and to make a conclusion of a realistic target strength, using parameters from a "real" mine. From the calculations in Appendix Q, pages 4 and 5, a target strength of +5 dB is determined. A beamwidth of 4.423 degrees is then adequate, which means that the circular transducer can be reduced from a diameter of 1 meter tc 0.22 meters. The necessary SL and DI will now change to 168.5 dB and 33.3 dB.

The horizontal beamwidth requirement has now been met, but the vertical beamwidth is left to be considered. The section on multipath propagation indicates that the vertical beamwidth must be at least 25 degrees in order to utilize all the direct paths to the target (considering the whole year). Since a circular transducer creates a pencil beam, this will not give an appropriate beam pattern. There is a possibility, of course, to use a pencil beam and then scan through the required search volume both vertically and horizontally. This takes time however, and the scan time must be made as short as possible. The original reason for choosing a circular transducer was a trade off between maximum transducer size (1 meter), practical handling and sonar dome shape. Since the sizes now turn out to be much

smaller, a planar array or aperture is an option. The advantage of a planar aperture is that a vertical beamwidth of 25 degrees is possible to achieve, together with a narrow horizontal beamwidth (fan beam). The following approximate equations can be used to calculate the planar aperture. [Ref. 32]

$$BW(v) = \lambda / L1$$
$$BW(h) = \lambda / L2$$

where BW(h) = horizontal beamwidth
BW(v) = vertical beamwidth
L1 = transducer width
L2 = transducer length

For the beamwidths above, a rectangular planar transducer will measure a length of 0.2 meters and a width of 0.04 meters. The new values for the directivity index and source level yields 25.5 dB and 176.3 dB.

The next question is, "Is it possible to transmit a SL of 176.3 dB with that aperture size due to the cavitation threshold?" When a transducer is excited, cavitation bubbles are developed on the front of the transducer.

> "These bubbles are a manifestation of the rupture of the water caused by the negative pressures of the generated sound field. These negative pressures tear the liquid apart, so to speak, when they exceed a certain value called the cavitation threshold." [Ref. 9:p. 76]

The cavitation threshold can be calculated using the following equation [Ref. 9]:

$$I_c = 0.3 * p \quad W/cm^2$$

where I_c = cavitation threshold, W/cm^2

p = peak pressure of sound wave causing cavitation (in atm)

The p value is determined by Urick [Ref. 9:Figure 4.6] for 100 kHz to be 2 atm (worst case). This gives a cavitation threshold of 1.2 W/cm^2. With a transducer area of 80 cm^2, the maximum power is 96 W. Using the following equation solves for the source level:

$$SL = 10 \log P + DI + 171 \quad re\ 1\ Pa$$

where P = power in W

With a DI of 25.5 dB re 1 Pa, the maximum source level will be 216 dB. Since the required source level is far under this level, the bubble cavitation is not a problem.

The calculations above have utilized the limiting value for the reverberation which occurs when the echo changes from being masked by noise to being masked by reverberation. Increasing the power further will not influence the range but only emphasize the reverberation limited performance. In an actual design it might be advisable to increase the SL for hardware reasons since a SL of 176.3 dB gives very low power values (0.01 W).

F. TRANSDUCER STUDY

The transducer can be designed as a planar array or a planar aperture. The advantage of using an array technique is that FFT beamforming and beamsteering can be utilized and the array itself need not to be scanned inside the dome. An array consist of many small transducer elements which must be amplitude and phase weighted together. This implies a more sophisticated signal processing technique. One disadvantage, in this case, is that the wavelength is only 0.015 meters for 100 kHz. When considering beamsteering with an array, the transducer elements must be spaced at a distance less then 1/2 wavelength in order to avoid grating lobes. This means that the element spacing must be less than 0.0075 meters. Narrow spacing can give unwanted radiation coupling between the elements. Also, in order for the

elements to act like point sources (which makes the beam pattern prediction easier), the element length must be small compared to a wavelength. In this case this means fractions of a millimeter. These facts makes a choice of a steerable array technique very difficult to pursue. However, an array technique might still be utilized in an unsteerable mode, where no phase weighting is performed. To simplify the calculations a planar aperture is chosen for the further transducer design.

The directivity function of a planar aperture can be calculated by taking the two dimensional spatial Fourier transformation of the transducer aperture function. The aperture function is the frequency response of the planar aperture, when it is excited by an input electrical signal. The directivity function is simply the beam pattern of the transducer. The aperture function is normally a complex function, but since, in this case, no beam steering will be used, only the amplitude window (real part) needs to be considered. There are many different amplitude windows to chose from and only a few of them have a closed form solution. It is important in probably all sonar designs to suppress the sidelobes in order to minimize the effects of noise and other unwanted signals. The design then becomes a trade off between the beamwidth and the sidelobe level (SLL), since normally suppressing the sidelobes broadens the beamwidth. A broadening of the mainbeam must be compensated with larger aperture size. Since the size in the design is relatively small, an increase in transducer size is recommended to get low sidelobes. Therefore a Blackman window is chosen as the amplitude window function. This choice results in a sidelobe suppression of -58 dB. A one dimensional Blackman amplitude window function is given by the expression:

$$a(f_1 x) = (0.42 + 0.5 \cos(@\, x/L) + 0.08 \cos(4\, x/L))\ \ \mathrm{rect}(L)$$

where x = transducer in the x direction, i.e., a linear aperture

L = length of the aperture

rect(L) = rectangular window, i.e., a constant.

This one dimensional case can be extended into two dimensions, i.e., a planar aperture. The development of a planar aperture directivity function is shown in Appendix R. The problems to physically manufacture an aperture with a Blackman window response will not be discussed here.

In order to compute the beam pattern, the measurements of the aperture must first be computed. The aperture size can be determined by using the following equation:

$$\Delta\theta := 2\sin^{-1}\left[\frac{\Delta u}{2}\right]$$

where Δu = 3dB beamwidth in direction cosine space

$\Delta\theta$ = horizontal beamwidth (in this case)

and $\Delta u = 1.6444\,\lambda/L$

where L = transducer length

Using this equation with the required horizontal and vertical beamwidths yields an aperture width of 0.319 meters and a height of 0.057 meters. The directivity index (DI) and the required source level stay approximately the same, that is 25.5 dB and 176.3 dB, since the mainlobe beamwidths have not been changed.

In order to make sure that the target is in the far field, the range to the far field must be computed. The following equation can be used [Ref. 33]:

$$R\ (\text{far field}) = \frac{\pi \cdot r^2}{\lambda}$$

where

$$r := \sqrt{\left[\frac{L_x}{2}\right]^2 + \left[\frac{L_y}{2}\right]^2}$$

For more details see Appendix R.

The range to the far field is 0.16 meters. Since this is much less than 700 meters, the target is in the far field. The closed-form solution for the normalized directivity function of the Blackman window is shown in Appendix R.

Appendix R also shows the computed directivity function or beam pattern for the aperture.

The planar aperture must cover a sector of 20 degrees. With a beamwidth of 4.423 degrees at 700 meters, the aperture must be able to turn ±7.8 degrees from the ahead direction (Figure 48).

G. DESIGN SUMMARY

The original objective was to design a sonar with the ability to detect a mine at a distance great enough to allow an avoiding maneuver. In addition, the sonar must fulfill "practical" objectives like size, cost and logistic handling. Different design approaches have been taken according to these objectives. Each approach had strengths and weakness whose relative importance had to be evaluated. One weak aspect of the resulting design is the lack of

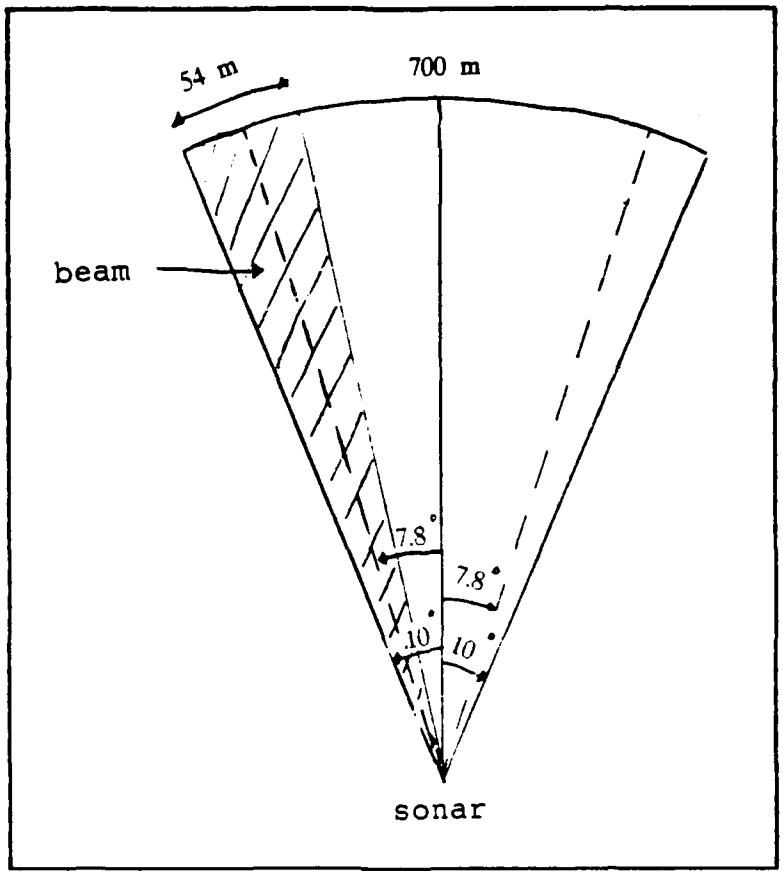

Figure 48. Transducer scan pattern

"real" measured values for parameters such as back scattering strength and target strength. The design, then, is based on the "reasonableness" of the estimates used. One strong aspect is that it is possible to achieve a practical solution for the given sonar objectives, despite the very complex water environment. In order to achieve a sonar design that allows ship operation the entire year, much more research and measurements must be done in the real environment. The sonar design result is summarized in Table 27 on the next page.

TABLE 27. SONAR DESIGN RESULT

Carrier frequency:	100 kHz
Source level:	>176.3 dB re 1 μ Pa
Transducer size:	0.32 X 0.06 meters
Sidelobe level:	-58 dB (Blackman window)
Pulse length:	0.8 msec
Beamwidths:	4.4 (H) X 25 degrees (V), tilted 5 degrees up from horizontal
Detection:	Incoherent detection (energy detection)
Waveform:	CW pulsed
Sonar range:	700 meters
Sonar depth:	10 meters
Sonar scan:	±7.8 degrees, against head direction

APPENDIX A. GENERAL ARRANGEMENTS OF TANKER

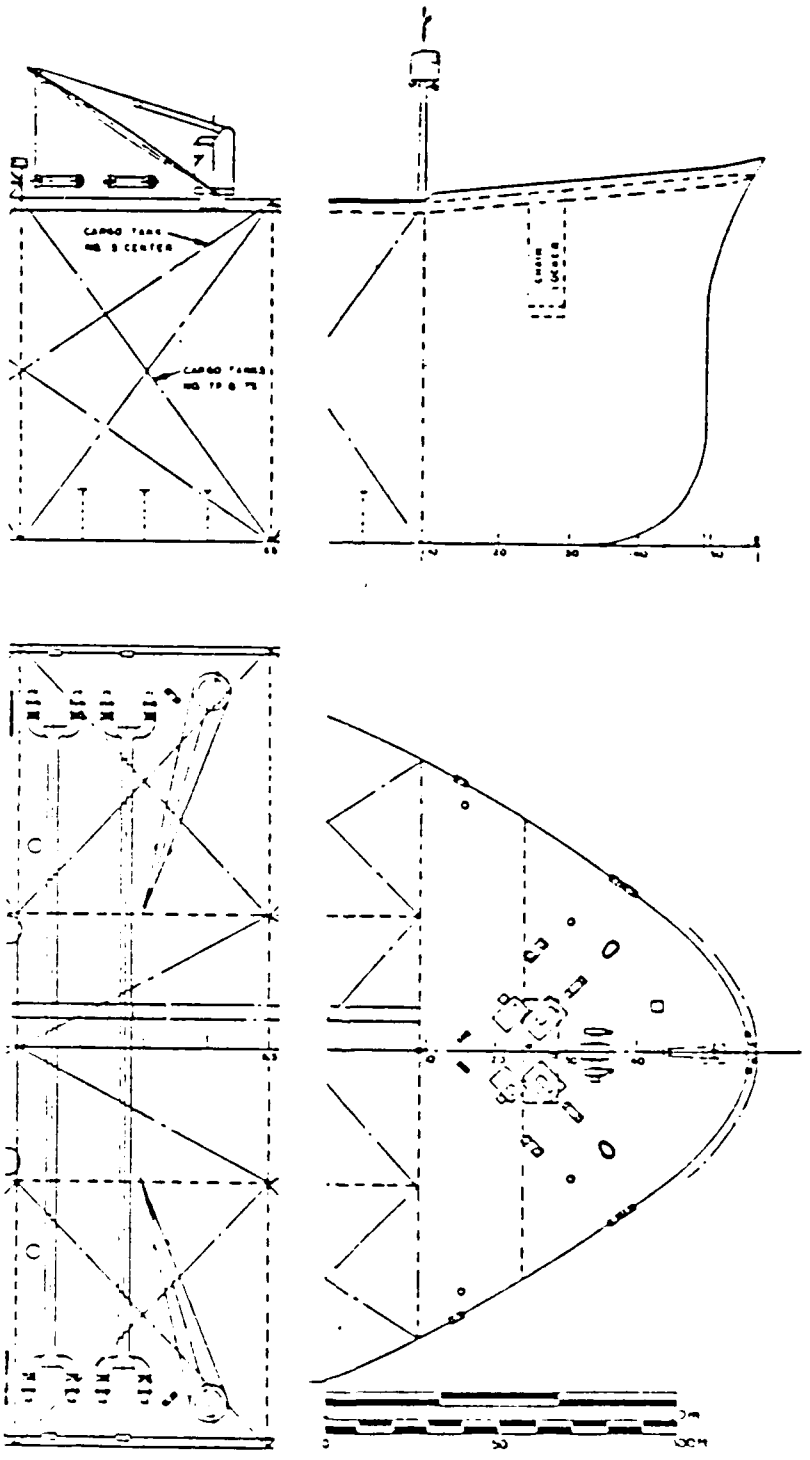

APPENDIX A (page 2)

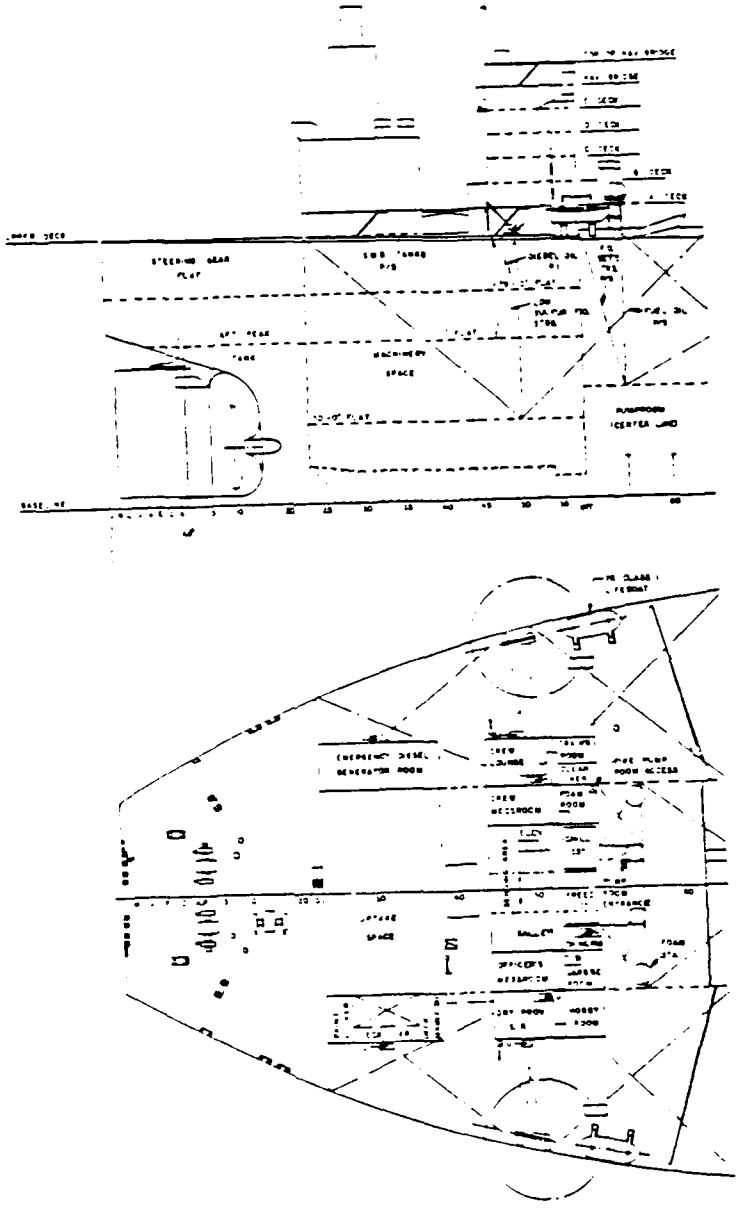

APPENDIX B. CRASH STOP AHEAD TEST

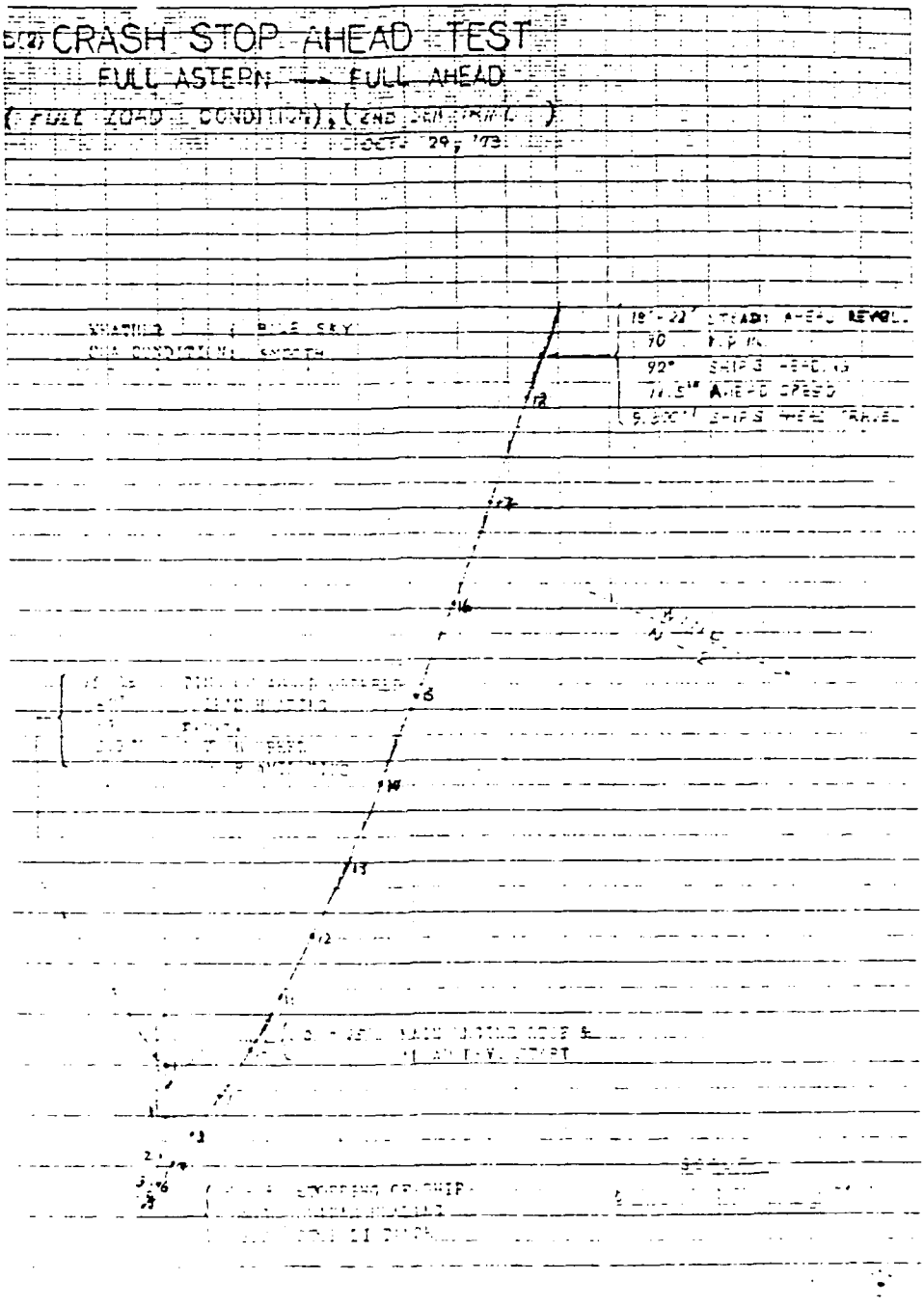

APPENDIX C. CRASH STOP ASTERN TEST

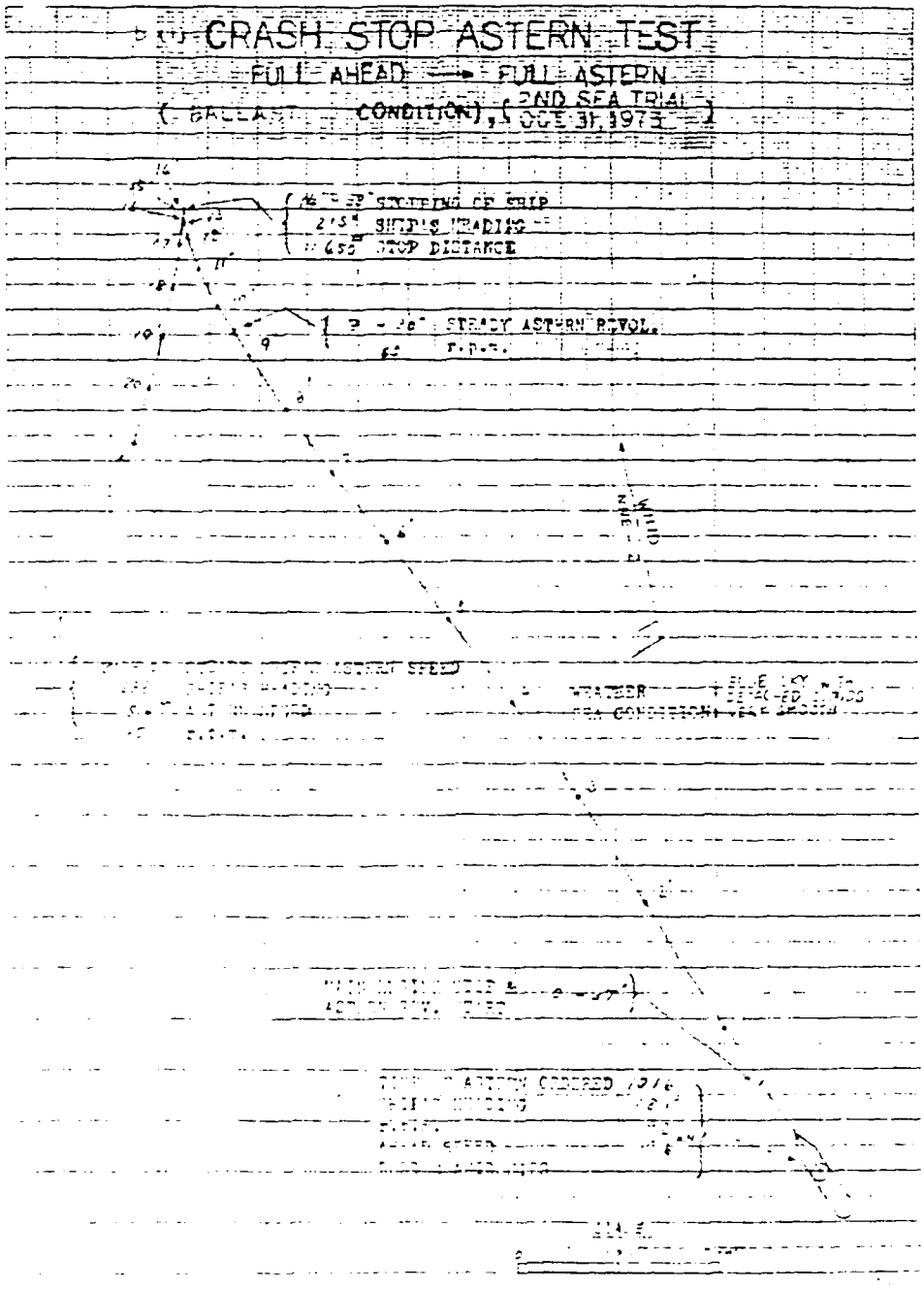

APPENDIX D. MODIFIED ZIP-ZAG TEST

4-(5)

MODIFIED ZIG-ZAG TEST

(UNOFFICIAL TEST)

BALLAST CONDITION (2ND SEA TRIAL)

FIRST HELM ANGLE	STARBOARD	PORT
ENGINE LOAD	NORMAL	NORMAL
DATE	OCT 31, 1973	OCT. 31 1973
WEATHER	BLUE SKY WITH DETACHED CLOUDS	
WIND	ENE - 2	ENE - 2
SEA CONDITION	SMOOTH	SMOOTH
TIME WHEN ORDERED	0614	0602
SHIPS HEAD WHEN ORDERED	[illegible]°	[illegible]°
SHIPS SPEED	[illegible] KN	17.6 KN
SHAFT R P M	92	92
[illegible]	[illegible]	[illegible]

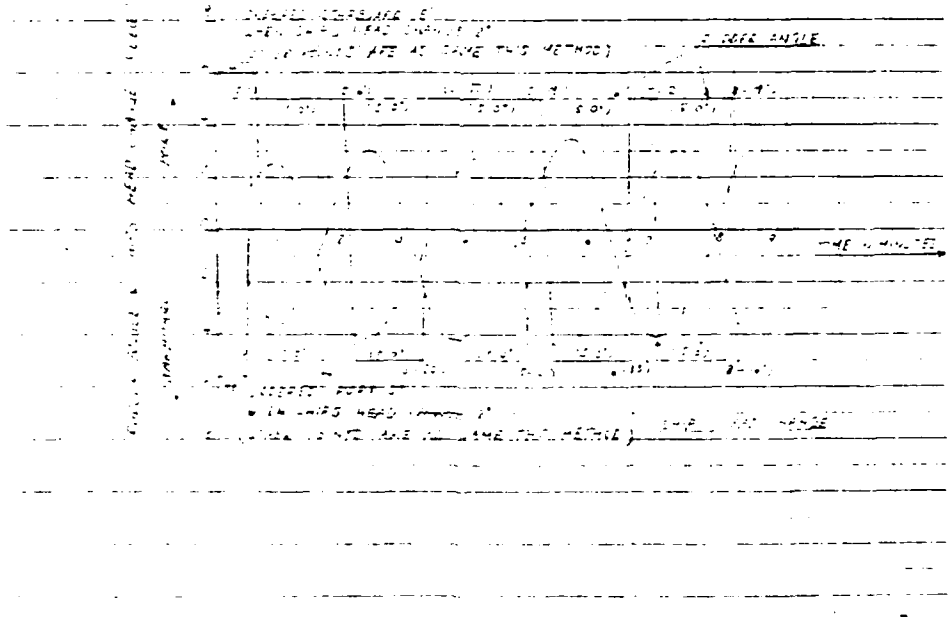

APPENDIX E. TURNING TEST

(BALLAST CONDITION) (2ND SEA TRIAL)

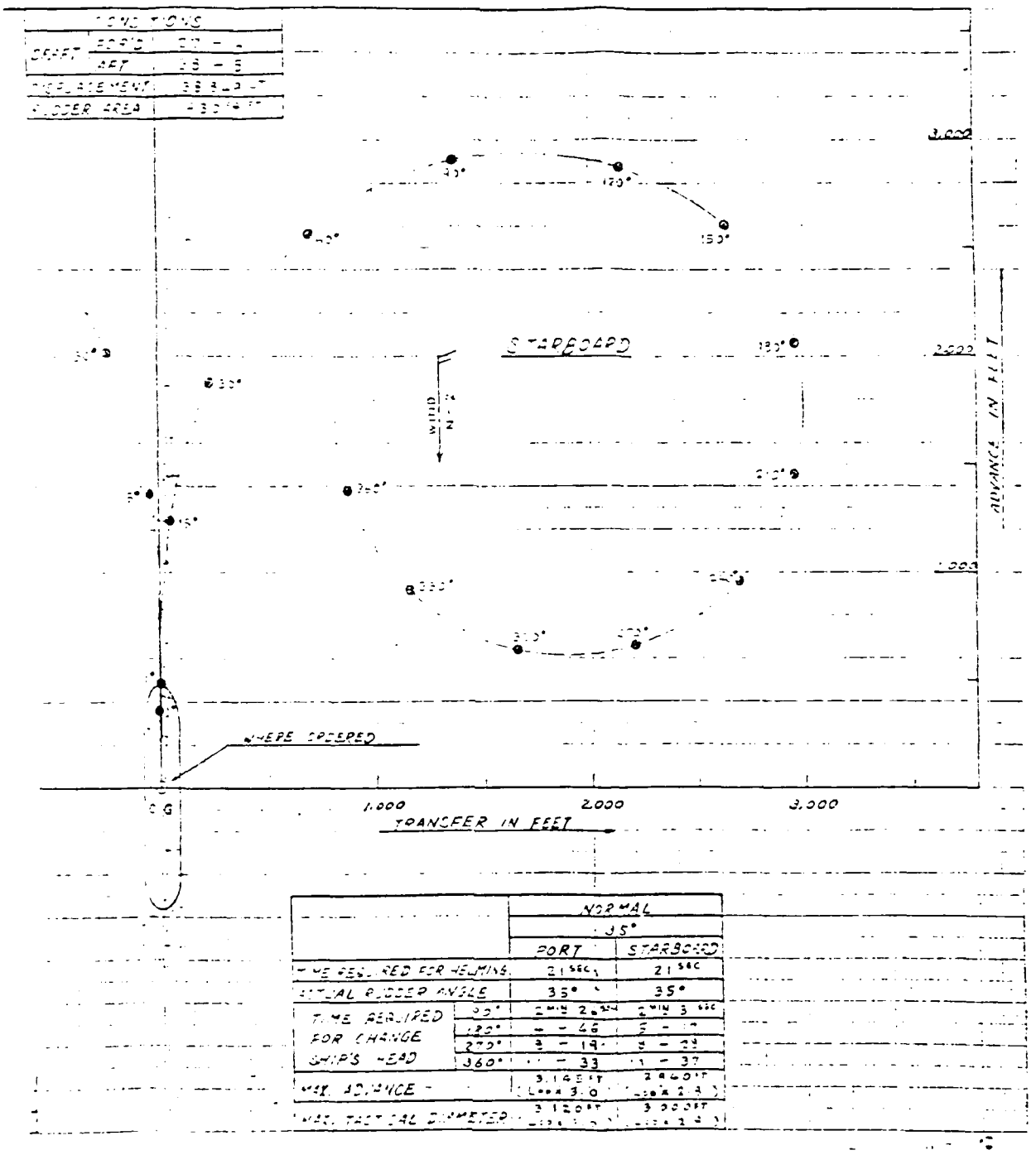

		NORMAL 35°	
		PORT	STARBOARD
TIME REQUIRED FOR HELMING		21 SEC	21 SEC
INITIAL RUDDER ANGLE		35°	35°
TIME REQUIRED FOR CHANGE SHIP'S HEAD	90°	2 MIN 2 SEC	2 MIN 3 SEC
	180°	— — 46	— — —
	270°	— — 19	— — 29
	360°	— — 33	— — 37
MAX. ADVANCE		3,145 FT (Lpp x 3.0)	2,960 FT (Lpp x 2.8)
MAX. TACTICAL DIAMETER		3,120 FT (Lpp x 3.0)	3,200 FT (Lpp x 3.0)

APPENDIX F. REVERSED SPIRAL TEST

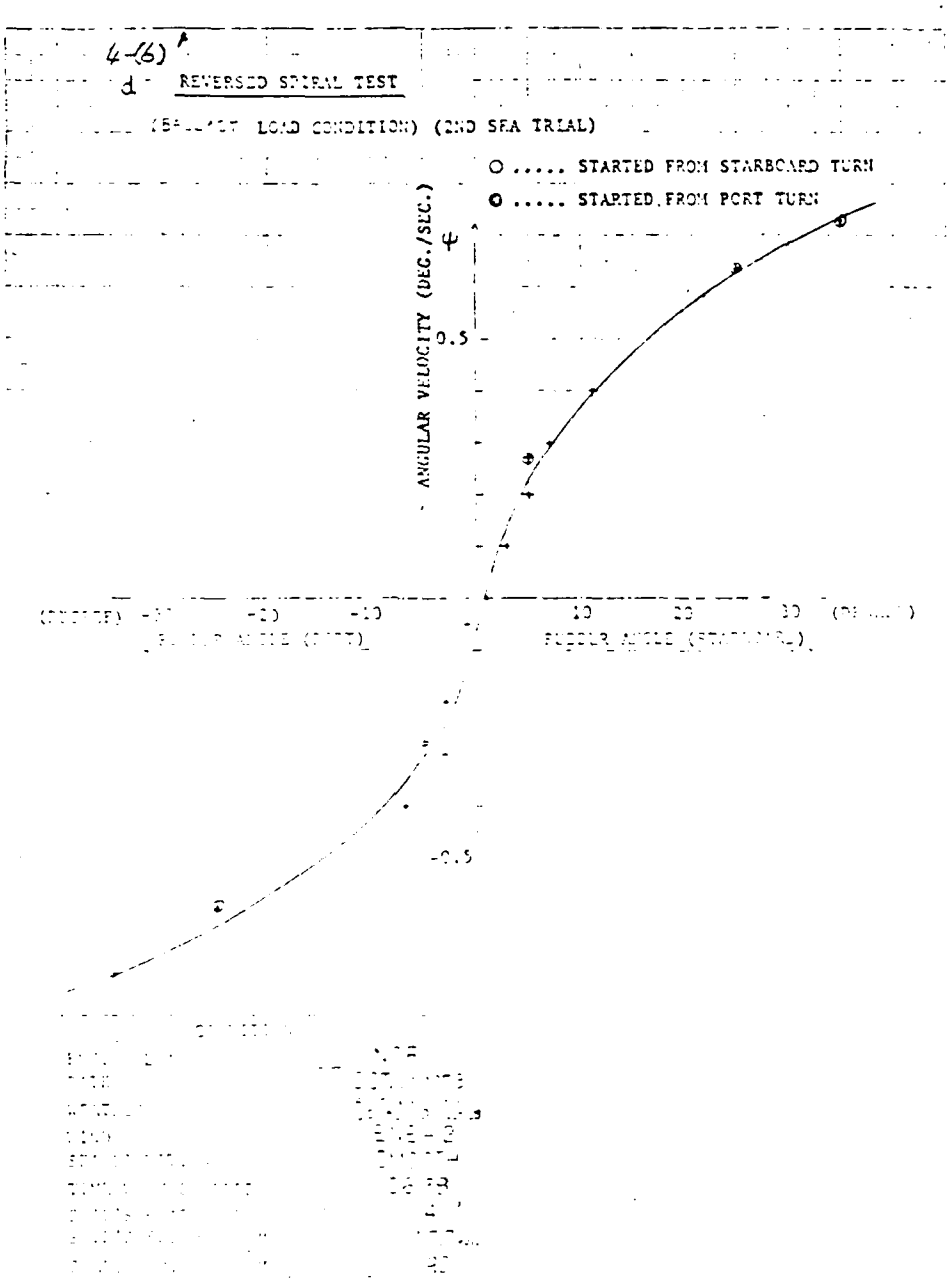

APPENDIX G. ECM ORGANIZATION

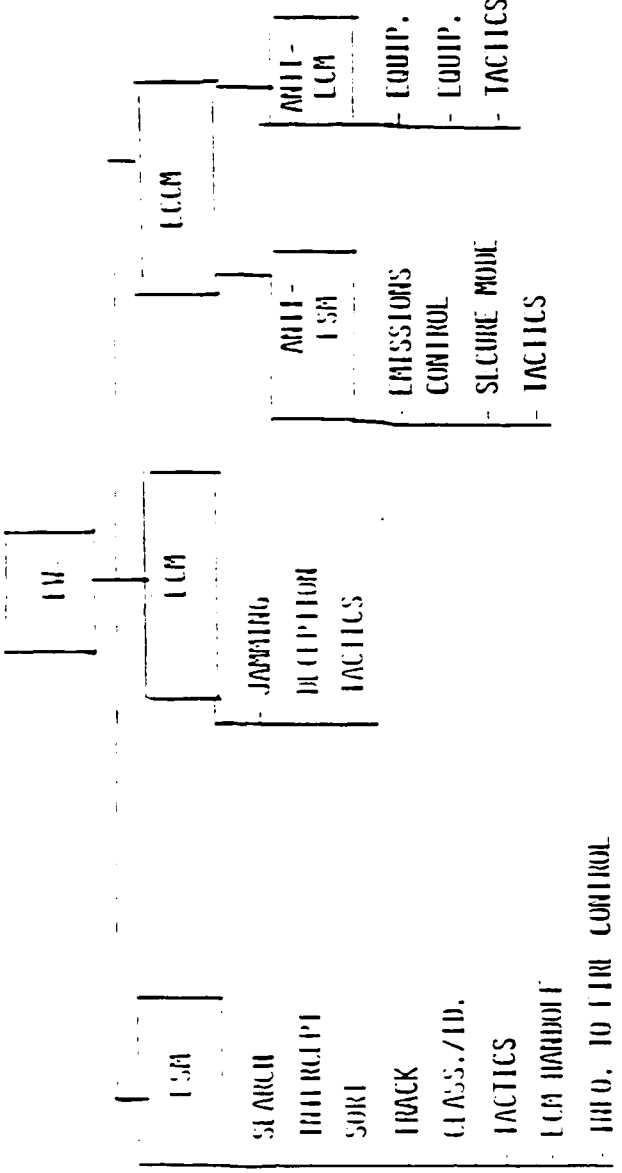

APPENDIX H. CALCULATION OF PULSE DENSITY

Let the height of the emitter and the ESM antenna be :-

$h_s := 10\ m$

The radar horizon limited LOS is :-

$$R := 2\ 1.23\ (nm)\ \sqrt{h_s \left[\frac{m}{ft\ m}\right]} \qquad \text{i.e.} \qquad R = 25\ km$$

The separation between ships at sea is assumed to average :-

$d_{sep} := 5\ nm$

Hence the total number of ships within LOS is :-

$$N_T := \left[\frac{\pi R^2}{d_{sep}^2}\right] \qquad \text{i.e.} \qquad N_T = 25$$

If the fraction of ships that are military is :-

$f := 0.1$

Then the number of civilian and military ships are :-

$N_C := (1 - f)\ N_T \qquad \text{and} \qquad N_M := f\ N_T$

The number of radars (assuming one per civilian ship and two per military ship is :-

$n_R := N_C + 2\ N_M \qquad \text{i.e.} \qquad n_R = 27$

There are also coastal radars and long range radars :-

$$N_{coast} := \frac{2\ R}{10\ km} \qquad \text{and} \qquad N_{long} := 2$$

For the short, medium and long ranges, we can determine the PRFs for maximum range without ambiguity. Let the various ranges be :-

$(\ i := 1\ ..3\ ) \qquad Rm_i :=$

30 nm
90 nm
150 nm

Then the corresponding PRFs are determined from :-

$c := 3 \cdot 10^{8}\ m\ sec^{-1}$ $\qquad PRF_i := \frac{c}{2} \cdot \frac{1}{Rm_i}$

PRF_i (Hz)
2700
1350
540

The number of radars in each range type (1 - short, 3 - long) are :-

$n_1 := N_C + N_M + N_{coast}$, $n_2 := N_M$ and $n_3 := N_{long}$

The number of radars in each category are :-

n_i
30
2
2

totalling $\sum_i n_i = 35$

And the PRFs in each radar range category are :-

$n_i \cdot PRF_i$ (Hz)
81449
3759
[illegible]

totalling $\sum_i n_i \cdot PRF_i = 85897$ Hz

APPENDIX I. MAP OVER THE BALTIC SEA

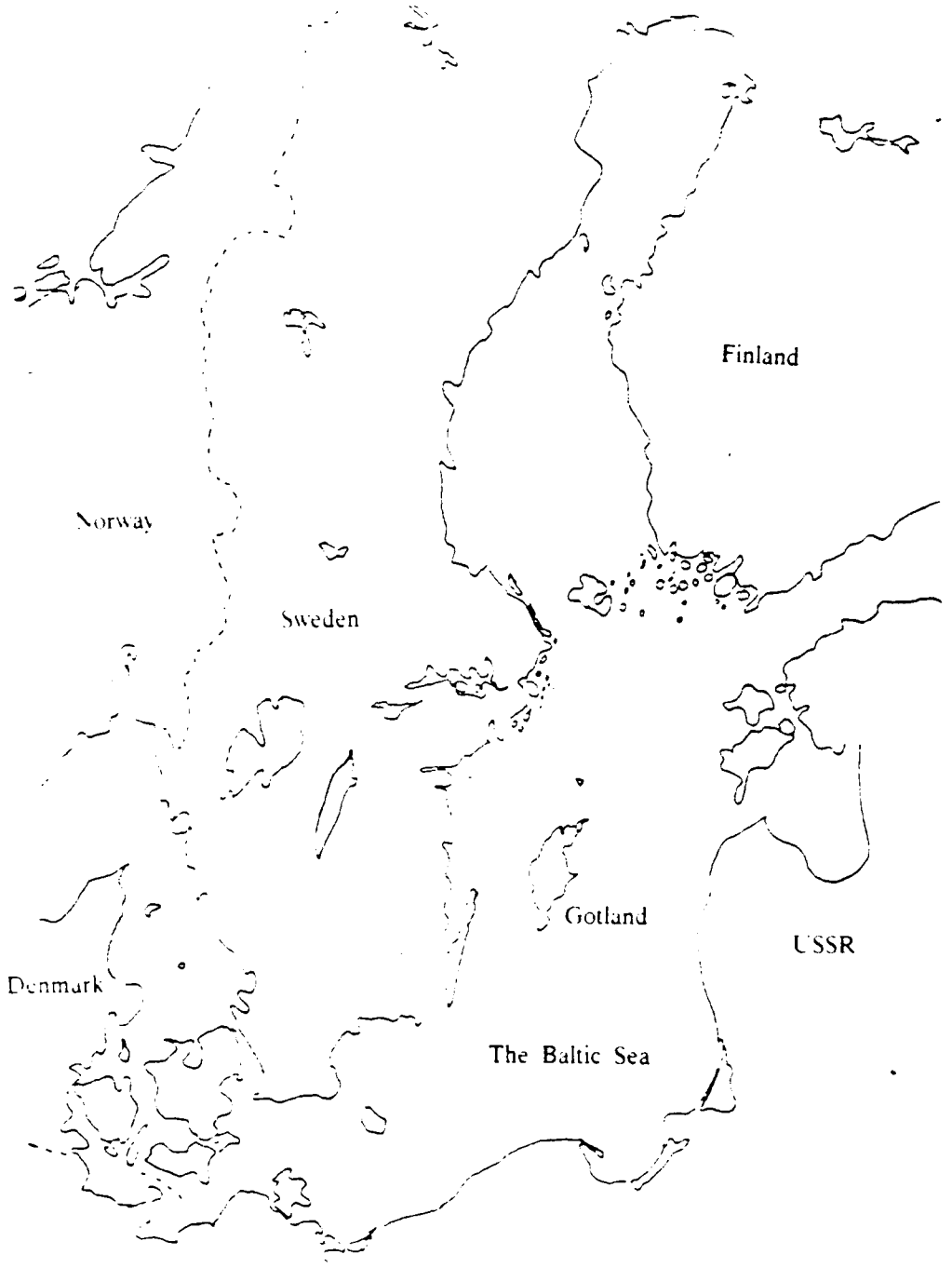

APPENDIX J. WAVE HEIGHT DETERMINATION

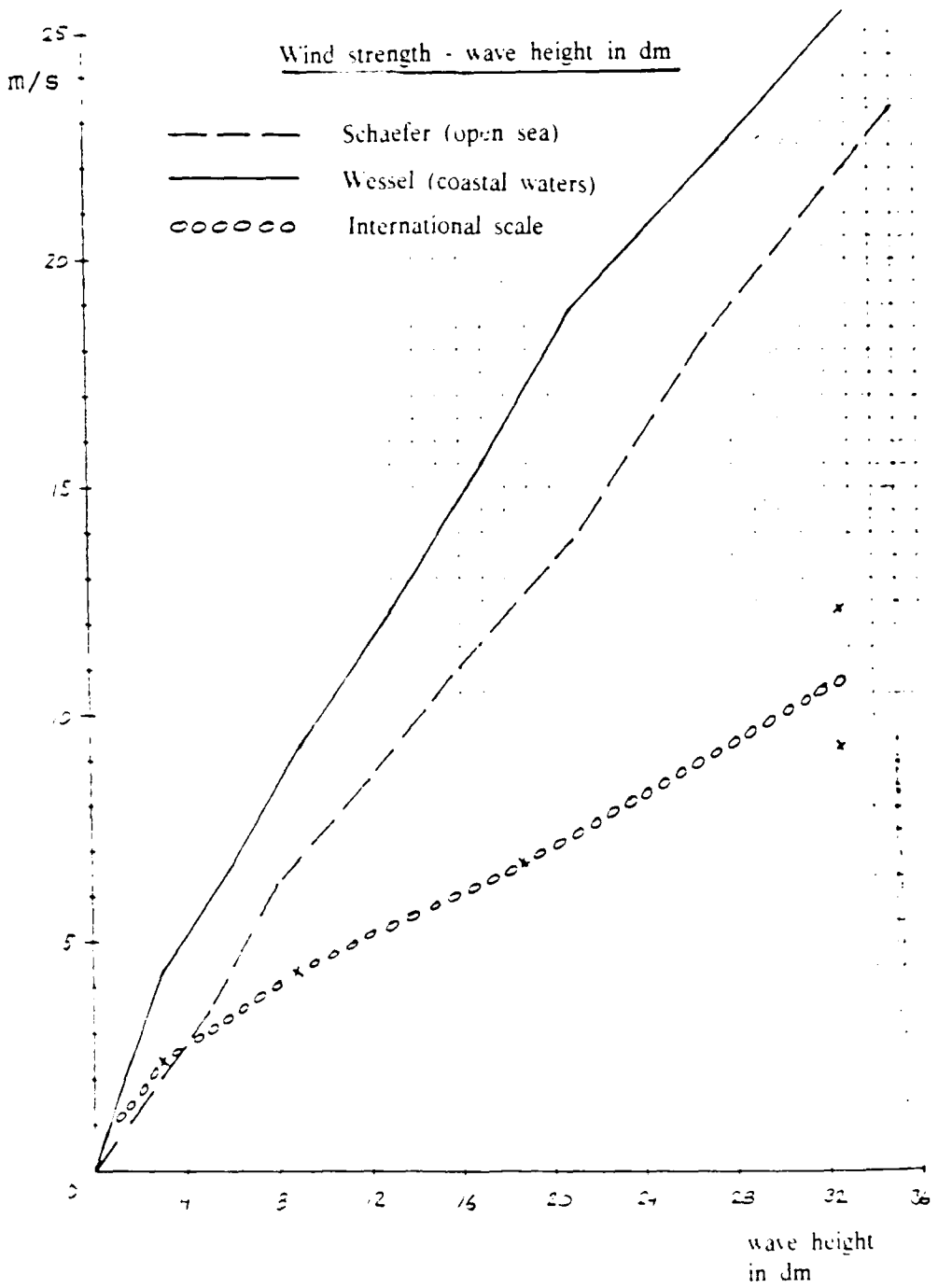

APPENDIX K. ABSORPTION IN dB/km VICE FREQUENCY

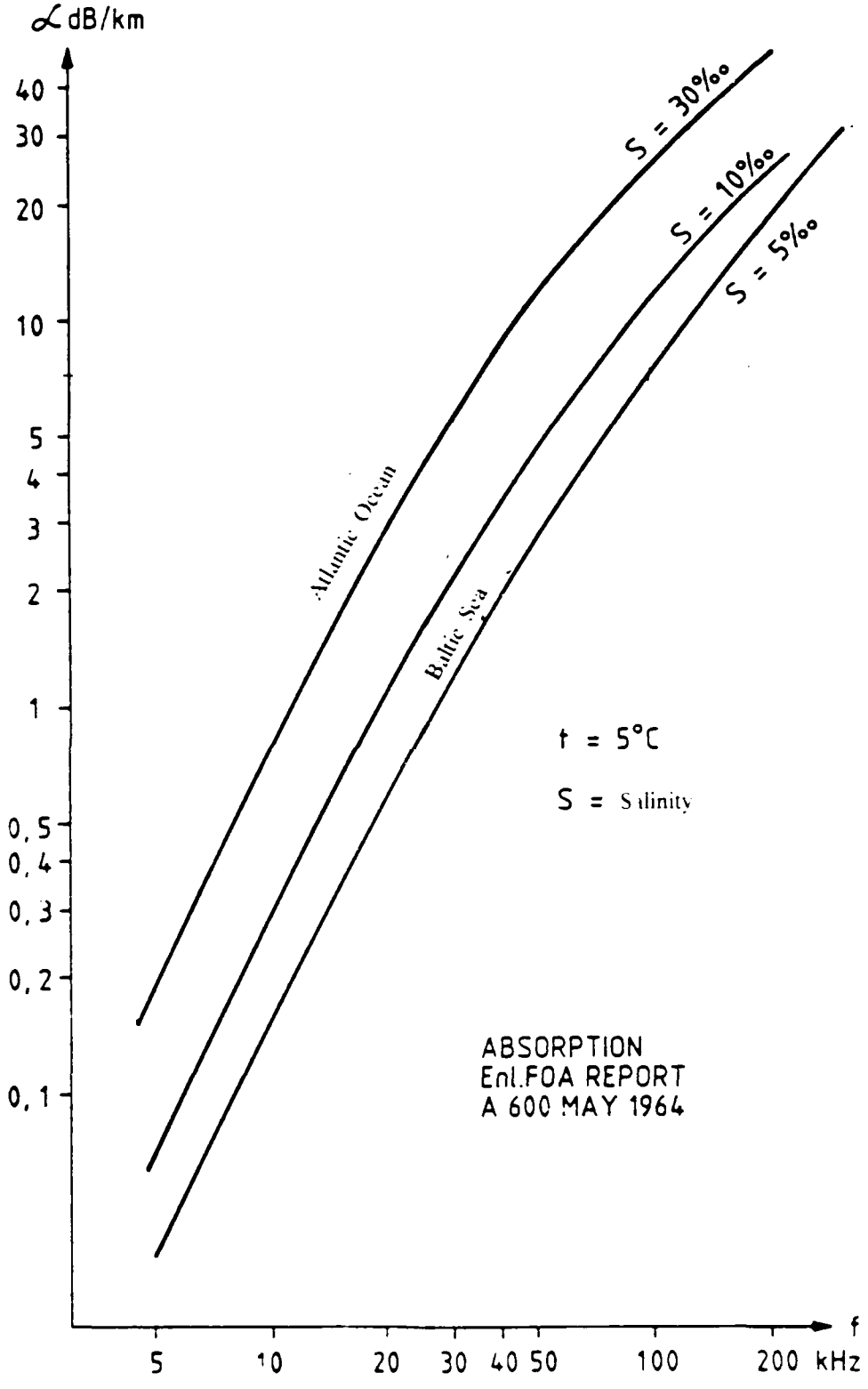

APPENDIX L. LOCATION OF REFERENCE WATER VOLUME

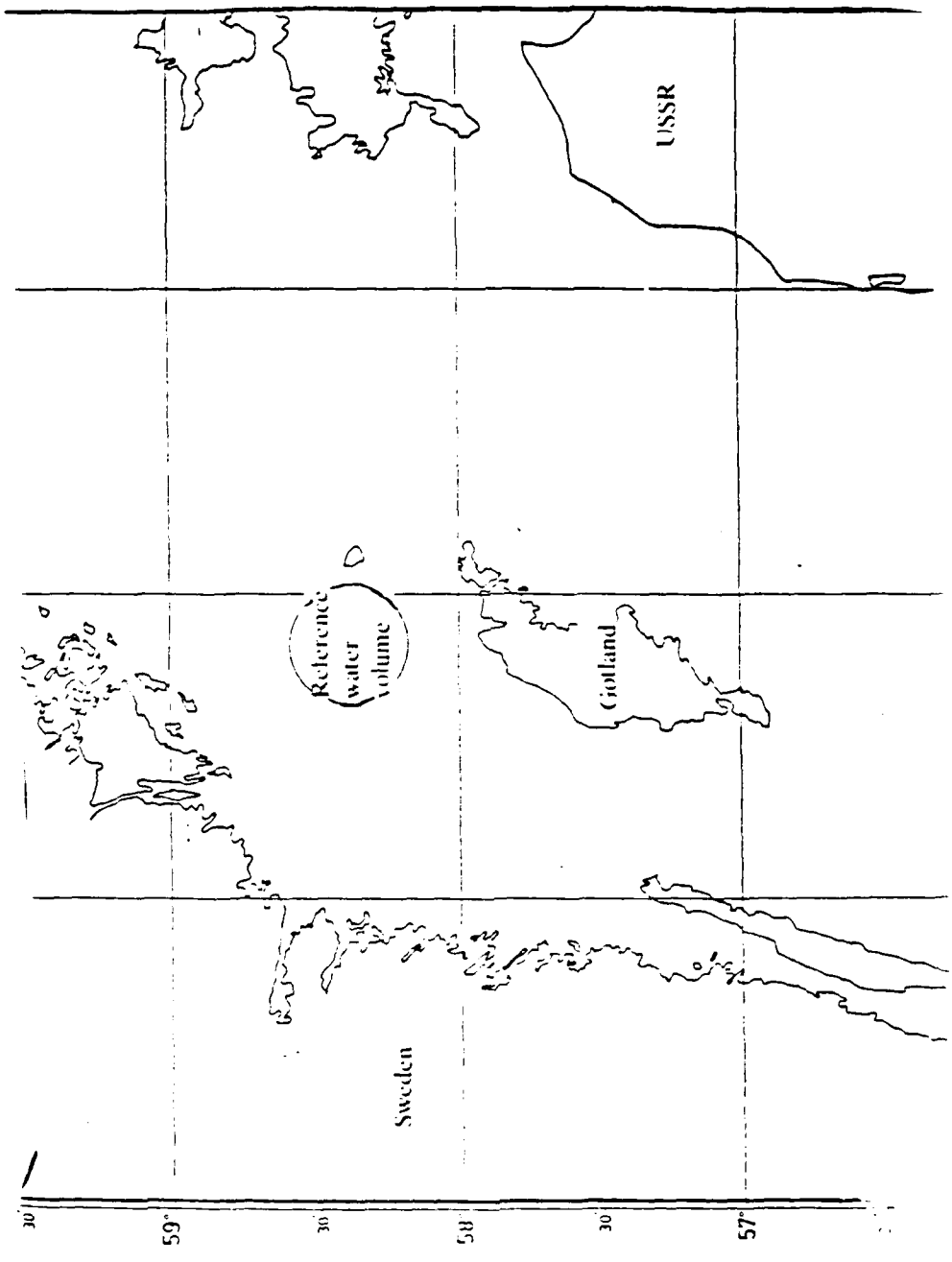

APPENDIX M. SPEED OF SOUND PROFILES WITH RAY TRACING

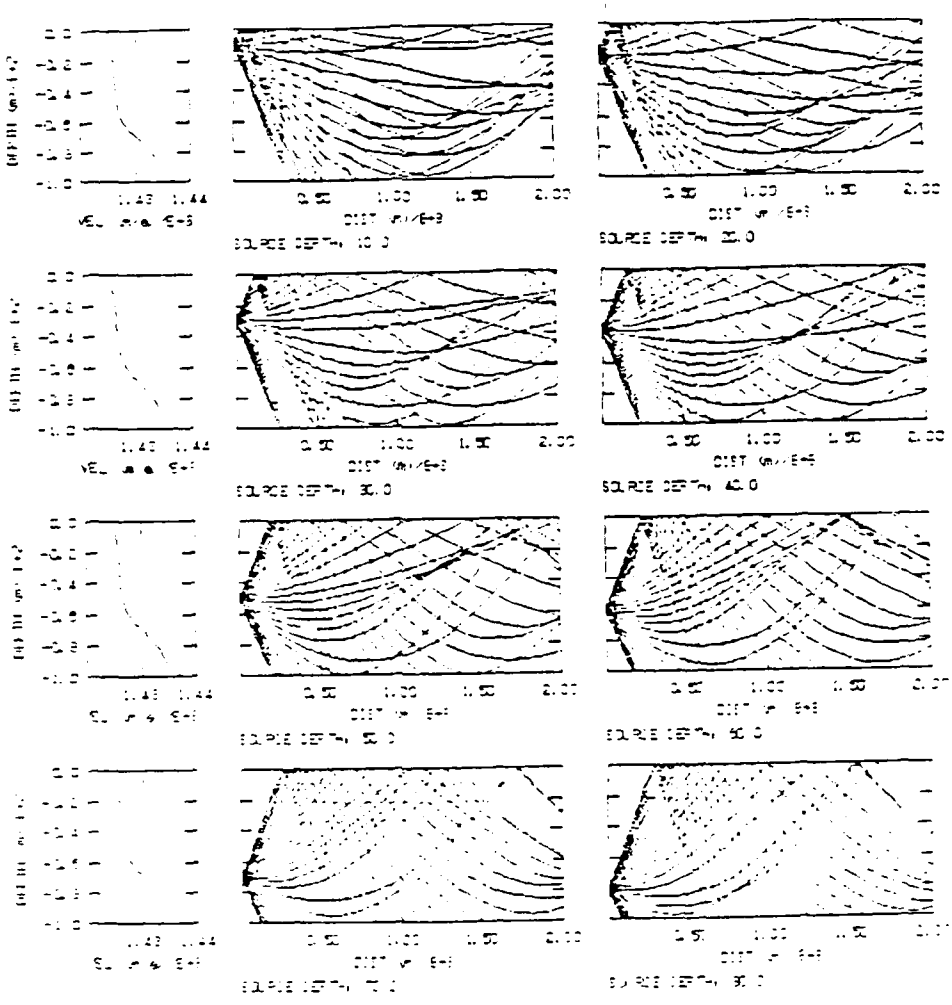

APPENDIX M (page 2)

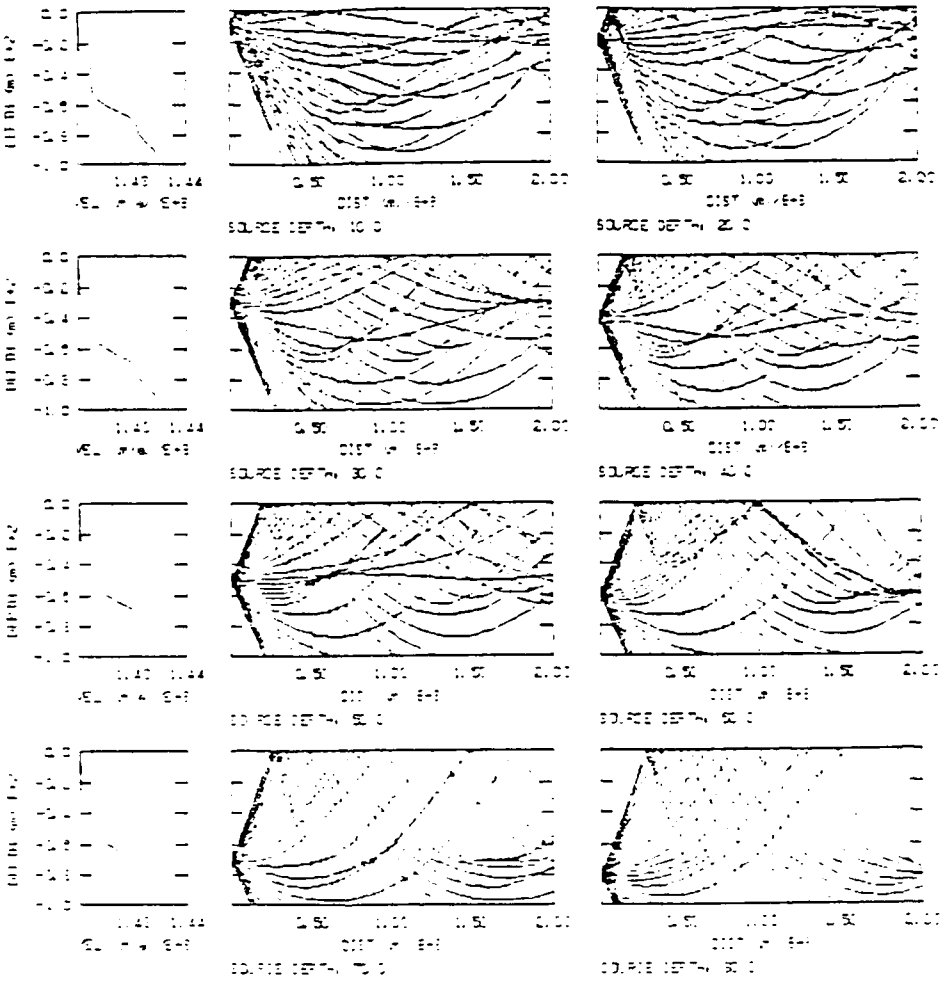

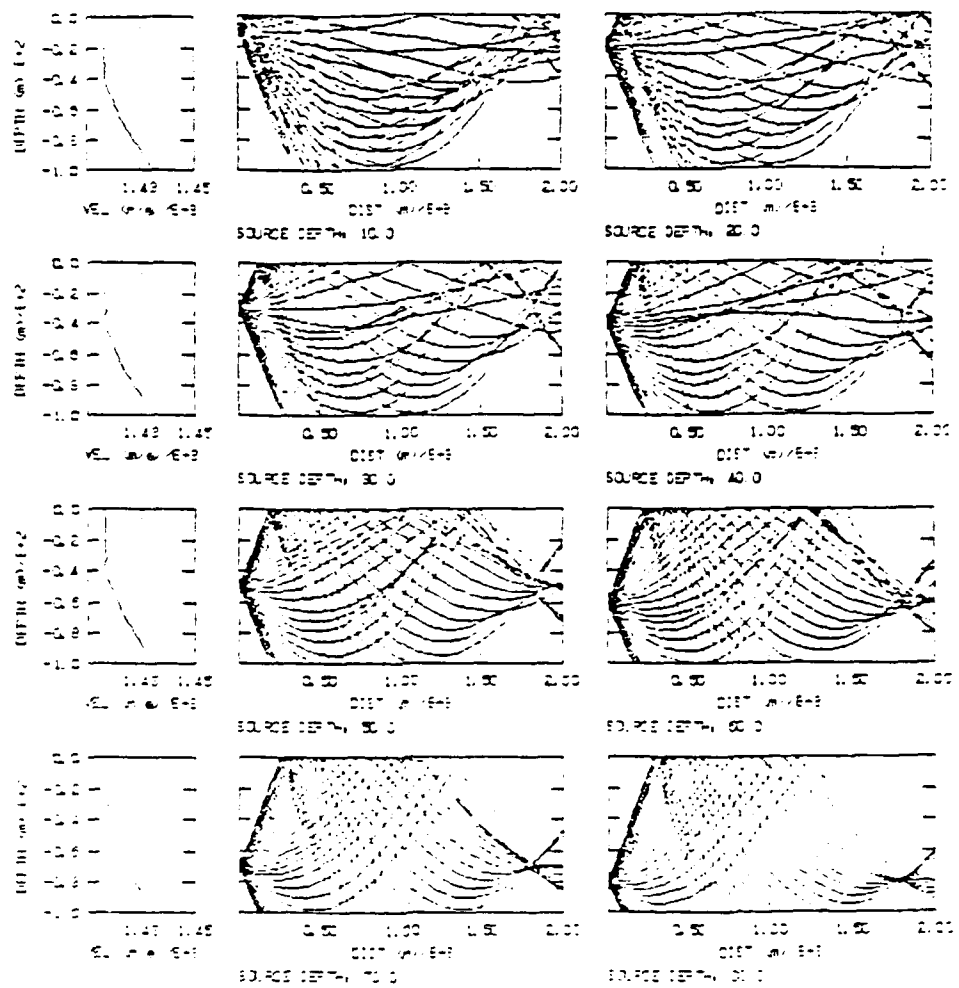

MARS, MARTIG-ET, MED

MIN RAY LAUNCH ANGLE: -15.00

MAX RAY LAUNCH ANGLE: 15.00

RAY LAUNCH ANGLE STEP: 1.00

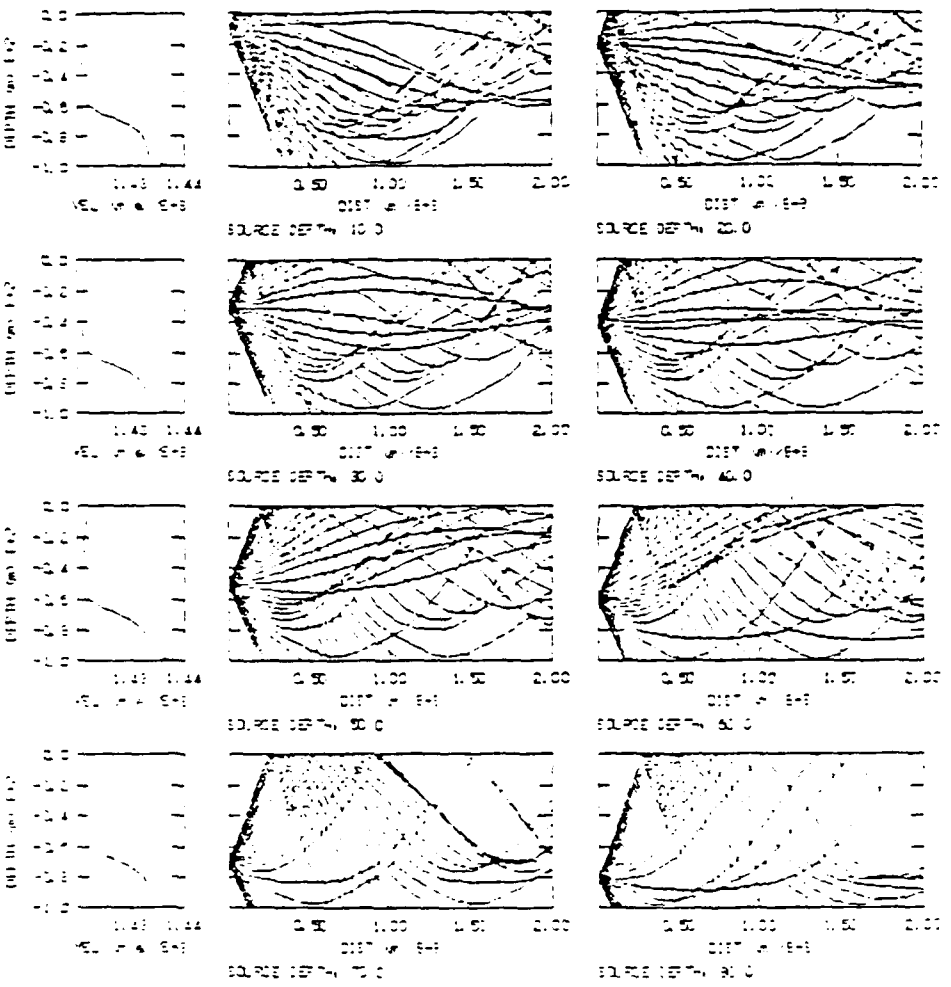

159

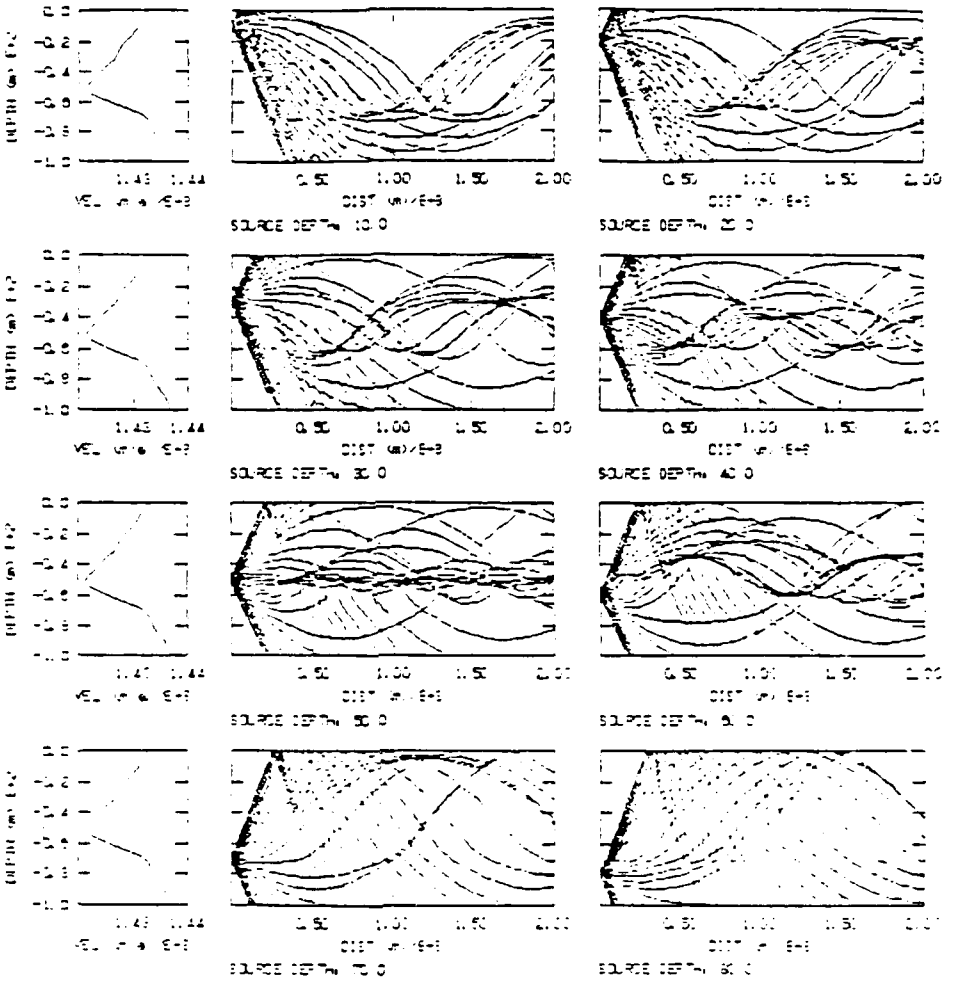

MAX RAY LAUNCH ANGLE: 15.00

RAY LAUNCH ANGLE STEP: 1.00

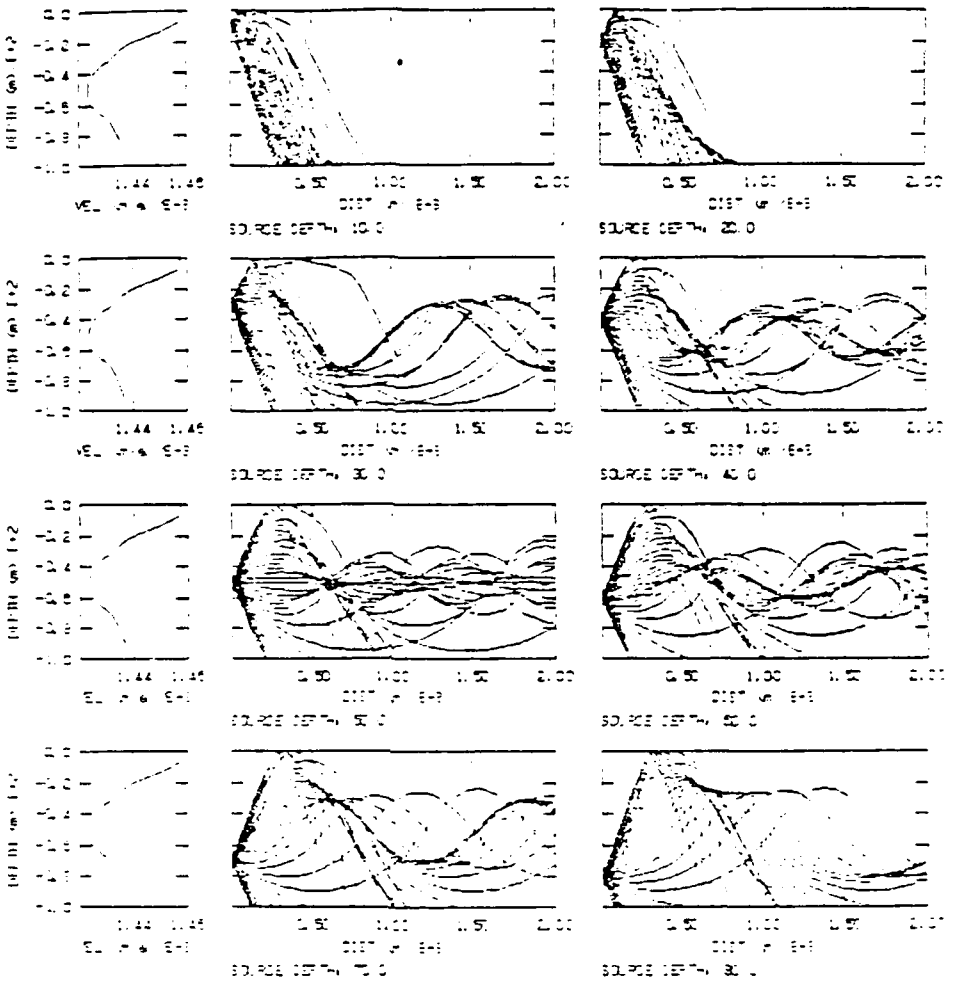

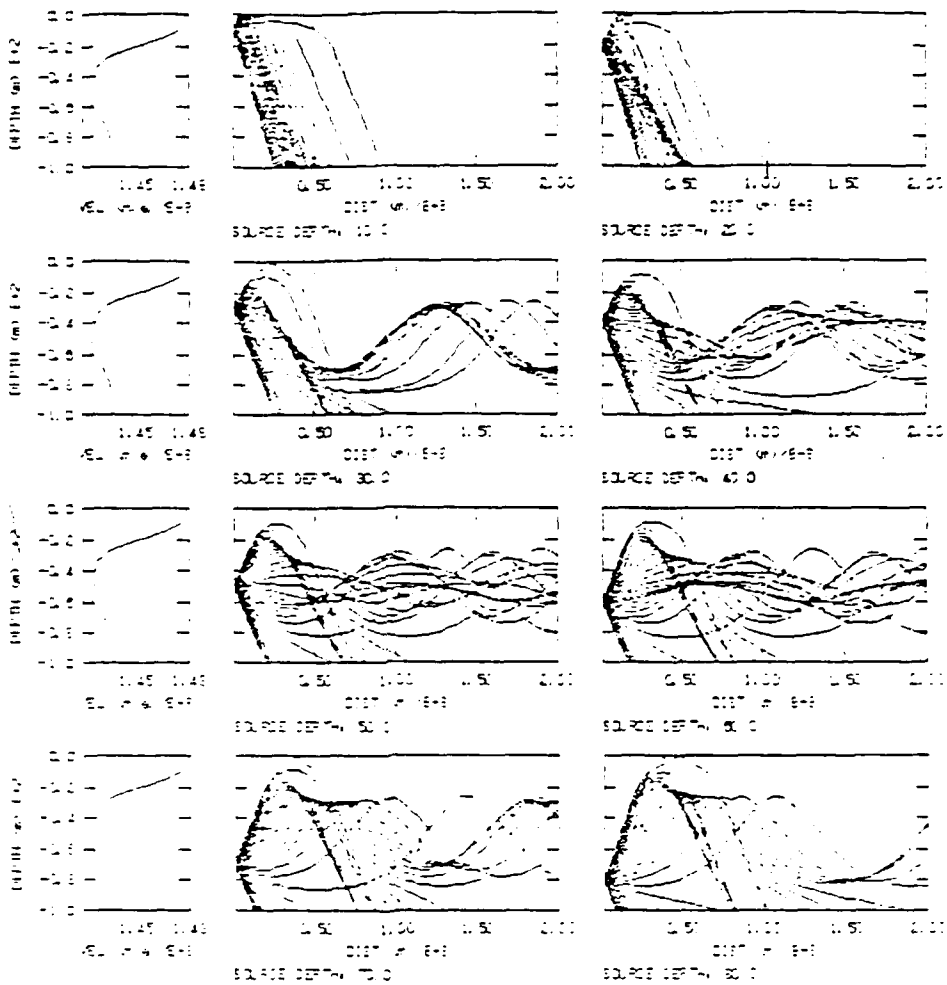

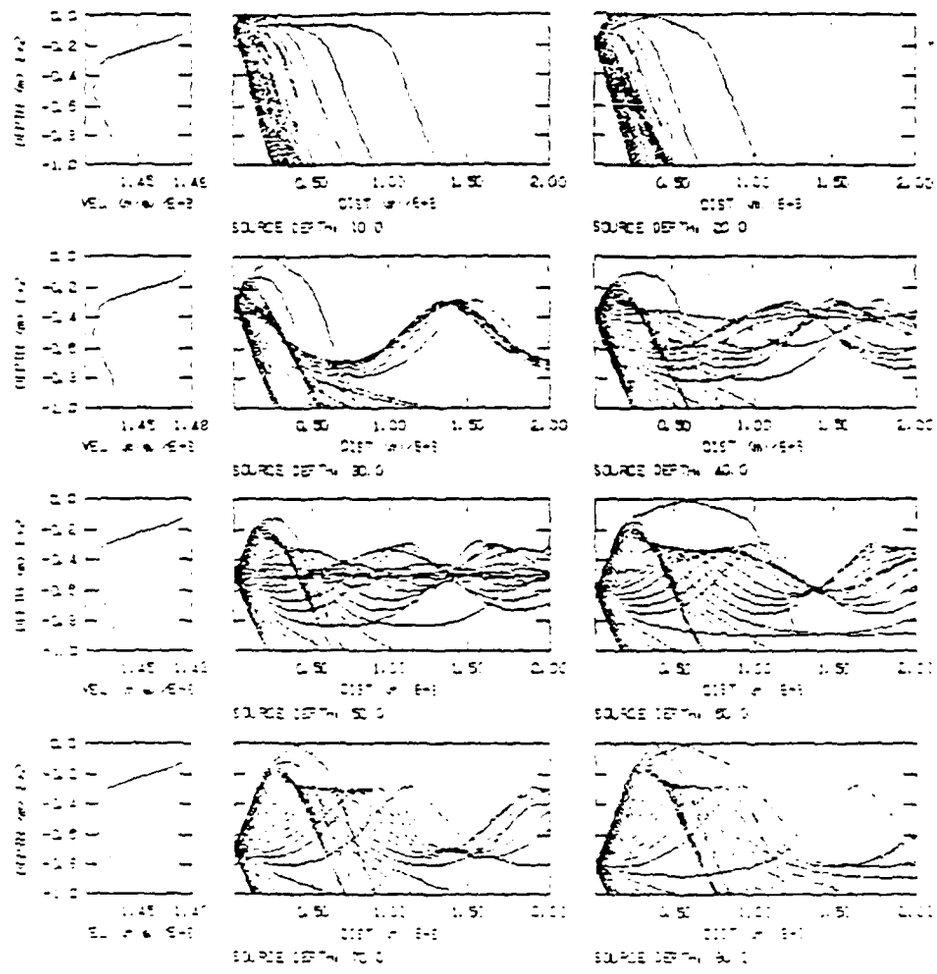

ACOUSTIC PARTICLE VEL

MIN RAY LAUNCH ANGLE: -15.00

MAX RAY LAUNCH ANGLE: 15.00

RAY LAUNCH ANGLE STEP: 1.00

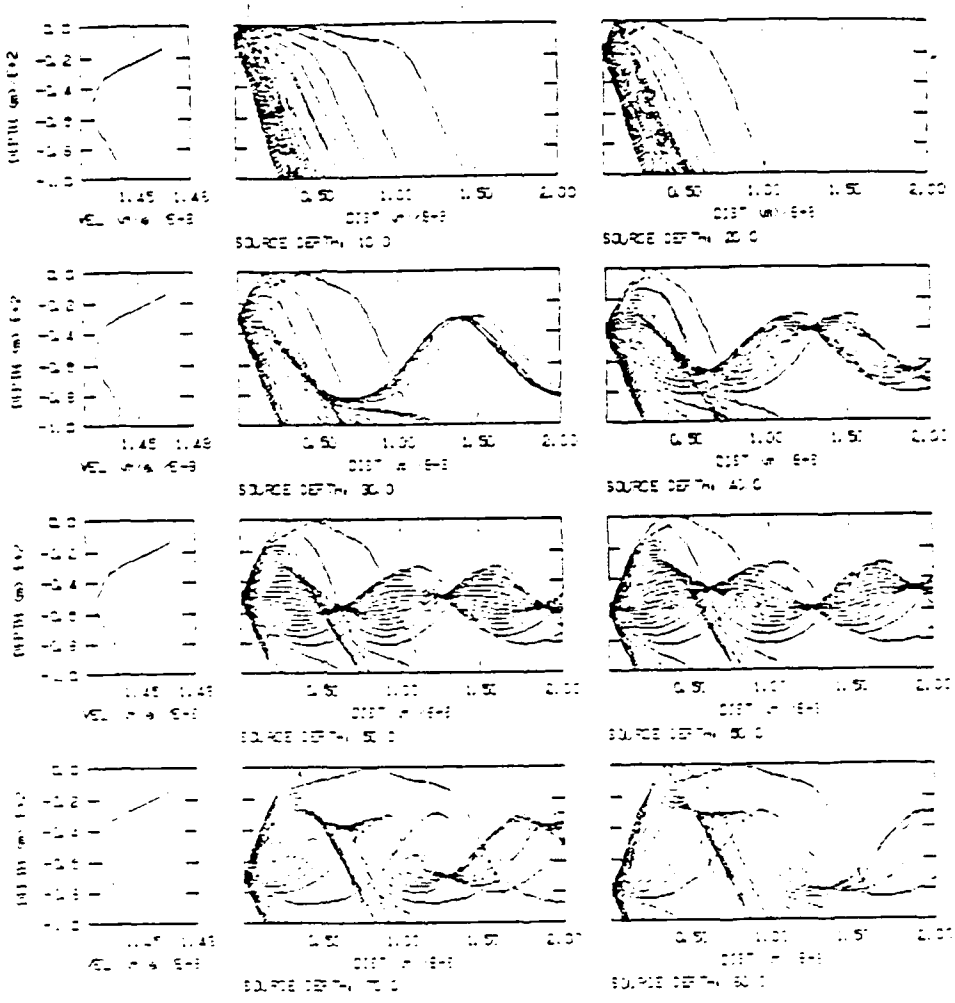

SEPTEMBER [illegible] MEC

MIN RAY LAUNCH ANGLE: -15.00

MAX RAY LAUNCH ANGLE: 15.00

RAY LAUNCH ANGLE STEP: 1.00

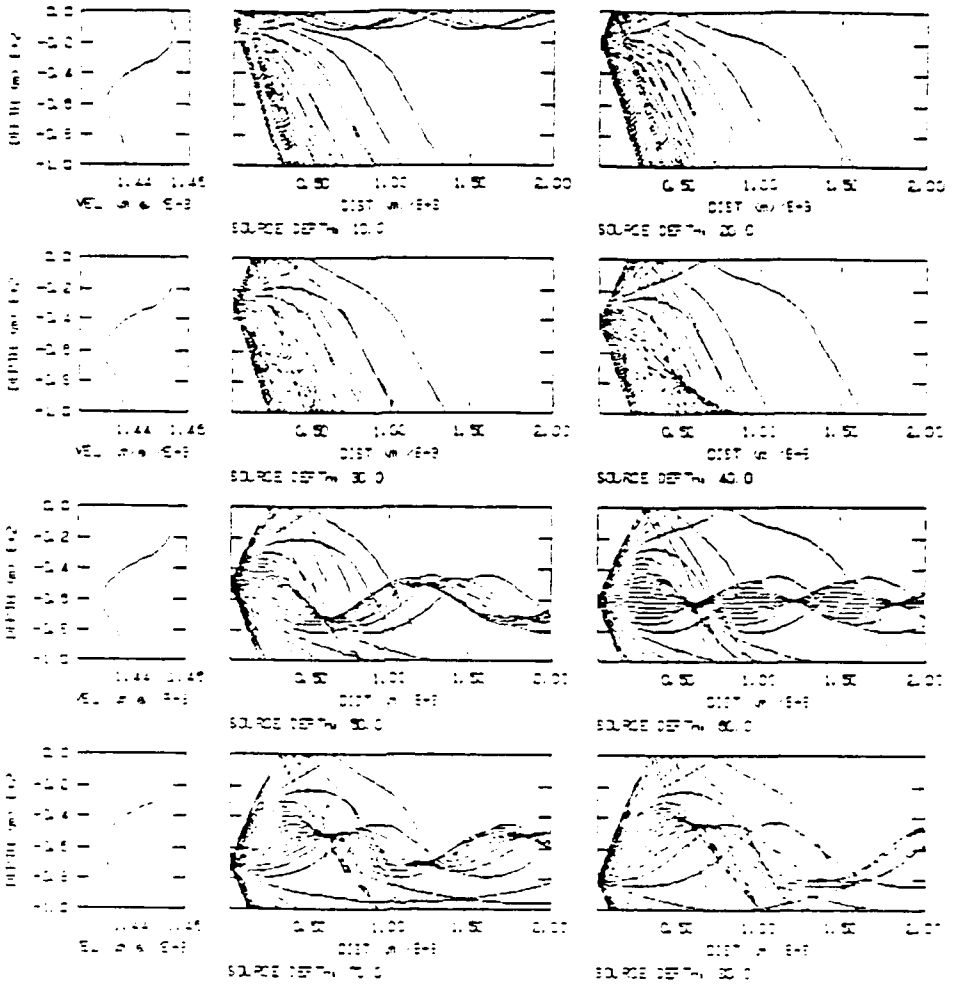

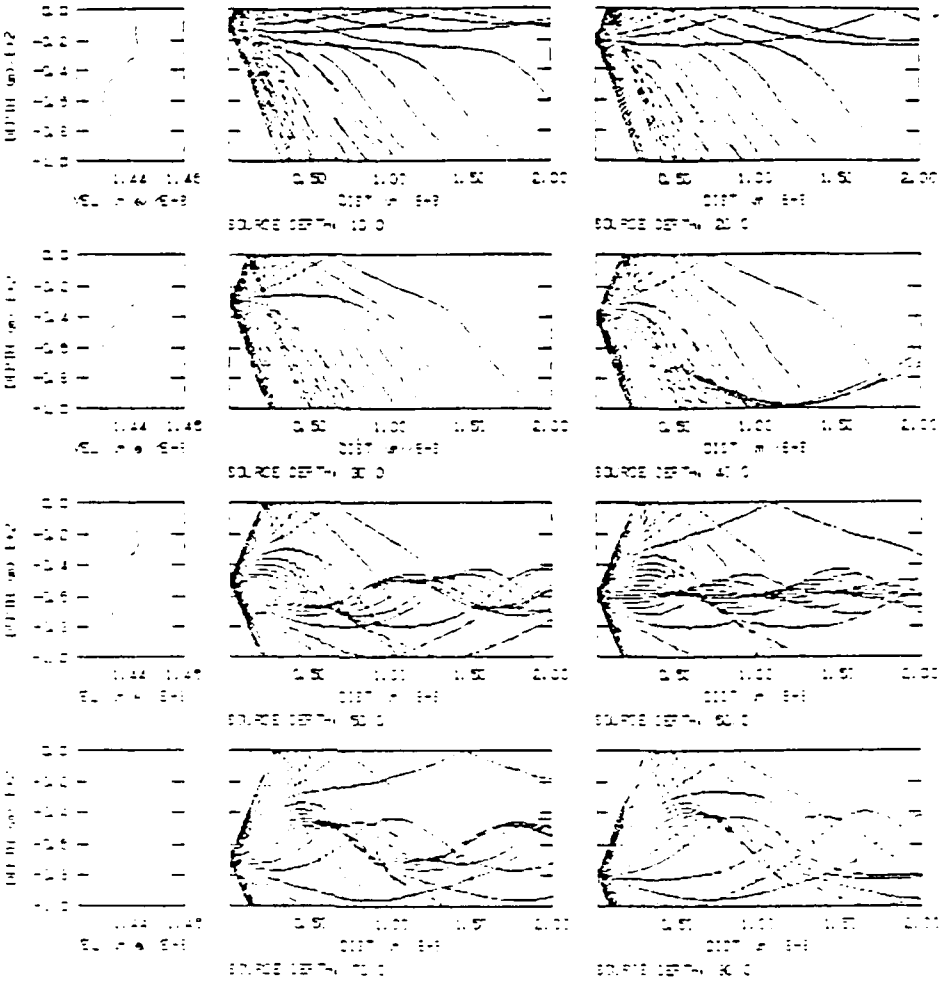

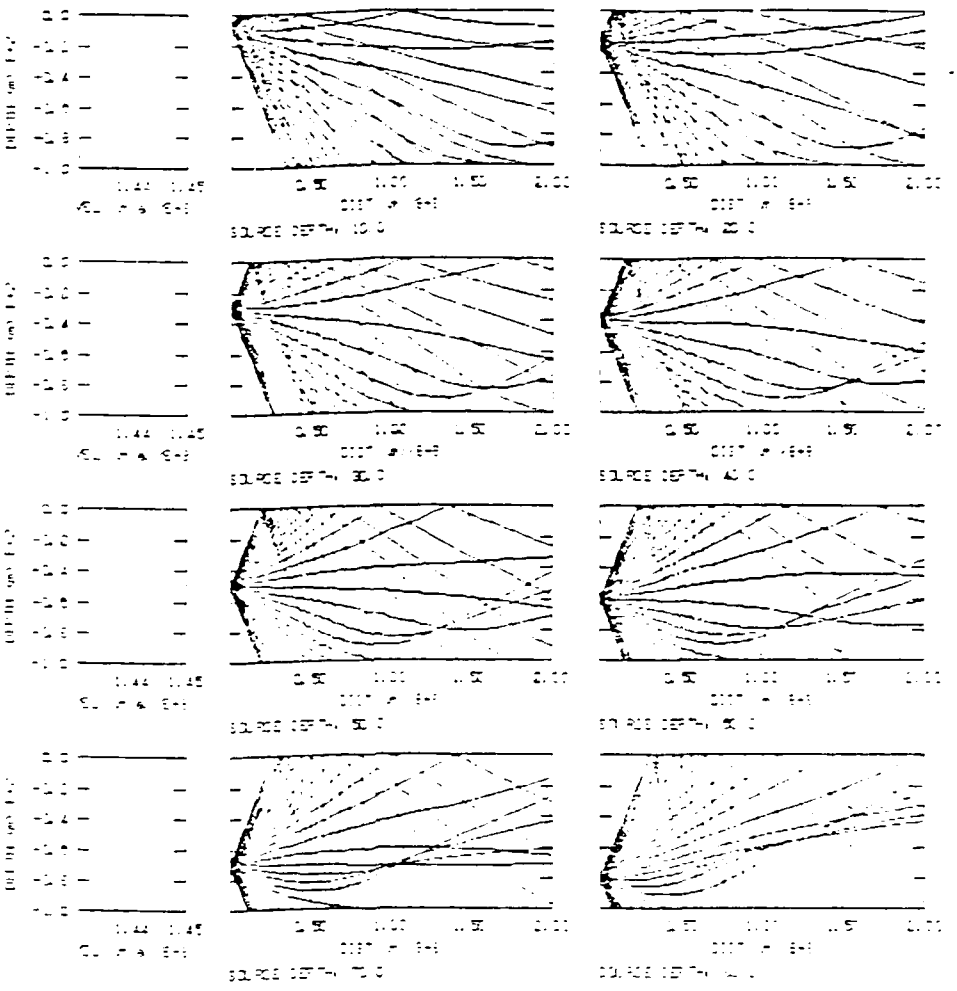

APPENDIX N. BOTTOM REFLECTION COEFFICIENT DIAGRAM

$rad \equiv 1$

$deg \equiv \frac{\pi}{180} \cdot rad$

$k := 0 \ldots 19$

$r1 := 1440000$

$r2 := 1950000$

$c1 := 1440$

$c2 := 1500$

$\theta_k :=$

0 deg
5 deg
10 deg
15 deg
20 deg
25 deg
30 deg
35 deg
40 deg
45 deg
50 deg
55 deg
60 deg
65 deg
70 deg
73.74 deg
75 deg
80 deg
85 deg
90 deg

$$\alpha_k := \operatorname{acos}\left[\sqrt{1 - \left[\frac{c2}{c1}\right]^2 \left[\sin\left[\theta_k\right]\right]^2}\right]$$

$$R_k := \frac{\frac{r2}{r1} - \left[\frac{\cos\left[\alpha_k\right]}{\cos\left[\theta_k\right]}\right]}{\frac{r2}{r1} + \left[\frac{\cos\left[\alpha_k\right]}{\cos\left[\theta_k\right]}\right]}$$

R_k
0.15
0.151
0.151
0.152
0.153
0.155
0.157
0.161
0.165
0.172
0.182
0.197
0.222
0.269
0.387
1 - 0.008i
0.817 - 0.577i
0.927 - i
-0.693 - 0.721i
-1

θ_k
0
0.087
0.175
0.262
0.349
0.436
0.524
0.611
0.698
0.785
0.873
0.96
1.047
1.134
1.222
1.287
1.309
1.396
1.484
1.571

$\lvert R_k \rvert$
0.15
0.151
0.151
0.152
0.153
0.155
0.157
0.161
0.165
0.172
0.182
0.197
0.222
0.269
0.387
1
1
1
1
1

magnitude of the reflection coefficient $\lvert R_k \rvert$

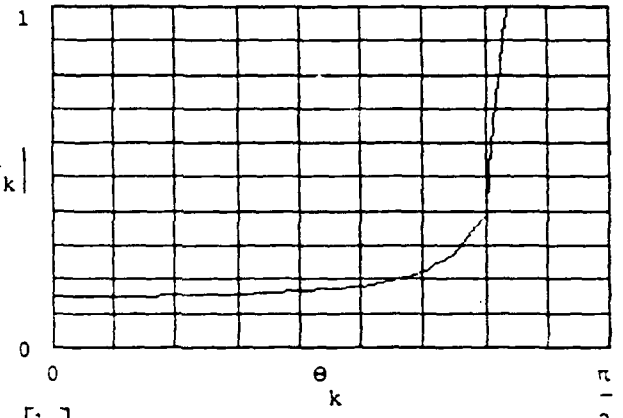

$$LdB_k := 20 \log\left[\frac{1}{R_k}\right]$$

Loss curve in dB

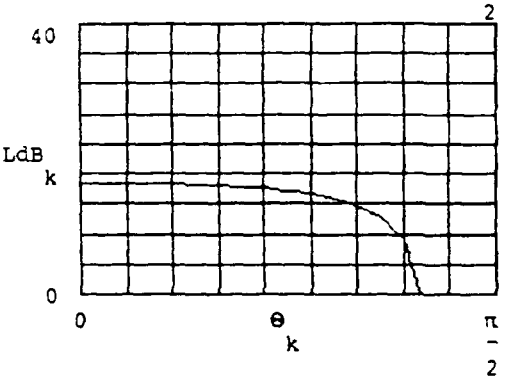

APPENDIX O. KNUDSEN'S CURVES FOR AMBIENT NOISE

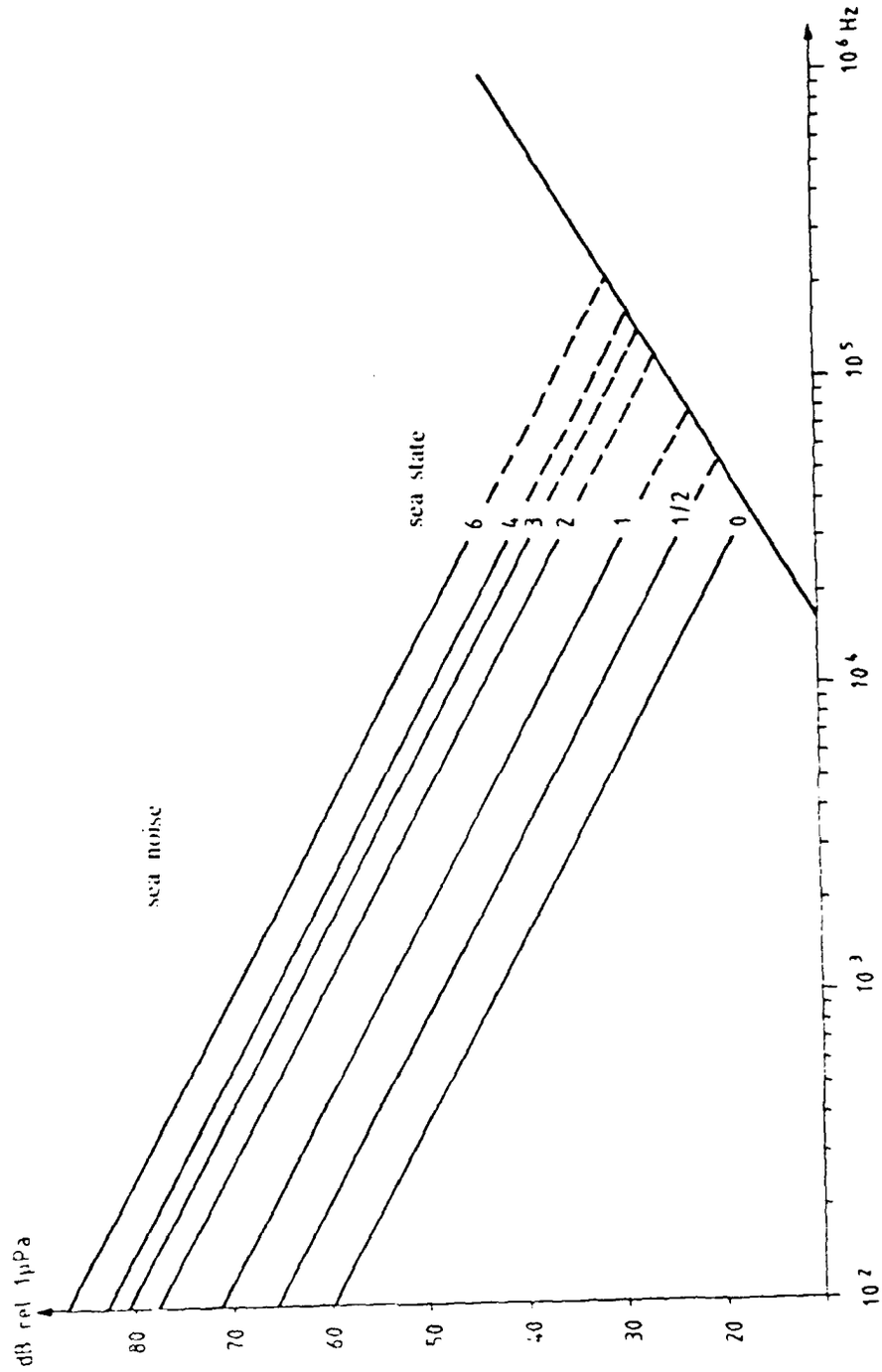

APPENDIX P. MISC. CURVES AND DIAGRAMS

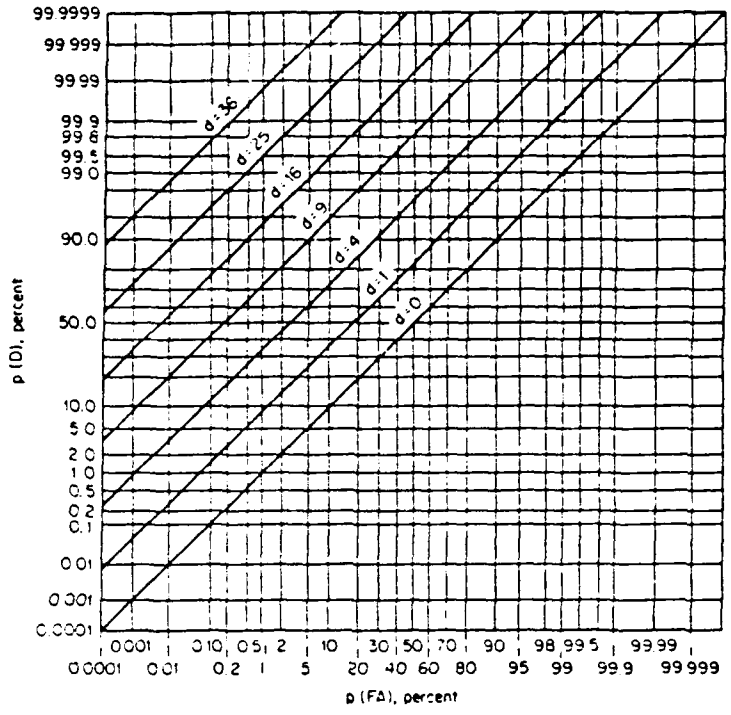

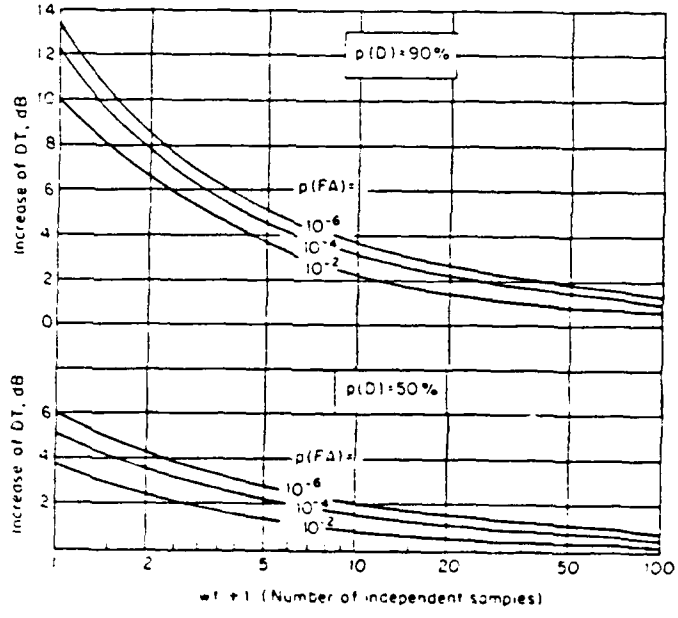

APPENDIX Q. BEAM PATTERN CALCULATIONS

Calculating NL - DI.

NL := 70 dB re 1 μPa (combining NSL(A), NSL(S) and within 840 Hz bandwith.)

DI for reference transducer yields:

k := 0 ..1

a := 0.5 meters

$\lambda_k :=$

0.015
0.003

Reference transducer:
circular with radius 0.5 meter

$$D_k := \left[2 \cdot \pi \cdot \frac{a}{\lambda_k}\right]^2$$

Noise floor (NF)= NL - DI

$$DI_k := 10 \cdot \log\left[D_k\right]$$

DI_k

46.421
60.401

dB ref 1 μPa

$NF_k := NL - DI_k$

NF_k

23.579
9.599

Determining the Source Level (SL)

SL = RL + 2*TL - TS + DT

k := 0 ..3

RL := k	r := k	a := k	TS := k	
23.579	500	10	0	100 kHz
23.579	700	10	0	100 kHz
9.599	500	100	0	500 kHz
9.599	700	100	0	500 kHz

$$SL_k := RL_k + 2 \cdot \left[20 \cdot \log\left[r_k \right] + a_k \cdot \frac{r_k}{1000} \right] - TS_k + 9$$

SL k	
150.538	SL for 100 kHz and 500 m range
160.383	SL for 100 kHz and 700 m range
226.558	SL for 500 kHz and 500 m range
272.403	SL for 500 kHz and 700 m range

Determining the horizontal beamwith.
Using expression for surface reverberation in ref [34] p.425.

$k := 0 \ldots 3$

$RL_k :=$	$SL_k :=$	$TL_k :=$	$SA_k :=$	$R_k :=$	
23.579	150.538	58.9	-19.1	500	100 kHz
23.579	160.383	63.9	-19.1	700	100 kHz
9.599	226.558	104	-15.1	500	500 kHz
9.599	272.403	126.9	-15.1	700	500 kHz

$$\frac{RL_k - SL_k + 2 \cdot TL_k - SA_k - 10 \cdot \log\left[R_k\right]}{10}$$

$\Theta(k) := 1.67 \cdot 10$

$$BW_k := \Theta(k) \cdot \frac{180}{\pi}$$

BW_k	Beam widths in degrees for
1.888	100 kHz and range 500 m
1.397	100 kHz and range 700 m
0.787	500 kHz and range 500 m
0.556	500 kHz and range 700 m

Sensitivity analysis; Varying the TS to investigate the performance limitations.

$k := -25 \ldots 12$ Target Strength variation

$SA := -19.1$ Scattering strength

$DT := 9$ Detection threshold

$$\Theta(k) := 1.67 \cdot 10^{\frac{k - SA - DT - 10 \cdot \log(700)}{10}}$$

$$BW(k) := \Theta(k) \cdot \frac{180}{\pi}$$ Beamwidth in degrees

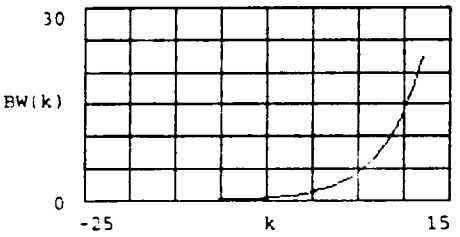

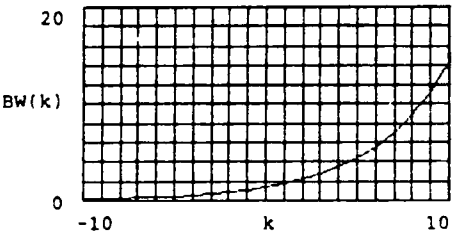

$a := 0 \ldots 9$

k := a	BW[k a]
-5	0.44[illegible]
-4	2.557
-3	0.721
-2	0.883
-1	1.111
0	1.399
1	4.423
2	13.988
3	27.274

Target Strength

Beamwidth in degrees

Calculating an assumed TS based on
a mine with a cylindrical form and with
a tactical aspect angle normal to the
axis of the cylinder. The mine parameters
are taken from an Italien mine, the
"SEPPIA" made by the Misar company.

TS formula for cylindrical shape [u]:

TS = 10 * log(a*L^2/(2*π))

where a = radius, L = cylinder length

a := 0.33

L := 1.33

λ := 0.015

$$TS := 10 \log\left[a \frac{L^2}{2\lambda}\right] \qquad TS = 12.891 \quad dB$$

This value is probably to high for a real mine, since one can expect
different kinds of TS reductions (see chapter 3.x) to be utilized.
Including TS reduction measures and variations in the aspect angle, a TS of
5 dB can be reasonable to assume.

Calculating different approx diameters for a circular transducer:

k := 0 ..8 D = transducer diameter

$ß_k :=$

k	$ß_k$
0	2.442
1	0.557
2	0.701
3	0.883
4	1.113
5	1.399
6	4.423
7	13.988
8	27.474

$$D_k := 65 \frac{0.015}{ß_k}$$

k	Diameter D_k	Target Strength (TS)
0	2.206	-5
1	1.75	-4
2	1.391	-3
3	1.104	-2
4	0.878	-1
5	0.697	0
6	0.22	5
7	0.07	10
8	0.036	12.9

So optimizing for a TS of 5 dB, a transducer with a diameter of
0.22 meters is required.

Recalculation for new required values for necessary SL and
DI gives:
SL = 138.534 dB
DI = 33.3 dB

APPENDIX R. BEAMWIDTH CALCULATIONS

Calculating horizontal and vertical beam pattern for a planar aperture with a Blackman amplitude window.
The aperture function for a planar aperture with separable functions (the aperture function can be written as a product of two functions) and with Blackman amplitude weighting used for both functions yields:

A(f,x,y) = Black(Lx) * Black(Ly)

The normalized directivity function or beam pattern yields:

D(f,fx,fy) = Dx(f,fx) * D(f,fy)

Calculating horizontal beampattern: (set v = 0,(see next page) which yields D(f,fy) = 1)

$\lambda := 0.015$

$u := -1, -0.999 \ldots 1$

$fx(u) := \frac{u}{\lambda}$ Where u = sin θ * cos ψ

$L := 0.319$

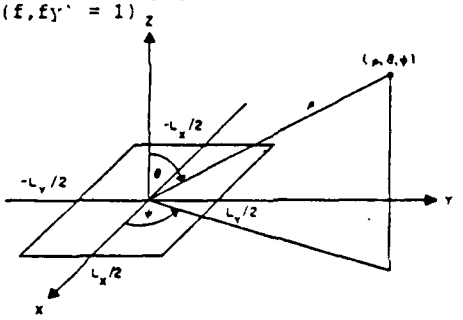

D(f,fx,fy) = Dx(f,fx) gives:

$$D(u) := \frac{\left[1.68 - 0.18\,(L \cdot fx(u))^2\right] \sin(\pi \cdot L \cdot fx(u))}{0.42 \cdot \pi \cdot L \cdot fx(u) \cdot \left[(L \cdot fx(u))^2 - 1\right] \cdot \left[(L \cdot fx(u))^2 - 4\right]}$$

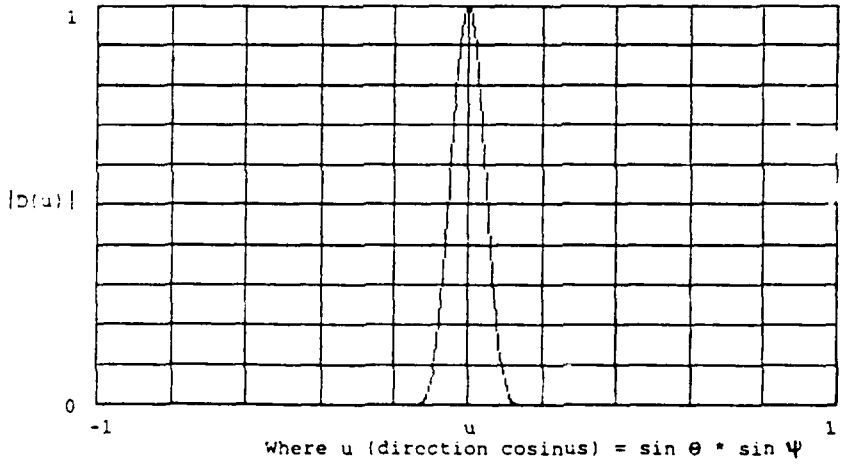

Where u (direction cosinus) = sin θ * sin ψ

Calculating vertical beam pattern: (set u = 0 which yields D(f,fx) = 1)

$L := 0.057$
$\lambda := 0.015$

$v := -1, -0.999 \ldots 1$

$fy(v) := \frac{v}{\lambda}$ Where v = sin θ * sin ψ

D(f,fx,fy) = D(f,fy) gives:

$$D(v) := \frac{\left[1.68 - 0.18 \cdot (L \cdot fy(v))^2\right] \cdot \sin(\pi \cdot L \cdot fy(v))}{0.42\ \pi \cdot L\ fy(v) \cdot \left[(L\ fy(v))^2 - 1\right] \cdot \left[(L \cdot fy(v))^2 - 4\right]}$$

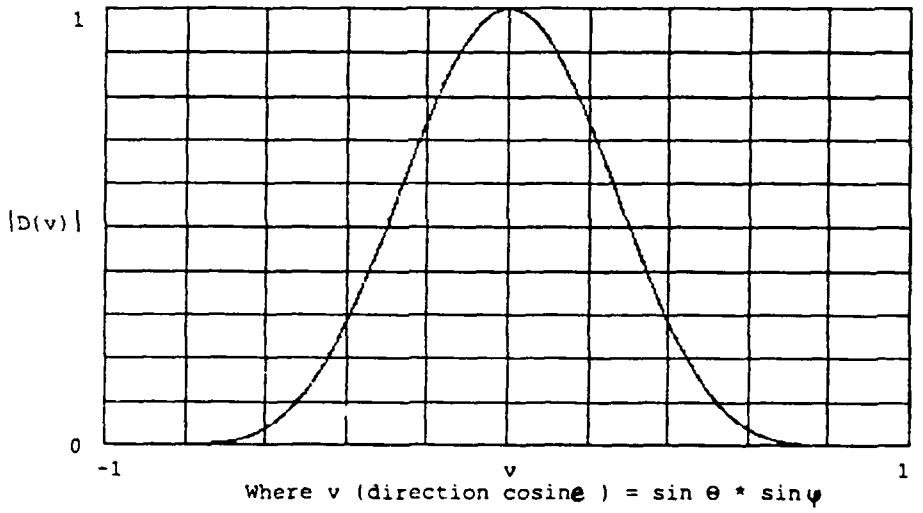

LIST OF REFERENCES

1. *The Scandinavian Shipping Gazette,* Sjofartens Bok, 1989.

2. Michel, Walter H., *The Mission Impact on Vessel Design, from Ship Design and Construction 1980,* Society of Naval Architects and Maritime Engineers, 1980.

3. Chevron Transport Corp., San Francisco CA, USA.

4. Skolnik, Merril I., *Introduction to Radar Systems,* McGraw Hill, 1980.

5. U.S. Naval Research Laboratory, Washington, D.C.

6. Ottosson, R., *MHS Kompendium i Radar, Tele and Telemotmedel Teknik,* MHS Stockholm, 1984.

7. Coppens, Alan B., Sanders, James V., and Dahl, Harvey A., "Introduction to the Sonar Equations," Text Material to Physics Course at Naval Postgraduate School, Monterey, CA, 1982

8. Cox, Albert W., *Sonar and Underwater Sound,* Lexington Books, 1974.

9. Urick, Robert J., *Principles of Underwater Sound, 3d edition,* McGraw-Hill Book Company, 1983.

10. Burdic, William S., *Underwater Acoustic System Analysis,* Prentice-Hall, Inc., 1984.

11. Kihlman, T. and Plunt, J., *Prediction of Noise Levels in Ships,* International Symposium on Shipboard Acoustics, 1976.

12. Brown, Neal A., *Cavitation Noise Problems and Solutions,* International Symposium on Shipboard Acoustics, 1976.

13. Cybulski, J., *Probable Origin of Measured Supertanker Radiated Noise Spectra,* Ocean'77 Conference Record, 1977.

14. Gillmer, Thomas C. and Johnson, Bruce, *Introduction to Naval Architecture,* Naval Institute Press, 1987.

15. Skudrzyk, E.J., and Haddle, G.P, *Noise Production in a Turbulent Boundary Layer by Smooth and Rough Surfaces,* J. Acoust. Soc. Am. 32, page 19, Jan. 1960.

16. *Chaff for Ships: Operational Considerations,* International Countermeasures Handbook, 1981.

17. Gunston, Bill, *Modern Airborne Missiles*, Prentice Hall Press, 1986.

18. Schleher, Curtis. *Introduction to Electronic Warfare*, Artech House Inc., 1986.

19. *Short Course Electronic Warfare*, EW group, Naval Postgraduate School, Monterey CA, USA.

20. Van Brunt, Leroy, *Applied ECM, Vol 1.*, 1978.

21. *Product Data Sheets*, Plessey Microwave, VA, 1987

22. Friedman, Norman, *The Offboard Countermeasures*, 1988.

23. Baranauskas, Tom, *Anti-Ship Missile Threat Drives Decoy Development*, Defense Electronics, March 1988.

24. Boyd, J.A., Harris, D.B., King, D.D. and Welch, H.W. Jr., *Electronic Countermeasures*, Peninsula Publishing, 1978.

25. Blanchard, Benjamin S. and Fabrycky, Wolter J., *Systems Engineering and Analysis*, Prentice-Hall, Inc., 1981.

26. *Sonobuoy Instruction Manual*, Direction of Commander, Naval Air Systems Command, USA, 1988.

27. Tsui, James Bao-Yen, *Microwave Receivers with Electronic Warfare Applications*, 1986.

28. Bonniers, Albert, *Bonniers 3-band lexikon*, forlag, Sweden, 1970.

29. *Svensk Lots del A (Swedish Pilot Guide)*, Sjofartsverket Sweden, 1985.

30. FMV, Swedish Defense Material Administration, Stockholm, Sweden.

31. Sveriges Geologiska Undersokning (Geological Survey), *Maringeologiska kartan Serie Am nr 1, SGU*, 1987.

32. Kinsler, Lawrence E., Frey, Austin R., Coppens, Alan B., and Sanders, James V., *Fundamentals of Acoustics*, John Wiley and Sons, 1984.

33. Ziomek, Lawrence J., *Underwater Acoustics*, Academic Press, Inc., 1985.

34. Ingham, A.E, *Hydrography for the Surveyor and Engineer*, BSP Professional Books, 1984.

35. FOA rapport C 30289-E1, *Activt Parametriskt Hydrofonsystem*, Pentelius Tore, Aug 1982.

36. FOA, Forsvarets Forskningsanstalt (Swedish Defense Research Establishment), Stockholm, Sweden

37. Wibaeus, Sten, *Sonarteknik*, Teleplan, 1985.

38. Kroenert, J.T., J. Acoust. Soc. Am. 71(2), page 507, Feb. 1982.

39. Sackman, George L., *High Resolution Sonar Concept Formulation*, Naval Postgraduate School, Monterey, CA, 1979.

40. Hecht, Eugene, *Optics (second edition)*, Addison-Wesley Publishing Company, 1980.

41. Urick, Robert J., *Sound Propagation in the Sea*, Peninsula Publishing, 1982.

42. Clay, Clarence S. and Medwin, Herman, *Acoustical Oceanography*, John Wiley and Sons, 1977

43. J. Geoph. Res., 71, 2037, Clay, C.S, *Coherent Relection of Sound From The Ocean Bottom, 1966.*

44. B. Aktiva hydrofonsystem, FOA rapport C 30168-E1, *Betydelsen av havets transmissionsegenskaper vid konstruktion av hydroakustiska system*, Pentelius, Tore, Nov 1979.

BIBLIOGRAPHY

Electronic Warfare -- The Future, Navy International March 1984.

The Falklands Campaign: The Lesson, Her Majesty's Stationary Office, 1972.

FOA 3 rapport C 3680-E1, Pentelius, Tore, *Ljudvagors Reflexion Mot Skiktad Havsbotten Med Speciell Hansyn Till Ostersjoforhallanden,* Aug 1971.

Norwegian Council for Technical and Scientific Research, Report B.0930.4502.1, *Noise Control in Ships,* 1985.

Ratcliffe, Mike, *Liquid Gold Ship,* Lloyd's of London Press Ltd., 1975.

Skolnik, Merril I., *Radar Handbook,* McGraw`Hill, 1970.

SSPA, Maritime Consulting. Gothenburg, Sweden.

Van Brunt, Leroy B., *Applied ECM, Vol 2.,* 1982.

Wiseman, Charles H., *Chaff Assists Anti-Ship Missile Defence,* EW: July/August 1977.

INITIAL DISTRIBUTION LIST

1.	Defense Technical Information Center Cameron Station Alexandria, Virginia 22304-6145	2
2.	Library, Code 0142 Naval Postgraduate School Monterey, California 93943-5002	2
3.	MHS Marinlinjen Valhallavägen 117 Box 80007 104 50 Stockholm SWEDEN	1
4.	Chairman, Code 73 Department of Electronic Warfare Naval Postgraduate School Monterey, California 93943-5000	1
5.	Chairman, Code 61 Ay Department of Physics Naval Postgraduate School Monterey, California 93943-5000	1
6.	Prof. L. Partelow 11 Paseo De Vaqueros Salinas, California 93908	1
7.	Prof. A. Coppens, Code 61 C2 Department of Physics Naval Postgraduate School Monterey, California 93943-5000	1